REVIEWS OF MODERN PHYSICS, VOLUME 75, JULY 2003

Recent trends in the determination of nuclear masses

D. Lunney*

CSNSM–CNRS/IN2P3, Université de Paris-Sud, F-91405 Orsay, France

J. M. Pearson†

Département de Physique, Université de Montréal, Montréal (Québec), H3C 3J7 Canada

C. Thibault‡

CSNSM–CNRS/IN2P3, Université de Paris-Sud, F-91405 Orsay, France

(Published 20 August 2003)

The mass of the nucleus, through its binding energy, continues to be of capital importance not only for various aspects of nuclear physics, but also for other branches of physics, notably weak-interaction studies and astrophysics. The authors first describe the modern experimental techniques dedicated to the particularly challenging task of measuring the mass of exotic nuclides and make detailed comparisons. Though tremendous progress in these and the associated production techniques has been made, allowing access to nuclides very far from stability, it is still not yet possible to produce many nuclides involved in stellar nucleosynthesis, especially the *r* process, leaving no choice but to resort to theory. The review thus goes on to describe and critically compare the various modern mass formulas that may be used to extrapolate from the data towards the neutron drip line. Special attention is devoted to the crucial interplay between theory and experiment, showing how new measurements far from stability can considerably reduce the ambiguity in extrapolations to nuclides even further away.

CONTENTS

*Electronic address: lunney@csnsm.in2p3.fr
†Electronic address: pearson@lps.umontreal.ca
‡Electronic address: thibault@csnsm.in2p3.fr

"*Paris is worth a mass.*"
—Henri IV

I. INTRODUCTION

The continuing interest in nuclear masses lies in the fact that the mass $M(N,Z)$ of a nucleus with N neutrons and Z protons is measurably less than the sum of the masses of its constituent free nucleons, whence a direct determination of the binding energy B of the nucleus is possible:

$$B(N,Z)=\{NM_n+ZM_p-M(N,Z)\}c^2, \quad (1)$$

where M_n is the mass of the neutron and M_p that of the proton. Given this inherent connection with the binding energy, the mass of the nucleus must be regarded as one of its basic characteristics. The steady growth over the years in the number of nuclides whose masses have been measured has contributed immensely to our understanding not only of nuclear structure but also of several other branches of fundamental physics.

The "mass defect" was discovered by Aston in the early days of his pioneering program, launched right after the First World War (Aston, 1920). He found that to within 1 part in 1000 all but one of the isotopes he measured had integral atomic weight (on the scale of 16 for oxygen), helium in particular having atomic weight 4.000. The one exception was hydrogen, for which a value of 1.008, rather than 1.000, was found, a result that had to be reconciled with the prevailing view that the helium nucleus consisted of four hydrogen nuclei and two electrons (more than a decade was to elapse before the discovery of the neutron). Aston attributed this mass defect to the unique feature of the hydrogen atom of "not containing any negative electricity in its nucleus," but Eddington (1920, 1926) interpreted it rather in terms of the binding energy of the helium nucleus, showing that the nuclear transmutation of hydrogen into helium could serve as an adequate source of stellar energy. A long-standing puzzle was thereby resolved, no other known source of energy being sufficient to account for the estimated output of the sun over the necessary time scale. Others had made a similar suggestion, but Eddington was the first to exploit the idea on a quantitative basis by making the connection with Aston's measurements. The intimate relationship between nuclear-mass measurements and astrophysics is thus seen to go back to the earliest days of our field, thanks to Eddington.

Aston for his part went on to make systematic measurements of some 200 nuclides, described in his book (Aston, 1933). By the mid 1930s his measurements, interpreted in terms of the new neutron-proton picture of the nucleus, established the near constancy at around 8 MeV of the binding energy per nucleon of most nuclides (with a weak maximum at ^{56}Fe). This observation, combined with the near constancy of nuclear densities, as indicated by the measured nuclear radii, led to the concept of the saturation of nuclear forces, i.e., the notion that any given nucleon in a nucleus interacts only with its nearest neighbors (see, for example, von Weizsäcker, 1935, and Bethe and Bacher, 1936).

This property of the nuclear forces was recognized as being consistent with their known short range, although other conditions on the forces have to hold as well. In any case, closely associated with the saturation property is the liquid-drop model of the nucleus, originally proposed by Gamow (1930), even before the discovery of the neutron. This picture of the nucleus became firmly entrenched during the 1930s, and before the end of the decade it had been extended, particularly in the hands of Niels Bohr, to account for both the compound-nucleus mechanism of nuclear reactions and the newly discovered phenomenon of fission [see, for example, Friedman and Weisskopf (1955) and Wheeler (1955) for these respective topics].

Later, shortly after the end of the Second World War, mass measurements played an important, although not exclusive, role in establishing the shell model (Haxel *et al.*, 1948, 1949a, 1949b, 1949c, 1950; Mayer, 1948, 1949, 1950). According to this model, also known as the independent-particle model, nuclei with so-called magic numbers of neutrons or protons, N_0 and $Z_0=8$, 20, 28, 50, 82, and $N_0=126$, have exceptional stability, i.e., extra binding beyond what is expected from the smooth systematics of the liquid-drop model. As far back as 1933 there had been some speculation, inspired by atomic

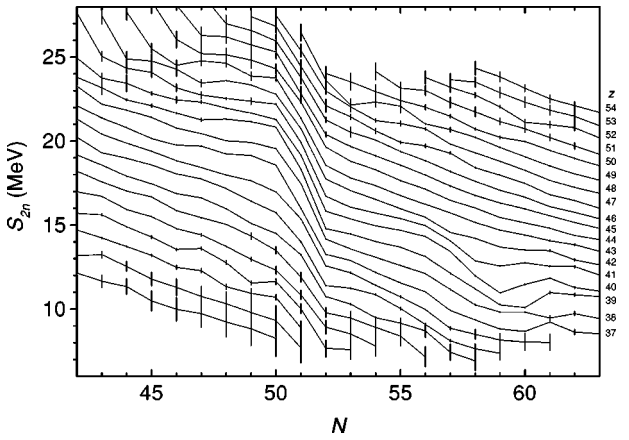

FIG. 1. Two-neutron separation energy S_{2n} of several elements in the range $Z\sim30-50$, as a function of neutron number N. Data are taken from Audi and Wapstra (1995).

physics, on possible shell structure (Elsasser, 1933, 1934a, 1934b), but Bethe and Bacher (1936) had stressed the need for better mass measurements before any firm conclusion could be drawn. Even more importantly, it was long believed that any shell structure in the nucleus would be impossible, since an essential condition for a shell structure in a given system of particles is the existence of a common field in which the particles can move more or less independently of each other. In the case of the atom the electric charge of the nucleus obviously generates such a field for the electrons, and moreover the interactions between the electrons, being long-ranged, can to a certain approximation be smoothed out into a supplementary field which simply modifies the Coulomb field of the nucleus. On the other hand, there is nothing within the nucleus itself that can play the same role that the nucleus plays within the atom, and it was furthermore difficult to see how the short-range interactions between the nucleons implied by the liquid-drop picture could conspire, even to a first approximation, to form a smoothed field.

Nevertheless, by 1950 the evidence for shell properties had become overwhelming, and it had to be admitted that in some way the nucleonic interactions do to some extent smooth themselves out into a common, or mean, field. Reconciling these aspects of nuclear structure with the equally well established liquid-drop features became one of the major challenges of nuclear physics. The necessary synthesis turned out to be a generalized independent-particle model, much closer to the shell model than to the liquid-drop model in spirit: the essential generalization lay in allowing the mean field to deform from spherical symmetry and also to be time dependent (see, for example, Rowe, 1970 and Brown, 1971). It was found that such a model could indeed have all the known liquid-drop attributes, although it is highly convenient for many purposes to retain the liquid-drop language.

The most striking way in which shell structure manifests itself in mass systematics is through the two-neutron separation energy

$$S_{2n}(N,Z)=B(N,Z)-B(N-2,Z) \tag{2a}$$

in the case of neutron shells, and the two-proton separation energy

$$S_{2p}(N,Z)=B(N,Z)-B(N,Z-2) \tag{2b}$$

in the case of proton shells. (Because of the pairing effect, the single-nucleon separation energy is a less clear-cut indicator: see below.)

Referring specifically to neutron shells, there is a general tendency for the two-neutron separation energy S_{2n} to fall steadily as the neutron number N increases with the proton number Z held constant: this is a liquid-drop characteristic, and follows from the von Weizsäcker mass formula of Eq. (9). However, at the magic numbers marking shell closure there is a sudden drop, after which the steady fall resumes. The situation is well illustrated in Fig. 1, where we show the variation with neutron number of S_{2n} for the elements $Z\sim30-50$: the magic number $N_0=50$ is conspicuous, corresponding to a sudden drop in the energy necessary to remove neutrons after a closed shell. Proton shell structure can likewise be displayed by plotting the two-proton separation energy S_{2p} as a function of Z for isotone chains.

The strong shell gap at $N_0=50$ is not the only departure from a steady fall of the S_{2n} vs N curve that is apparent in Fig. 1: between $N=56$ and 61 there is a trough visible for the elements Rb ($Z=37$) to Ru ($Z=44$), having a maximum depth at $N=59$ for Zr ($Z=40$). This corresponds to the mean field associated with the shell structure undergoing a sharp change from a spherical to a deformed shape. However, mass measurements are by no means the only indicator of such shape changes, a more characteristic signature of deformation being the existence of rotational spectra, at least in the case of nuclei close to the stability line.[1]

The magic numbers that we have quoted above were established from the earliest days of the shell model (Haxel *et al.*, 1950; Mayer, 1950), at which time the data were limited to nuclei lying close to the line of beta stability (hereafter referred to as the stability line). There is an ongoing interest concerning the extent to which these numbers remain magic as one moves out towards either the neutron drip line or the proton drip line.[2] Specifically, one would like to know whether there

[1]Such spectra were originally interpreted in terms of the classical rotations of a deformed liquid drop (Bohr and Mottelson, 1953), but they arise also in the generalized independent-particle model as a necessary consequence of angular momentum conservation, once the mean field is deformed (see, for example, Mottelson, 1962).

[2]By neutron drip line is meant the locus of points corresponding to the minimum value of N for which $S_n<0$ at each value of Z. The proton drip line is likewise defined in terms of the minimum value of Z for which $S_p<0$ at each value of N (see Fig. 4 below). All nuclides lying between these lines will be stable with respect to nucleon emission, although some iso-

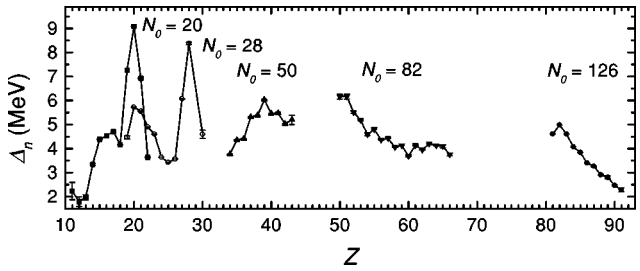

FIG. 2. Experimental neutron-shell gaps as a function of Z for $N_0=20$, 28, 50, 82, and 126. Data are taken from Audi and Wapstra (2001).

is any quenching, in the sense of either a weakening or a total extinction, of the shell gaps, as defined by

$$\Delta_n(N_0,Z)=S_{2n}(N_0,Z)-S_{2n}(N_0+2,Z) \tag{3a}$$

and

$$\Delta_p(N,Z_0)=S_{2p}(N,Z_0)-S_{2p}(N,Z_0+2). \tag{3b}$$

From Fig. 2, showing the variation of the $N_0=20$, 28, 50, 82, and 126 neutron-shell gaps with Z, we see that in the first three cases there is definitely a weakening of the gaps as the neutron excess (or equivalently, proton deficiency) increases, although only in the case of $N_0=20$ do the presently available data approach the neutron drip line. This is the region of the famous "island of inversion," which has been the subject of intense investigation by a variety of complementary techniques [see, for example, Thibault *et al.* (1975), Orr *et al.* (1991a, 1991b), and Lunney, Audi, Doubre, *et al.* (2001)]. As for $N_0=82$ and 126, there is a tantalizing suggestion that quenching might be setting in on the neutron-rich side. Certainly, there are no data counterindicating quenching. We return to this question in Sec. III.B.4.

The existence of shell quenching naturally raises the question of whether new magic numbers might appear in these neutron-rich or proton-rich regions of the nuclear chart. In fact it would seem so, as evidenced by recent studies (including mass measurements) around $N=16$ (Ozawa *et al.*, 2000). On the other hand, while recent Coulomb-excitation measurements by Sorlin *et al.* (2002) suggest that $N=40$ could be magic in the case of Ni ($Z=28$), there is no other evidence of a shell gap in this region.

There is also the long-standing question of whether there might not be new magic numbers lying beyond the heaviest known nuclei. Actually, it was recognized a long time ago that in a purely liquid-drop picture nuclei with $Z>104$ would, because of the disruptive nature of the Coulomb force, be completely unstable with respect to spontaneous fission. The very existence of such elements thus depends on the potentially stabilizing influence of shell effects, and it was realized during the 1960s that new magic numbers might give rise to "islands of stability,"[3] essentially because of the large increase in fission-barrier height that could be expected in the vicinity of doubly magic nuclei (Myers and Swiatecki, 1966). Early calculations (Meldner, 1967) indicated that $Z=114$ and $N=184$ should both be magic, with the corresponding doubly magic nucleus $^{298}114$ being close to beta stability. After enormous experimental efforts [see the reviews of Armbruster (2000), Hofmann and Münzenberg (2000), Hofmann (2002), Oganessian (2001, 2002), and Oganessian *et al.* (2002)], the superheavy nuclide $^{289}114$ was discovered (Oganessian *et al.*, 1999), but it remains to be seen whether $Z=114$ and $N=184$ are indeed magic; other theoretical candidates are discussed by Kruppa *et al.* (2000) and by Berger *et al.* (2001). The experimental signatures for the production of these elements, in most cases with only one or two events recorded over weeks of experiments, are invariably the alpha-decay sequences that generally lead to spontaneously fissioning nuclides. Knowing the masses of these descendants is important, not only for validating mass predictions in this region, but also for confirming the very existence of the superheavy nuclide in question.

In the light-mass region of the nuclear chart, experiments have reached, and even crossed, the drip lines. One of the surprises, discovered by Tanihata *et al.* (1985), was the existence of halo nuclides. The archetypal example is ^{11}Li, consisting of a more or less inert ^{9}Li core and an extended halo of two very weakly bound neutrons. The radial wave function of a halo nucleus depends critically on the one- or two-neutron separation energy. Modern, three-body models now require this quantity as an input parameter. Recent reviews of halos and their models are given by Hansen *et al.* (1995), Tanihata (1996), and Riisager *et al.* (2000).

As a final item in our summary of the various contributions that mass measurements have made, and continue to make, to our knowledge of nuclear structure, we mention the two different kinds of pairing phenomena that are encountered. The better known of these refers to the tendency for nuclei with an even number of nucleons of one type or the other to be more strongly bound than nuclei with an odd number. While this property was already well established in the 1930s,[4] understanding its

lated nuclides lying *beyond* the lines will also be nucleon stable. Also, many nuclides just beyond the proton drip line are energetically capable of emitting protons but will, because of the Coulomb barrier, be effectively stable against proton emission, positron decay being so much more rapid [see Novikov *et al.* (2002), who describe this phenomenon as forming a "littoral shallow"].

[3]This metaphor makes sense provided one works in terms of the binding energy B rather than the internal energy $E=-B$. However, there is some confusion of terminology here, since one often refers to nuclei lying close to the stability line as constituting a "valley of stability," a metaphor that makes sense only in terms of E.

[4]It was his familiarity with pairing that led Niels Bohr as early as 1939 to identify ^{235}U, rather than the much more abundant ^{238}U, as the isotope responsible for the fissioning of natural uranium under bombardment by thermal neutrons (Bohr, 1939).

behavior in nuclei lying far from the stability line is very much a matter of current interest (see, for example, Bennaceur *et al.*, 1999). More subtle is the pairing between a neutron and a proton coupled in an isospin state of $T=0$. This appears to be related to the so-called Wigner effect, i.e., the tendency for nuclei with $N=Z$ to be more strongly bound than neighboring nuclei (see Sec. III.B.3). Mass measurements have played an important role in elucidating this phenomenon (Jensen *et al.*, 1984; Brenner *et al.*, 1990; Satula *et al.*, 1997).

While new and better mass data still contribute to our understanding of nuclear structure, a large part of the motivation driving the continuing effort in the field derives simply from the realization that a knowledge of the masses of all the nuclei involved in a given reaction, or other process such as beta decay or fission, leads to a determination of the energy release. One important application of this is the determination of the possible decay modes of a system. For example, the recent discovery of two-proton emission (Giovinazzo *et al.*, 2002; Pfützner *et al.*, 2002) began with inspection of mass surface (specifically, seeking a negative S_{2p} and positive S_p). Another example is in the prediction of cluster radioactivity, e.g., ^{12}C emission. A recent experimental determination of the Q value for this decay from the alpha-decay studies of Mazzocchi *et al.* (2001) is very important, since this quantity has an enormous influence on the partial half-life.

Particle physics is another, but quite different, area in which measurements of nuclear masses are, because of their implications for energy release, absolutely essential. Neutrinoless double-beta decay (Elliott and Vogel, 2002) is one example where the mass differences of the parent and daughter precisely determine the location of the double-beta peak, revealing the putative existence of Majorana neutrinos (Klapdor-Kleingrothaus *et al.*, 2001; Aalseth *et al.*, 2002). Other motivation comes from the electroweak sector of the Standard Model of particle interactions, in connection with the hypothesis of the conserved vector current (CVC), and with the extent to which the Cabibbo-Kobayashi-Maskawa (CKM) matrix (Particle Data Group, 2002) satisfies unitarity. Both can be tested by means of an accurate determination of the weak vector-coupling constant G_V, accessible via superallowed $0^+ \rightarrow 0^+$ nuclear beta decays. The clean extraction of G_V from the comparative half-life of a given decay requires precise knowledge of the available phase space, which in turn depends sensitively on the energy released by the beta decay in question, whence the need for accurate mass measurements of both mother and daughter nuclides. At the present time the CVC hypothesis appears to be well verified, but there is a tantalizing indication of a deviation from unitarity of the CKM matrix. Confirming this possible breakdown of the Standard Model will require *inter alia* measuring the masses of nuclei whose half-lives are less than 100 ms with an accuracy of much better than 1 keV (see, for example, Hardy and Towner, 2001, 2002). This is an interesting example of an indispensable contribution made by low-energy (actually, zero-energy) nuclear physics to a field generally held to be the property of high-energy physicists.

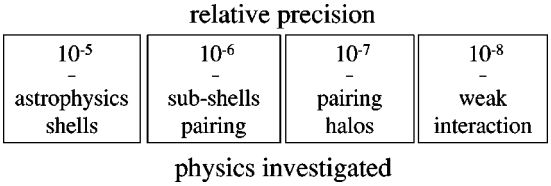

FIG. 3. Correlation between the relative uncertainty on the measured mass $\delta m/m$ and the associated physics that can be probed.

Yet another domain in which the determination of energy releases is of prime importance is that of stellar nucleosynthesis, and it is fair to say that the needs of the astrophysics community are at least partially responsible for the current growth of activity in the field of nuclear masses. (Another astrophysical context in which new mass data could clarify matters is discussed at the beginning of Sec. III.)

Having discussed the importance of mass determinations for many different areas of physics, we now summarize the approach we have adopted in the present review. Even if there will always be some interest in remeasuring with ever-increasing precision the masses of particular nuclides, the predominant experimental thrust, described in Sec. II, is to explore regions of the nuclear chart further and further away from the stability line. Continuing technical advances at an expanding number of radioactive-beam facilities now allow us to probe relatively exotic nuclear systems, in some cases at—and beyond—the drip lines (Ravn, 2002). The main problem facing experiments with exotic nuclides is the fact that as these species are produced in very limited quantities (see Sec. II.A), the associated measurement techniques require very high sensitivity. Since the determination of the mass requires very high precision, this means that great effort must be made to identify and eliminate systematic error and to ensure consistency. One of the many challenges facing mass spectrometrists is that exotic nuclides are by definition very short lived. The development of a fast measurement technique is therefore imperative, but such techniques must also be of sufficiently high resolution to make precision measurements.

The precision required on the mass depends on the physics being investigated. This idea is summarized in Fig. 3. As can be seen from the above discussion concerning nuclear structure, the first indications of shell effects (see Fig. 1) are somewhat gross, of the order of a few MeV, corresponding to a relative precision of about 10^{-5}. Probing the shell openings and closures of more exotic nuclides requires somewhat higher precision, roughly 10^{-6}. Halo nuclides, having very small separation energies that are themselves input parameters for microscopic models, require a precision approaching 10^{-7}, while the stringent weak-interaction studies de-

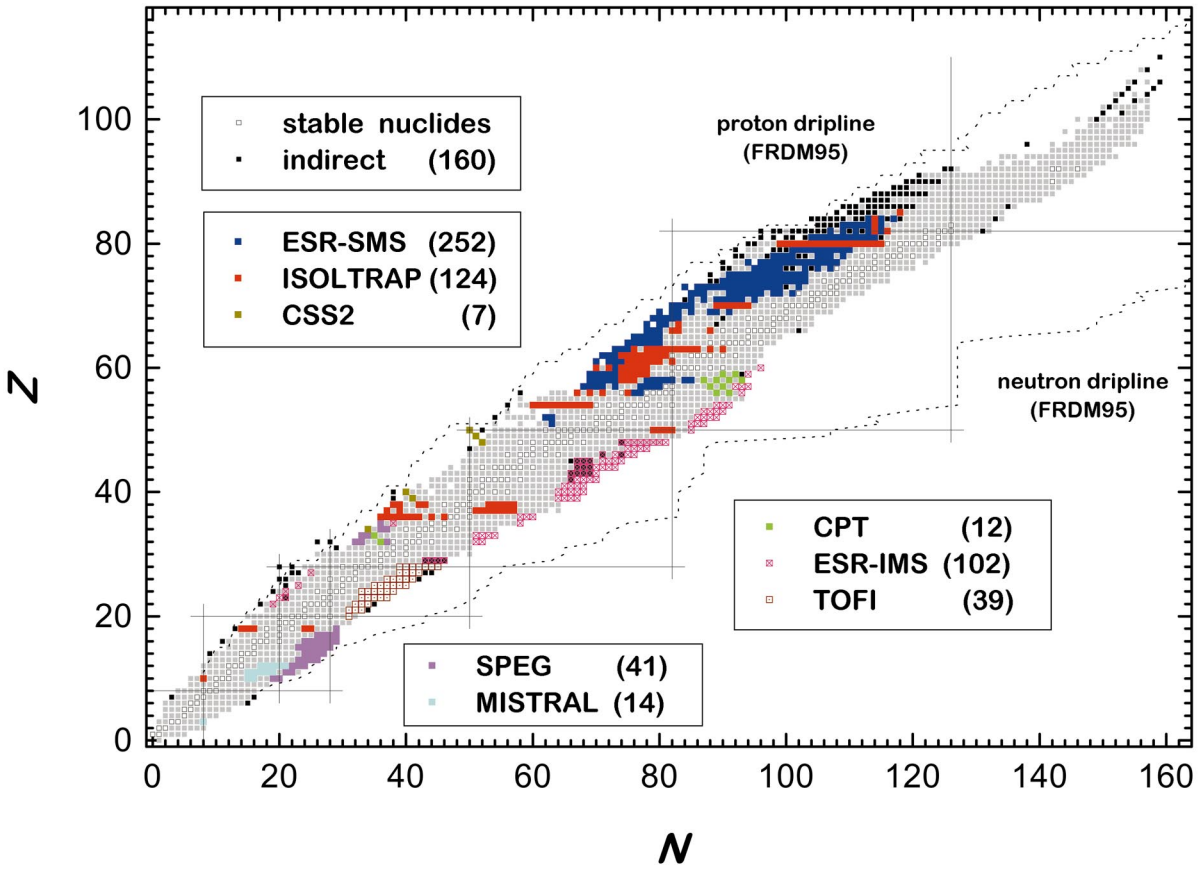

FIG. 4. (Color) Nuclear chart showing the regions where measurements have been made (since 1994) by the various dedicated mass programs using direct techniques and those determined by indirect measurements. Stable nuclides are shown as well as the drip lines calculated by the finite-range droplet model (Möller *et al.*, 1995). CPT, Canadian Penning Trap; CSS2, Separated Sector Cyclotron at GANIL; ESR-IMS, Experimental Storage Ring-Isochronous Mass Spectrometry; ESR-SMS, Experimental Storage Ring-Schottky Mass Spectrometry; ISOLTRAP, Isolde Penning trap; MISTRAL, Mass measurements at ISOLDE with a Transmission Radio frequency spectrometer on-Line; SPEG, Spectromètre à Perte d'Energie au GANIL; TOFI, Time-Of-Flight Isochronous spectrometer.

scribed above require a measurement precision of 10^{-8} or better.

Masses can be determined in a variety of ways, notably in the form of differences resulting from the Q value of a radioactive decay or nuclear reaction (Sec. II.B). While decay measurements can be quite accurate, one must be careful to have sufficient knowledge of the level scheme in order to correctly determine the ground state and feedings, and also to link this relative difference value to a known mass value, sometimes very far away and causing cumulative error. Methods that are complementary, and generally less prone to error, are based on mass spectrometry to determine masses via time-of-flight or frequency measurements. Furthermore, they generally make measurements with respect to a well-known reference mass, eliminating error accumulation. We describe the several experimental programs currently dedicated to the measurement of masses of radioactive ions by mass spectrometry in Sec. II.C. A detailed comparison is given in Sec. II.D and a look into future developments in Sec. II.E.

Since the mass of any given nucleus can be measured in many ways, a comprehensive assessment of all the currently available data is published every few years as the "Atomic Mass Evaluation" (AME), the most recent of which contains over 2200 consistently adjusted values and is available via the Internet (Audi and Wapstra, 1995). The AME is maintained not only to provide a repository for the wealth of atomic mass data but especially to attempt to reconcile often conflicting mass values determined by different techniques (see Sec. II.F).

Because of difficulties in production, a large number of nuclei far from the line of stability have still not had their masses measured and are unlikely to do so in the near future (see Fig. 4).[5] But many of these unmeasured nuclei play a vital role in the stellar synthesis of the stable nuclides, and an understanding of these processes requires a knowledge of the masses of all the nuclei involved. The problem is particularly acute in the case of the heavy, highly neutron-rich, nuclei that are involved in the r process (rapid neutron capture) of nucleosyn-

[5]Recently the drip-line nuclide ^{37}Na (as well as ^{34}Ne) was detected at RIKEN (Notani *et al.*, 2002) and GANIL (Lukyanov *et al.*, 2002)—*twenty years* after the first detection of ^{35}Na (Langevin *et al.*, 1983)!

thesis, an understanding of which may require the masses of nuclei containing 30 or so neutrons more than the heaviest measured isotope of the same element [see, for example, Meyer (1994); Wallerstein *et al.* (1997); Arnould and Takahashi (1999); Kratz *et al.* (2000); Goriely (2003)]. A similar problem also arises occasionally in connection with the synthesis of proton-rich stable nuclides through the *rp* process (rapid proton capture), although the problem is less acute than in the case of the *r* process since the available measurements extend much closer to the proton drip line than to the neutron drip line [see, for example Wallerstein *et al.* (1997); Schatz *et al.* (1998); Arnould and Takahashi (1999)]. Faced with this unenviable situation, one has no choice but to resort to a theoretical determination of the mass. We devote Sec. III to this question, surveying the various theoretical methods that are now available for this purpose. It will be seen there that the only methods that have any hope of success in all regions of the nuclear chart are those that have an essentially "semiempirical" character, in the sense that the theoretical description of the nucleus that is adopted always has a number of free parameters that are fitted to the measured masses (and maybe to other nuclear data). Thus theory is used here simply as a means of extrapolating from the mass data to the unknown nuclides (and, as discussed at the beginning of Sec. III, to the system known as infinite nuclear matter).

II. EXPERIMENTAL METHODS

Mass measurements are pursued worldwide.[6] In some cases, they are the fruit of detailed spectroscopic efforts or reaction studies (indirect techniques) but there are also various programs dedicated to the more direct determination of masses. Apart from the efforts dedicated to stable nuclides (discussed in Sec. II.E), these programs are naturally associated with radioactive-beam facilities using various production mechanisms and their specific mass separation schemes. In fact, the technique employed by a given mass measurement program is very strongly conditioned by the production-separation method, as outlined below. New experimental developments of ion cooling have had an enormous impact as well. This section will first briefly describe the various production mechanisms before giving an overview of indirect techniques, followed by a presentation of the direct techniques used at the radioactive-beam facilities with mass spectrometry programs. A detailed comparison of the various techniques will follow, as well as an overview of the projects that are under development.

[6]In this paper only a summary of the various techniques and associated programs is given (with no figures) accompanied by detailed comparisons. For up to date and detailed descriptions—all compiled into one volume—the reader is referred to the proceedings of the conference on Atomic Physics at Accelerators APAC2000 (Lunney, Audi, and Kluge, 2001).

A. Production of exotic nuclides

The study of radioactive nuclides requires their production, for which several types of nuclear reactions may be used. A large range of nuclides are produced, often including less interesting but more abundant species closer to stability. Two general techniques for separating the reaction products from the primary production projectiles are used: in-flight and on-line. Mittig *et al.* (1997) and Lepine-Szily (2001) give thorough reviews of these production and separation questions. More general discussions, accompanied by brief descriptions of the existing installations exploiting these two techniques, are given by Grunder (2002) and Nolen (2002) for North American facilities, and by Jonson (2002) and Guerreau (2002) in the case of Europe. An earlier article by Tanihata (1998) covers Asian installations. A survey of the different reactions themselves is given by Schmidt *et al.* (2002).

1. In-flight separation

When a heavy, high-energy primary beam is directed onto a thin target, the resulting primary beam fragments can be quite exotic in nature, in addition to being in excited states [see reviews by Geissel *et al.* (1995) and Morrissey (2002)]. The target must be thin enough not to destroy the fragments and to minimize the effects of straggling, which degrade the momentum and angular distribution of the fragment beam. In addition to separating the primary beam using magnetic rigidity selection and a velocity filter, for example, the produced fragments can be time-tagged and after suitable drift time at a velocity depending on the target thickness, identified by time of flight as well as standard energy-loss techniques.

Projectile fragmentation favors the production of exotic nuclides at relatively high energies (a few tens to a few hundred MeV/A) and their high velocity makes unambiguous Z selection possible. This point is important since a disadvantage of working with such beams is the charge-state distributions of different elements that can overlap. Spectrometers with large angular acceptance must be used, which limits the intrinsic accuracy with which the mass might be determined (unless there is a way of cooling the fragments in flight, such as in a storage ring, as described below).

At lower energies (a few MeV/nucleon) fusion-evaporation reactions can be used in combination with in-flight separation. These are the best reactions for producing very proton-rich nuclides. Accelerated beams of fissile elements can also be used with a thin, light target to condition the resulting distributions of exotic nuclides. Major fragmentation facilities are: in Europe, GANIL in Caen (France), GSI in Darmstadt (Germany), and JINR in Dubna (Russia); in Japan, RIKEN; in China, the Lanzhou facility; and in the USA, NSCL in East Lansing and ANL near Chicago.

2. Isotope separation on-line

The technique of isotope separation on line (ISOL), which provided the very first beams of exotic nuclides [see review by Jonson and Richter (2000)], uses a primary beam (e.g., high-energy protons or heavy ions) to produce large quantities of radioactive nuclides in a very thick target. Depending on the chemical composition of the target, nuclides are created by spallation, fragmentation, or even fission in the case of uranium or thorium carbide. Unlike in-flight separation, where the reaction products are barely slowed, here they are stopped and consequently must be coaxed out of the target by diffusion, i.e., by heating the target matrix. After the atoms have been transferred into an ionization chamber, different techniques of varying chemical selectivity can be applied to produce the ions of interest. As the target-ion source ensemble is mounted on a high-voltage platform (typically 60 keV), once ionized, the beam is accelerated, focused, and mass separated using a magnet. The great advantage of the ISOL technique is the superior beam quality, which is particularly amenable to use with precision apparatus. The high quantity of exotic species produced in the thick target is generally offset by the fact that the produced nuclides must diffuse out of the voluminous target matrix. Depending on chemical composition, this process can take a few hundred milliseconds for alkali elements, to several seconds and longer for more refractive species.

A detailed description of production and separation by the ISOL technique is given by Ravn *et al.* (1994) and by Köster (2000, 2002a), and the mother of all ISOL facilities, ISOLDE, has most recently been described by Kugler (2000) and Lindroos (2003). Other facilities (see review by Jonson, 2002) where mass measurements have been (or will be) pursued using ISOL include GSI, where fusion-evaporation reactions with heavy-ion beams are used; Jyväskylä (Finland), where heavy-ion-induced fission is used with the gas-jet, ion guide system IGISOL; Studsvik (Sweden), where the OSIRIS facility uses thermal neutrons to the same end; Japan's new KEK-JAERI joint facility, and Caen (France), where the GANIL-SPIRAL facility uses projectile fragmentation in a thick target.

B. Indirect mass measurement techniques

Often a distinction is made between so-called "indirect," i.e., reaction and decay, measurements and "direct" techniques due to the fact that the former yield mass differences. In fact, the distinction is somewhat academic, since the latter techniques all make use of a mass reference with respect to which the unknown mass is determined. Absolute measurements are impracticable due to the fact that it would be otherwise impossible to measure the magnetic-field values to anywhere near the desired precision (see Sec. II.C).

1. Reactions

Nuclear reactions are traditionally one of the most accurate mass measurement techniques, but they are of somewhat limited breadth, since the incoming and outgoing particles must be known in addition to the target mass. The kinematics of the unknown mass or the reaction Q value must be determined by a relatively precise (and well-calibrated) mass spectrometer. Two techniques are generally used: *missing mass* and *invariant mass* (see recent review by Penionzhkevich, 2001).

In the missing-mass method, a suitable reaction $A(a,b)B$ is selected in which the masses of target A, projectile a, and ejectile b are known. The mass of the unknown product B is determined by measuring the Q value. While the spectrometer used to measure the Q value will suffer from a certain limitation in resolution, the great advantage of this technique is that B need not be a bound nuclide. No direct technique is applicable in this case, since the measurement time will be too long. Recent measurements using this technique were performed on $^{13-16}$B by Kalpakchieva *et al.* (2000) at HMI (Berlin); on ^{13}Be by Belozyorov *et al.* (1998) at JINR (Dubna); and by Lu *et al.* (1998) at the Lanzhou facility. An original technique using pion reactions was also used at the Los Alamos meson facility (LAMPF) for masses of exotic nuclides. The last paper on this technique was presented at the 1995 conference on Exotic Nuclei and Atomic Masses (ENAM) by Seth (1996).

The invariant-mass method is particularly well suited for unbound nuclides and very similar to a decay measurement in that the mass of the unknown parent nuclide B is determined by detecting the kinematics of the recoiling decay product b and decay particle x. The unknown (unbound) nuclide is created from a reaction in a thin target with detectors placed at forward angles for the particles x and a large-acceptance spectrometer used to determine the momentum of b. The invariant-mass peak is reconstructed from the kinematics of x and b events recorded in coincidence. This technique suffers greatly from sensitivity limitations, since covering a large solid angle with particle detectors is difficult, and a small surface area is required in order to have sufficient position resolution. A recent result on ^{18}Na was obtained by Zerguerras (2001) using this technique at GANIL.

Neutrons offer the possibility of excellent accuracy via (n,p) or (n,α) reactions (Wagemans *et al.*, 2001) and (n,γ) decays. For example, Kessler *et al.* (1999) have determined the energy of the $^1\mathrm{H}(n,\gamma)^2\mathrm{H}$ reaction to only 0.4 eV. These reactions are especially suitable for nondestructive measurements on macroscopic samples (Paul *et al.*, 2001). (p,γ) reactions can likewise provide tremendous accuracy.

2. Decays

Radioactive decay Q values can provide relatively accurate mass differences between parent and daughter nuclides. However, in order to derive mass values, these differences must be linked to a known mass which can be sometimes quite far away, inducing cumulative error. In addition, it is often very difficult to get the complete spectroscopic information, and errors can occur if a (par-

ticularly high-lying) decay branch has not been detected. This is especially true in the case of beta decay, for which the additional determination of the detector response function, required to correctly unfold the endpoint energy, can also render such mass determinations somewhat hazardous.

A recent example is given by Barton *et al.* (2003), who prudently determined a lower limit for the mass of ^{80}Y (see Sec. II.D). Other recent mass results from beta decay have been published by Brenner *et al.* (1998) for $^{150-151}$Er, Fogelberg *et al.* (1999) around ^{132}Sn, and Brenner (2001) for ^{73}Br. Recent semiempirical results (measurements incorporating, for example, Coulomb energy corrections) have been obtained by Canchel *et al.* (2001) for ^{27}S with the LISE spectrometer using a fragmented beam at GANIL, and from the GSI ISOL facility by Mazzocchi *et al.* (2001) for ^{60}Ga and Jokinen *et al.* (2002) for ^{57}Zn. Masses determined this way can be thought of as by-products of a wealth of detailed spectroscopic information. While beta decay was, for a long time, the principal source of mass determinations, this situation has now been reversed. A precise mass value, when determined by a direct technique, can be used as a stringent constraint on the total energy window available for establishing level schemes, as requested by Oinonen *et al.* (1999) for the case of ^{61}Ga, for example. Roeckl (2001) and Roeckl *et al.* (2003) discuss the perils of deriving masses from beta-decay measurements and review the GSI ISOL results for $N \approx Z$ nuclides.

Q_α measurements are more straightforward and at the drip line, together with Q_p values, are a very powerful method for determining masses with excellent accuracy—if the subsequent decay chains can be linked to a known mass. Unlike beta particles, alpha particles do not share their energy with a neutrino, and the energy differences are direct, providing that the decay starts from and ends at the ground state (or an isomeric state with a known energy). In addition to the work at Argonne National Laboratory with the ATLAS facility along—and even beyond—the proton drip line (see Davids *et al.*, 2001), a large contribution to mass knowledge in the very heavy region comes from the GSI superheavy-element research. Alpha particles are the dominant decay mode and several chains have been identified (see Heßberger *et al.*, 2000, 2001 and Hofmann *et al.*, 2001) to which known mass values can be linked. Another rich source of alpha measurements is the gas-filled RITU separator at Jyväskylä (Kettunen *et al.*, 2001), with other contributions coming from Japan's JAERI recoil mass spectrometer (Tagaya *et al.*, 1999) and RIKEN (Mitsuoka *et al.*, 1997) facilities as well as heavy-ion radioactive-beam facilities in China at Lanzhou (Gan *et al.*, 2001) and in Russia at Dubna (Oganessian, 2001).

C. Direct mass spectrometry techniques

The closing of the Chalk River TASCC facility in 1996 deprived the nuclear structure community of the last mass program that relied on deflection-voltage measurements.[7] Now, all direct mass determination techniques, i.e., those of mass spectrometry, rely on measurements of time-of-flight or (cyclotron) frequency, which are inherently more accurate. These various techniques are correlated with the production and, notably, the separation mechanism. Generally speaking, the ISOL method allows the use of higher-precision methods, while in-flight separation is more amenable to high sensitivity. Until very recently, mass programs based on direct techniques were found at only three installations (all in Europe):[8] ISOLDE, GANIL, and GSI. At GANIL, the masses of exotic fragments are accessed naturally through the ion time of flight combined with a rigidity determination. Also starting from fragmentation, the Experimental Storage Ring at GSI is run in two different operating modes to derive the mass from the ion revolution frequency. Two experiments at ISOLDE rely on measurement of the cyclotron frequency of an ion in a homogeneous magnetic field to access the mass. One of these, the Penning trap, represents a significant breakthrough in terms of measurement accuracy. In each of the following subsections we shall briefly describe the technique, its advantages and disadvantages, and some recent results. A recent, very concise review is also given by Scheidenberger (2002).

The present European domination will be challenged very soon with new projects under construction at MSU and TRIUMF, and the Penning trap program at ANL (transferred there when TASCC was closed), which has already started to produce results (Wang *et al.*, 2002; Clark *et al.*, 2003). European presence will by no means decline, however, since two new projects at GSI as well as at Jyväskylä and Munich are also well underway. [In the meantime, the new Penning trap in Jyväskylä has produced some prelimary mass data on Zr isotopes (Äystö *et al.*, 2003).] It is very important to note that all (save one of the GSI projects) are based on Penning traps. These future mass measurement programs are discussed in Sec. II.E.

1. Mass measurement programs at GANIL: SPEG and CSS2

a. SPEG: time-of-flight combined with rigidity analysis

At GANIL, exotic nuclides are produced by bombarding a production target with an intense heavy-ion beam (10^{13} pps) at intermediate energy ($50-100$ MeV/u). The dominant mechanism at these energies is projectile fragmentation, after which the forward-directed GeV fragments are selected in flight by an α-shaped spectrometer and transported to the high-

[7]The University of Manitoba continues with such an instrument for stable nuclides, having recently published results for ^{183}W and ^{199}Hg (Barillari *et al.*, 2003).

[8]From 1985 to 1995, Los Alamos National Laboratory in the US played an important role on the mass measurement scene with the TOFI (Time-Of-Flight Isochronous) experiment. The final TOFI data set was presented at the 1998 ENAM conference (Bai *et al.*, 1998).

resolution spectrometer SPEG. The mass measurement technique using SPEG is discussed by Savajols (2001), while the spectrometer itself is described by Bianchi *et al.* (1989).

The mass is deduced from the relation

$$B\rho = \frac{\gamma m v}{q}, \tag{4}$$

where $B\rho$ is the magnetic rigidity of a particle of rest mass m, charge q, and velocity v, and γ is the Lorentz factor. This technique requires a precise determination of the magnetic rigidity and of the velocity of the ion, which is determined from a time-of-flight measurement.[9]

The time of flight, typically of the order of 1 μs, is measured using microchannel plate detectors located near the production target (start signal) and at the final focal plane of SPEG (stop signal), over an 82-m (isochronous) path. From the detector response, the time-of-flight resolution $\Delta t/t$ is about 2×10^{-4}.

The magnetic rigidity of each ion is derived from two horizontal position measurements, and a momentum resolution of 10^{-4} is commonly achieved. The identification of each ion arriving at the focal plane of SPEG is achieved by the measured flight time and the energy loss and total energy signals from a detector telescope. As the resolution of the system is not sufficient to resolve isomeric states, a 4π NaI array surrounds the telescope for the detection of γ rays.

Systematic errors due to electronics nonlinearity, beam-optics effects, and element-dependent energy loss in the detectors, are corrected with a calibration function that requires reference masses as far as possible along a given isotopic chain (Savajols, 2001). The thicker target necessary for the less exotic reference nuclides produces too much beam for the sensitive detection system required by the exotic nuclides. To avoid this problem, the production-target wheel has a narrow section of increased thickness that sends short bursts of reference ions as it turns.

The mass resolution of $2-4\times10^{-4}$ obtained from the combination of the time-of-flight and the magnetic rigidity measurement is relatively modest. However, the excellent transmission and ion-by-ion elemental identification feature of SPEG provides a sensitivity that is unsurpassed by any other technique. This allows a rough mapping of the mass surface very far from stability.

Measurements with SPEG are limited to about $A\leqslant70$ due to rigidity of the beam transport system, as explained by Chartier *et al.* (1998), who published masses of the proton-rich ^{70,71}Se nuclides. Those measurements have since been improved by more careful analysis performed after discovery of detector defects. Moreover, thanks to additional calibration masses that became available in the meantime, mass values for three additional exotic nuclides (Lima *et al.*, 2002) could be obtained. A recent campaign has provided a wealth of data around the failing $N=28$ shell closure (Sarazin *et al.*, 2000). An extension of these measurements, made possible by cleansing the fragmented beam of light particles (protons, deuterons, and alphas) using a thin foil, is under analysis and a new proposal covering the *n*-rich region up to $A\sim70$ was recently approved (Savajols, 2002).

b. Cyclotrons: a lengthened time-of-flight base

For a given time resolution, the overall resolution in time-of-flight measurements is limited by the total flight time. If this can be increased, then a corresponding gain in resolution is possible. At GANIL, a cyclotron has been used to achieve this end. The circular orbits in the cyclotron increase the flight path to over 1 km. The cyclotron uses an alternating voltage to accelerate ions of different charge-to-mass ratio $\delta(m/q)/(m/q)$ according to

$$\frac{\delta(m/q)}{(m/q)} = \delta t/t = \delta\phi/\phi, \tag{5}$$

where the accelerating frequency phase $\delta\phi/\phi$ between different ions corresponds to a time difference $\delta t/t$. This quantity is measured by inserting a radial telescope detector system and recording the ion arrival time compared to the accelerating frequency phase over the corresponding energy range.

The GANIL facility is now home to four cyclotrons, two of which may be used for mass measurements: the first, CSS1 (for separated sector), accelerates the projectile beam to a few MeV/A to bombard a production target, creating proton-rich nuclides via fusion-evaporation. It is the second, CSS2, that is used for the time-of-flight measurement. The details of this scheme were elaborated by Auger *et al.* (1994), while the first results were published by Chartier *et al.* (1996) for ^{100}Sn and Lalleman *et al.* (2001) for ^{80}Y. The so-called energy-phase plot is calibrated using a well-known reference mass that must be simultaneously accelerated within the narrow acceptance window of the cyclotron. Therein lies the difficulty with this installation, since the cyclotron providing the primary beam uses the same acceleration frequency as the one accelerating the exotic beam. This problem can be circumvented by using a cyclotron with an independent acceleration frequency, as planned for the new CIME machine at the GANIL-SPIRAL facility (Chartier *et al.*, 2001). This feature was employed by Issmer *et al.* (1998) using the SARA cyclotron in Grenoble to measure ^{80}Y (see Sec. II.D); however, a price was paid in transmission, due to a reduction in the acceleration acceptance phase.

2. Mass measurements at GSI using the Experimental Storage Ring

Circulating ions with well-defined orbits offer excellent conditions for cumulative time-of-flight detection. Mass measurements have now been performed at GSI

[9]In a similar way, the TOFI experiment at LANL produced a very large quantity of mass data using fragmented beams focused into a series of three dipoles, with the resulting isochronous trajectories used to determine the mass.

by operating the Experimental Storage Ring (ESR) in two different ion-optical modes, recording successive lap times of the ions coasting around the ring. The ions in question are produced by fragmentation of very heavy projectiles (e.g., Au and Bi) at very high energies (about 0.5 GeV/A). The fragments are sent through a fragment separator and injected into the 108.4-m-circumference ESR, the optical lattice of which is tuned to accept a certain magnetic-rigidity window.

The mean revolution frequency of an ion in a storage ring is determined by its speed divided by its orbit circumference, which in turn will depend on the ion optical conditions of the storage ring [its operating point—see Franzke *et al.* (1995), Schlitt *et al.* (1996), and Geissel *et al.* (2001) for more extended descriptions]. For mass measurements, it is desirable on the one hand to have a large range of simultaneously stored ions, but on the other hand to minimize the magnetic-field volume sampled by the ions, which will be a source of uncertainty. The relative difference in revolution frequencies $\Delta f/f$ depends on two components: the different charge to mass ratios $\Delta(m/q)/(m/q)$ and the different velocities $\Delta v/v$ according to

$$\frac{\Delta f}{f} = -\frac{1}{\gamma_T^2}\frac{\Delta(m/q)}{m/q} + \left(1 - \frac{\gamma^2}{\gamma_T^2}\right)\frac{\Delta v}{v}, \tag{6}$$

where γ is the Lorentz factor, determined from the beam velocity, and $\gamma_T^2 = [\delta(p/q)/(p/q)]/(\delta C/C)$ where (p/q) is the magnetic rigidity and C the orbit circumference. The so-called *transition point* γ_T^2 (related to another parameter called the *momentum compaction factor* $\alpha_p = 1/\gamma_T^2$), is determined by the optical setting of the ring. For the mass measurement, γ_T must be determined using known mass values. In order to render this relation velocity independent, the second term must be eliminated. Two methods have now been used to achieve this end, as described below.

a. ESR-SMS: Schottky mass spectrometry

One way of eliminating the second term in the above relation is to directly minimize the velocity dispersion, i.e., to indroduce an ion-cooling mechanism.

Ions circulating in a storage ring can be cooled by electronic active feedback [the famous technique of stochastic cooling developed by Van der Meer (1985) for the discovery of the intermediate vector boson] or by using laser excitation [originally achieved by Schröder *et al.* (1990) and more recently by Madsen *et al.* (1999)]. A third possibility is to use electrons [see short description by Danared (1995) and comprehensive review by Poth (1990)], which can also be interesting for experiments in ion-electron recombination. The ESR includes an electron cooler that merges its electron beam with the circulating ion beam at a similar velocity. A stored ion finds itself repeatedly bathed in a sea of cold electrons and, feeling the Coulomb attraction from all quarters, eventually takes up the pace. Once cooled, the ion-beam energy can in fact be controlled by that of the electron beam. Electron cooling reduces the phase space of the circulating ion beam, allowing better beam definition, very small velocity spread, and higher stored ion density. The momentum dispersion $\delta p/p$ can be decreased to $\approx 10^{-6}$ for stored-ion intensities below a few thousand. The beam temperature as a function of stored-ion density even showed a phase transition, similar to the sudden vanishing of resistance in superconductors (Steck *et al.*, 1996).

A charged particle passing near a conductor induces a detectable signal called Schottky noise (Cocher and Hofmann, 1990). A pair of parallel plates, a few centimeters from the beam axis, is used to "listen" to the circulating beam. Since the cooled beam in the ESR has a well-defined trajectory, the ions induce a well-defined signal at the harmonics of their revolution frequency. For better signal-to-noise ratio, a high harmonic is used and frequency mixed with a local oscillator before being Fourier transformed to obtain the revolution frequency.

The resolving power obtained from these Schottky signals depends on the operating point of the ring. For typical momentum compaction $\alpha_p = 0.14$ and beam energy 370 MeV/A ($\gamma = 1.4$) resolving powers up to 7.5×10^5 have been obtained (Geissel *et al.*, 2001).

When a large number of ion species is present in the ring, the masses of unknown fragments are determined according to the above equation by comparing their Schottky peak positions to those of the well-known masses.

An added advantage of the storage ring that merits comment is the fact that it is possible to monitor the Schottky signal with time and glean information on decay processes. This option was exploited in measurements of the beta-decay lifetimes as a function of charge state, with a dramatic result in the case of the cosmochronometer ^{187}Re: practically stable as an atom ($T_{1/2} = 5 \times 10^{10}$ yr), the removal of all its electrons reduces its half-life almost ten orders of magnitude to a mere 14 years—a case of bound-state beta decay (Bosch *et al.*, 1996).

As is usual in science, all good things come with a compromise, and in the case of cooling the injected fragments, it is the required duration of several seconds. This obviously limits the application of the mass measurement technique to nuclides having half-lives of this order. (Note that a stochastic precooling technique that could reduce the cooling time is available at the ESR but has not yet been used for mass measurements.)

While measurement campaigns using the ESR have not been frequent (two in 1995 and another in 1997, with the ring being dismantled and reassembled in the meantime), the amount of data produced from these runs is staggering: from 1995, 104 masses of p-rich nulides measured and a further 64 masses derived from existing links to alpha-decay sequences that reach the proton drip line. The preliminary results, validating this new technique, were first published by Radon *et al.* (1997) and the complete measurement harvest by Radon *et al.* (2000). A more detailed analysis concentrating on the physics derived from these measurements has recently appeared (Novikov *et al.*, 2002). In 1997, the same projectile and

target combination was used with improved data acquisition, and a further 89 new masses were determined with 88 more masses determined via links. Improved storage ring and electron cooler performance will contribute to a reduction of experimental uncertainties. The only source so far for this data set is the dissertation of Falch (2000); however, Geissel *et al.* (2001) give an update on these measurements, and Litvinov *et al.* (2003) will provide the details and final numbers.

b. ESR-IMS: Isochronous mass spectrometry

An alternative method of minimizing the second term in the above equation, and one that avoids the lengthy cooling procedure, is to operate the ring in isochronous mode where $\gamma_T = \gamma$ (see, for example, Trötscher *et al.*, 1992; Geissel *et al.*, 2001). While the isochronous mode offers access to very-short-lived fragments, the high-quality Schottky diagnostic system is no longer applicable. For this application, a special thin-foil detection system has been developed that registers each passage of the stored ions. The recorded time-of-flight spectrum of the different ions of various mass is analyzed using a sort of pattern recognition algorithm that seeks series of equidistant peaks which are then regrouped and assigned a mass when compared with reference ions. Typically several hundred passages can be recorded before the ion is lost. Resolving powers of over 10^5 have been obtained, and the technique has been successfully used to determine several masses including ^{68}As, $^{70-71}$Se, and ^{73}Br (Hausmann *et al.*, 2001). In a recent (2002) experiment, fission fragments were injected into the ring and several time-of-flight spectra were recorded for neutron-rich nuclides in the range $28 \leqslant Z \leqslant 80$ (Litvinov and Scheidenberger, 2002). This exciting development shows what a versatile tool the storage ring can be and is sure to have an important impact on the mass landscape (see Fig. 4).

3. The ISOLDE mass measurement program: MISTRAL and ISOLTRAP

A great advantage of ISOL-produced radioactive beams of interest for high-precision apparatus is their relatively good optical quality, as well as the fact that they are created at low energy. At ISOLDE, two experiments exploit these characteristics: the transmission spectrometer MISTRAL and the tandem Penning trap spectrometer ISOLTRAP, both of which have homogeneous magnetic fields B in which a manipulation of the ion trajectory is performed in a controlled and coherent way to determine the mass m via the cyclotron frequency $f_c = qB/2\pi m$ (Lunney and Bollen, 2000).

a. MISTRAL: radio-frequency transmission spectrometer

The radio-frequency transmission spectrometer MISTRAL works by injecting the ISOLDE beam at its full transport energy of 60 keV, after which it follows a two-turn helicoidal trajectory through a homogeneous magnetic field and is transported to a secondary electron multiplier for counting. In order to obtain the high resolution needed for precision measurements, a sinusoidal modulation of the longitudinal kinetic energy is effected using a radio-frequency signal applied to electrode structures located at the one-half and three-half turn positions inside the magnetic field. This way the ions make one complete cyclotron orbit between the two modulations. The radio-frequency voltage is applied to the common, central modulator electrode and the resulting trajectories are all isochronous. Depending on the phase of this voltage when the ions cross the gaps, the resulting longitudinal acceleration produces a larger or smaller cyclotron radius than that of the nominal trajectory. The ions are transmitted through the 0.4-mm exit slit when the net effect of the two modulations is zero. This happens when the modulation frequency is an integer-plus-one-half multiple of the cyclotron frequency

$$f_{RF} = (n + 1/2) f_c , \tag{7}$$

which means that during the second modulation the ions feel exactly the opposite of what they felt during the first. The ion signal recorded over a wide frequency scan shows consecutive transmission peaks, evenly spaced by f_c. The resolving power $R = m/\Delta m$ depends on the harmonic number n, the exit slit size w, and the amplitude of modulation of the trajectory diameter D_m (Coc *et al.*, 1988):

$$R = 2\pi n \frac{D_m}{w}. \tag{8}$$

The great advantage of this scheme is that, like the time-of-flight techniques described above, there is no half-life limitation incurred by preparation or measurement time, nor is there a need to slow the beam in any way. The great disadvantage is the limiting spectrometer acceptance—five 0.4 mm$\times$5 mm slits required to precisely define the nominal trajectory and limit the sampled magnetic-field volume to ensure measurement precision.

After its installation in 1997, MISTRAL had its first beam time at the end of that year for a (successful) proof of principle. In 1998, the first test measurements were performed on $^{23-30}$Na—some of these nuclides having particularly short half-lives (e.g., ^{28}Na with $T_{1/2} = 31$ ms). A second run on these same nuclides was performed in order to check the reproducibility. The ensemble of these measurements was published by Lunney, Audi, Doubre, *et al.* (2001) with considerable improvement in accuracy for $^{28-30}$Na. Using the plasma ion source in 1999, they measured two short-lived isotopes of Ne in addition to ^{32}Mg (Monsanglant, 2000; Lunney, Monsanglant, *et al.*, 2001). The fact that each species gives rise to a series of peaks can make it extremely difficult to unfold more than two or three isobars for which the mass peaks corresponding to different harmonic numbers may overlap. For this reason, the Mg isotopes were remeasured but using the chemically selective ISOLDE laser ion source (Köster, 2002b; Fedosseev *et al.*, 2003). With no isobaric contamination it was possible to relax the required mass resolution, and the consequent gain in transmission allowed measurements

of $^{29-33}$Mg, currently under analysis. A sucessful measurement was also performed on the short-lived superallowed beta emitter ^{74}Rb (Vieira *et al.*, 2003), and in early 2002 the very short-lived (8.6 ms) halo nuclide ^{11}Li was also measured (Lunney, Audi, *et al.*, 2003).

b. ISOLTRAP: Penning trap spectrometer

The Penning trap offers the possibility of storing an ion for long periods, essentially at rest, in a clean, unperturbed environment. Consequently, the measurements performed with Penning traps (as well as the related Paul trap) are of such high precision that the 1989 Nobel prize was awarded to the inventors of these instruments: Dehmelt (1990) and Paul (1990).

Consisting of a quadrupole electric field formed by a set of electrodes placed along the axis of a static magnetic field, the Penning trap confines ion movement in three dimensions. The magnetic field provides radial confinement whereas the electric field ensures longitudinal confinement. The static quadrupole field also defocuses in the radial plane, slightly slowing the cyclotron motion to f_+ in addition to introducing a second, very slow radial eigenmode (called magnetron motion) f_-. While slightly complicating the ion motion (by the addition of a radial mode), the use of a quadrupole field does render it more exactly controllable since for a quadrupole field $f_c = f_+ + f_-$. A detailed description of the ion dynamics in Penning traps is given by Brown and Gabrielse (1986). Other detailed works concerning Penning traps are those of Ghosh (1995), Vedel and Werth (1995), and Savard and Werth (2000) for nuclear measurements.

Penning traps have been used for mass measurements on stable species (mostly created *in situ*) by a number of groups (see Sec. II.E.1). The tandem Penning trap spectrometer ISOLTRAP at CERN's ISOLDE facility has for a long time been the only such device used for measurements of radioactive ions. Consisting of a beam-collection trap, followed by a cooling and isobaric cleaning trap, and finally the measurement trap, ISOLTRAP has now measured more than 200 masses over a broad range of the nuclear chart. A complete description of ISOLTRAP is given by Bollen *et al.* (1996), and more recent status reports by Bollen *et al.* (2001), Blaum *et al.* (2003), and Herfurth *et al.* (2003).

In order to collect ions into a Penning trap, they must be brought to rest—a very delicate procedure requiring high efficiency for weakly produced radioactive species. The good optical quality of ISOL-produced beams is more amenable to this excercise but, although produced at relatively low energy, the beam velocity is still considerable compared to that required to stay trapped. In early experiments with ISOLTRAP, a collection foil was used for stopping the fast ions, which were then reevaporated at thermal energies, effectively limiting measurement possibilities to surface-ionizable species. Now, a gas-filled linear Paul trap is used for this task. Not only is it now possible to collect ions of any species and deliver them as low-energy bunches, but also the efficiency has been greatly improved. This new system is described by Herfurth, Dilling, Kellerbauer, Bollen, *et al.* (2001) and in Sec. II.E.2.

A general difficulty with radioactive beams is isobaric contamination by less exotic, stable, or molecular ions of greatly superior abundance. This necessitated the development of an isobaric separation trap in order to isolate the ion of interest. This so-called cooler trap, of a larger and more open, cylindrical geometry, uses a buffer-gas cooling scheme that is mass dependent. Collisions with gas molecules reduce the amplitude of the trapped-ion motion except in the case of the magnetron motion, where the amplitude increases, causing a loss. Since it is possible to couple the two radial modes using an azimuthal excitation at the cyclotron frequency (Bollen *et al.*, 1996; Raimbault-Hartmann *et al.*, 1997), the magnetron motion is converted to cyclotron motion, for which cooling *reduces* the amplitude. Thus ions of a given mass are cooled and centered, enabling a true mass separation. A mass resolving power of over 10^5 (Raimbault-Hartmann *et al.*, 1997) and isobaric contamination suppression of more than 10^4 (Beck *et al.*, 2000) have been achieved.

The cooler trap delivers the ions of interest to the high-precision, hyperbolic measurement trap (Becker *et al.*, 1900). Trapped for a final time, the ions are manipulated into well-defined initial conditions before an azimuthal excitation of the cyclotron motion is again performed. After an excitation time that will determine the mass resolving power (see Sec. II.E), the ions are extracted from the trap and their time of flight is recorded as a function of excitation frequency. Ions in resonance at f_c will have greater kinetic energy, and therefore reach the detector sooner, forming a dip in the spectrum [see Bollen *et al.* (1996) for a complete explanation]. When the half-life permits, the trapped ions can be excited for several seconds, allowing a mass resolving power of more than 10^7. This feature is important in cases where certain species can be produced in isomeric states. ISOLTRAP is in fact the only mass spectrometer capable of resolving—and measuring—isomers. As with all other techniques, the mass is determined by comparing the cyclotron frequency with that of a reference ion of a well-known mass.

The following is a summary of ISOLTRAP mass measurements since 1995. Though the heated-foil technique was only applicable to surface-ionizable elements, it nonetheless permitted many early measurements on alkali elements (see Bollen *et al.*, 1996) and a relatively bountiful harvest of 44 rare-earth nuclides in the vicintity of the semi-doubly-magic ^{146}Gd, from five runs in 1995 and 1996 (Beck *et al.*, 2000). This work was the fruit of the commissioning of the cooler trap in which isobaric separation was beautifully demonstrated. The installation of a large, cylindrical Paul trap collector system was then undertaken in order to render the apparatus universal. This system allowed measurements of a long chain of Hg isotopes, as described by Schwarz, Ames, Audi, Beck, Bollen, Coster, *et al.* (2001) and

Schwarz, Ames, Audi, Beck, Bollen, Dilling, *et al.* (2001), as well as heavier isotopes of Pb, Bi, Po, and At. The effect of these results on the mass surface is remarkable since there are many links to long alpha-decay chains. The S_{2n} plots of the affected region shown before and after by Schwarz, Ames, Audi, Beck, Bollen, Dilling, *et al.* (2001) resemble something like a tumble-dried cotton shirt before and after ironing. The mid-shell Hg isotopes were particularly challenging due to the necessity of resolving the very-low-lying (50–250 keV) isomeric states, and in fact, Schwarz, Ames, Audi, Beck, Bollen, Coster, *et al.* (2001) were the first to report the actual determination of isomeric levels (for ^{187}Hg and ^{191}Hg) by mass spectrometry. Due to the limited efficiency of the cylindrical Paul trap, however, this system was subsequently replaced by the currently used linear Paul trap (Herfurth, Dilling, Kellerbauer, Bollen, *et al.*, 2001). The increase in efficiency brought about by the linear cooler buncher has made possible measurements on more exotic nuclides, particularly the very short-lived ^{33}Ar ($T_{1/2}=174$ ms) among other Ar isotopes, as reported by Herfurth, Dilling, Kellerbauer, Audi, *et al.* (2001), and ^{74}Rb ($T_{1/2}=65$ ms), reported by Herfurth *et al.* (2002) together with proton-rich Kr isotopes, notably ^{74}Kr for weak-interaction physics. ^{74}Rb is the shortest-lived nuclide ever to be held in a Penning trap. Additional measurements were made on Xe isotopes by Dilling, Audi, *et al.* (2001), on proton-rich Sr isotopes and neutron-rich Sn isotopes (including ^{132}Sn) by Sikler, Audi, *et al.* (2003), and on proton-rich Bi isotopes out to ^{189}Bi by Weber and the ISOLTRAP Collaboration (2003).

D. Comparisons of the various techniques

Summarizing the above sections, there are currently three installations at which direct mass measurements are performed on radioactive nuclides: GANIL, GSI, and ISOLDE.[10] Mass determinations using reaction and decay experiments are pursued within the framework of more general nuclear-spectroscopic studies at these and other installations. [See Wapstra and Audi (2002) for a summary of the "present knowledge."]

1. Measurement domains of the various methods

It is always difficult to make global comparisons since each technique is adapted to a particular production mode, which strongly conditions the choice of nuclides and hence the nuclear properties, e.g., half-lives, isomeric states, etc. Before giving detailed comparisons of the various methods, therefore, it is instructive to survey the regions of the nuclear chart, shown in Fig. 4, where the different established mass measurement experiments have focused their attention.

Probably the most striking point in Fig. 4 is the sheer volume of ESR measurements. In addition to the nuclides shown here, links have been fused to previously established alpha chains, allowing the extension of mass values out to the proton drip line. The recent SPEG results (and the last of TOFI[11]) are concentrated on the light, neutron-rich side. Like the ESR measurements, they offer an ensemble of results over which one can establish systematic behavior, only much further from stability. Given the production mode, these techniques produce a broad range of elements, the mass spectra being accumulated in parallel. Using the same production mode (but not necessarily the same reaction mechanism), CSS2 and ESR-IMS have smaller rigidity acceptance, producing a smaller data set, but are more optimized for nuclides of particular interest. For example, in the case of CSS2, a measurement of ^{100}Sn was achieved. With the ESR in isochronous mode, proton-rich masses of Se and Br were measured (see below) only a short time after test measurements. The recent ISOLTRAP measurements cover $A=32-203$, probably the largest range of all. Since the ISOLDE target-ion sources are generally optimized for a given chemical species, a sequence of isotopes of a particular element is usually measured, allowing for systematic studies along chains. Note that in Fig. 4, most of the Hg masses and some of the rare earths measured by ISOLTRAP were also measured by the ESR (see comparisons in Fig. 5). MISTRAL has provided some shorter chains, in the neutron-rich region of light nuclides having particularly short half-lives. Like ISOLTRAP, MISTRAL is capable of measuring the masses of any of the 64 elements produced by ISOLDE.

Finally, Fig. 4 shows that, despite the fact that masses derived from spectroscopy (i.e., indirect measurements) require additional constraints (e.g., links and assumptions on nuclear structure, as discussed above) and as such are often less accurate, they do provide us the mass data that are farthest from stability.

Given so many techniques, each with favored regions of application, it is interesting to compare cases in which the same nuclide is measured by differing techniques. This is done for several cases shown in Fig. 5. Plotted are the differences (in keV) with respect to the values with the smallest uncertainty.

Figure 5 (top) compares heavy masses measured by ESR-SMS (Radon *et al.*, 2000) to those determined by ISOLTRAP (Beck *et al.*, 2000; Bollen *et al.*, 2001; Schwarz, Ames, Audi, Beck, Bollen, Coster, *et al.*, 2001). While the ISOLTRAP uncertainties are five times smaller, the agreement is generally excellent.

Figure 5 (middle) shows values for $^{68,70-71}$Se and ^{80}Y. ^{68}Se was measured at GANIL by Lalleman *et al.* (2001) with the CSS2 cyclotron, by Lima *et al.* (2002) using SPEG, and very recently at Argonne using the Canadian

[10]As also mentioned, measurements with the Canadian Penning Trap (CPT) at Argonne have been reported, but as yet no mass values or errors have been published.

[11]The final TOFI data set (Bai *et al.*, 1998) seems to be strongly correlated with the 1994 results (Seifert *et al.*, 1994), so they are all included in the following discussions.

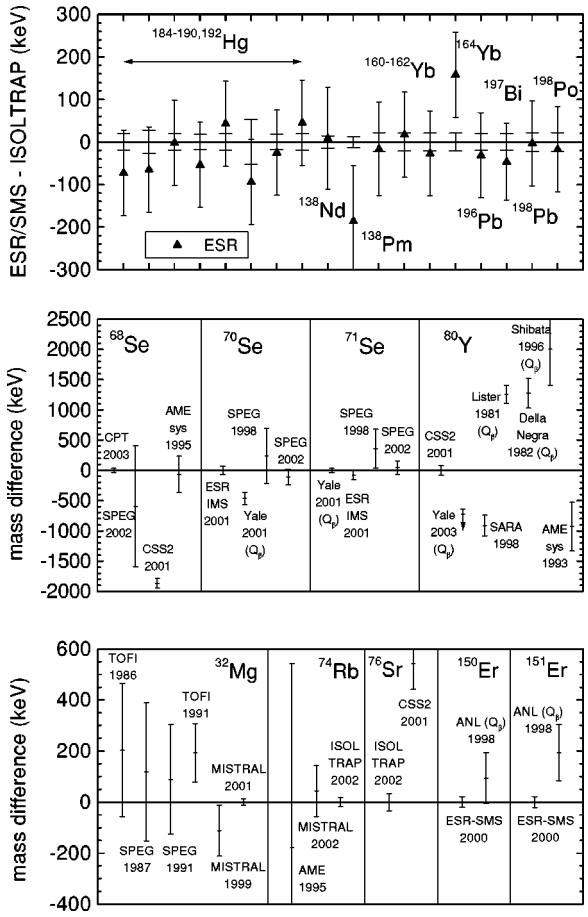

FIG. 5. Comparisons of mass data as measured by the various techniques described in this section. Plotted are the differences (in keV) with respect to the value with the smallest uncertainty. Top: chain of Hg isotopes (left) and various others (right) measured by ESR-SMS (Radon *et al.*, 2000) compared to those measured by ISOLTRAP (Beck *et al.*, 2000; Bollen *et al.*, 2001; Schwarz, Ames, Audi, Beck, Bollen, Coster, *et al.*, 2001). Middle: ^{68}Se measured by the Canadian Penning Trap (Clark, Sharma, and Savard, 2003, preliminary result) compared to that of SPEG (Lima *et al.*, 2002), CSS2 (Lalleman *et al.*, 2001), and the value derived from systematics from the 1995 evaluation (Audi and Wapstra, 1995); ^{70}Se and ^{71}Se from SPEG (Chartier *et al.*, 1998) and Q_β-derived masses (Brenner, 2001) compared to ESR-IMS (Hausmann *et al.*, 2001); a preliminary ^{80}Y mass measured by Lalleman *et al.* (2001) using CSS2 with respect to the one determined by Issmer *et al.* (1998) using the SARA cyclotron, some older Q_β results (Lister *et al.*, 1981; Della Negra *et al.*, 1982; Shibata *et al.*, 1996), and a new Q_β result from Barton *et al.* (2003) using the Yale Tandem, as well as a systematic prediction from Audi and Wapstra (1993). Bottom: ^{32}Mg recently measured by MISTRAL (Gaulard *et al.*, 2003) compared with a previous MISTRAL result (Lunney, Monsanglant, *et al.*, 2001) and older values from TOFI (Zhou *et al.*, 1991) and SPEG (Orr *et al.*, 1991a); ^{74}Rb as determined by MISTRAL (Vieira *et al.*, 2003) compared to ISOLTRAP (Herfurth *et al.*, 2002); ^{76}Sr measured by ISOLTRAP (Sikler, Audi, *et al.*, 2003) and CSS2 (Lalleman *et al.*, 2001); ^{150,151}Er measured by ESR-SMS (Falch, 2000) and by Q_β (Brenner *et al.*, 1998).

Penning Trap (Clark, Sharma, and Savard, 2003). The preliminary CPT value, in perfect agreement with SPEG and with a value from the 1995 mass evaluation derived from systematic trends (Audi and Wapstra, 1995), is almost 2 MeV away from the CSS2 result. The masses of $^{70-71}$Se measured by Hausmann *et al.* (2001) via ESR-IMS are compared to the older SPEG values from Chartier *et al.* (1998), the recent reanalysis of the same SPEG data by Lima *et al.* (2002), and the Q_β values from Brenner (2001). There is very satisfactory agreement for ^{71}Se while the Q_β mass value for ^{70}Se is slightly at odds with the direct measurement results, all of which are in agreement. It is interesting to note that the uncertainty assigned to the older SPEG measurements was conservative enough that they are completely compatible with the new ones. These masses were very recently measured by ISOLTRAP, whose superior precision should be decisive.

The right part of Fig. 5 (middle) shows the ^{80}Y mass measured by CSS2 (Lalleman *et al.*, 2001) compared with that determined by the SARA cyclotron (Issmer *et al.*, 1998) and some (older) Q_β results from Lister *et al.* (1981); Della Negra *et al.* (1982); and Shibata *et al.* (1996). While the Q_β results are all in agreement, the ensemble deviates by about 2 MeV from the SARA result, with the CSS2 value falling in between. Unlike the SARA cyclotron measurement, the CSS2 experiment did not record the total time of flight, and therefore the number of turns made by the different accelerated nuclides remains uncertain. A confirming measurement is planned with CSS2 in an attempt to resolve this difficulty. It is interesting to note that in the Atomic Mass Evaluation of both 1993 (Audi and Wapstra, 1993) and 1995 (Audi and Wapstra, 1995), the older Q_β results were replaced by a recommended mass based on systematics (see Sec. III.E). From the behavior of the S_{2n} plot in Borcea *et al.* (1993), it is easy to see why. This systematic value, also shown in the figure, is in perfect agreement with the SARA value. A very recent Q_β measurement at Yale (Barton *et al.*, 2003) has shed some light on this issue. In their measurement, Barton *et al.* (2003) paid particular attention to high-lying decay strength, some of which indeed escaped detection, explaining the large deficits of the older measurements. They very prudently placed an upper limit on their derived mass and have produced a value that would seem to vindicate the SARA measurement, as well as the analysis of Audi and Wapstra (1993, 1995) in the evaluation.

In Fig. 5 (bottom) the mass of ^{32}Mg, measured twice with compatible results by MISTRAL (Lunney, Monsanglant, *et al.*, 2001; Gaulard *et al.*, 2003), is compared with the older values of TOFI (Zhou *et al.*, 1991) and SPEG (Orr *et al.*, 1991a). Both the compatibility with SPEG and the disagreement with one data set of the TOFI results was also seen for the case of ^{30}Na (Lunney, Audi, Doubre, *et al.*, 2001). A detailed study by Monsanglant (2000) of the two data sets published by Zhou *et al.* (1991), recorded with different spectrometer settings, revealed a systematic deviation of 270 ± 70 keV

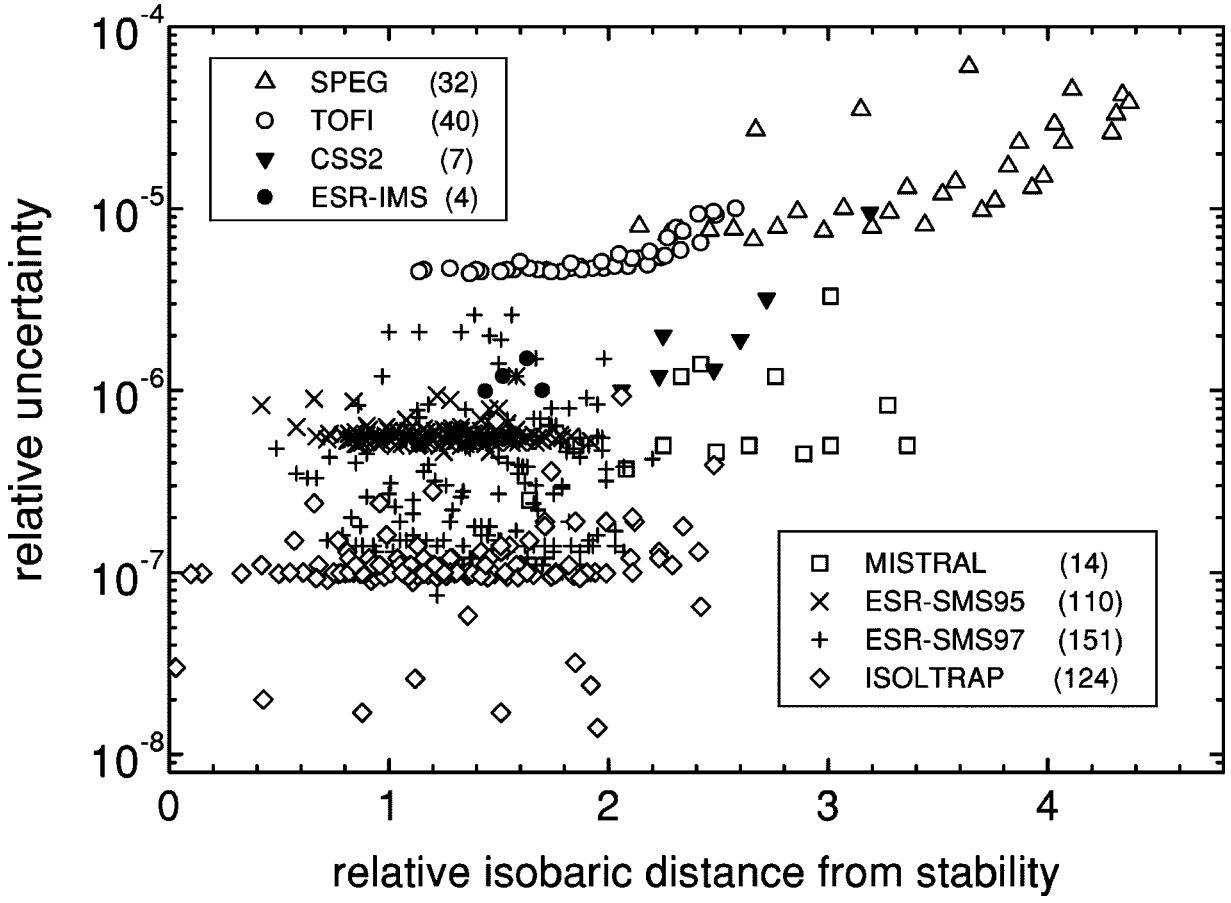

FIG. 6. The published, relative experimental uncertainties of mass measurements carried out since 1994 by the direct techniques: SPEG (Sarazin *et al.*, 2000), TOFI (Bai *et al.*, 1998; Seifert *et al.*, 1994), MISTRAL (Gaulard *et al.*, 2003; Lunney, Audi, *et al.*, 2001, Lunney, Monsanglant, *et al.*, 2001; Vieira *et al.*, 2003), CSS2 (Chartier *et al.*, 1996; Lalleman *et al.*, 2001), ESR-IMS (Hausmann *et al.*, 2001), ESR-SMS (Falch, 2000; Radon *et al.*, 2000), and ISOLTRAP (Beck *et al.*, 2000; Bollen *et al.*, 2001; Dilling, Ackermann, *et al.*, 2001; Herfurth, Dilling, Kellerbauer, Audi, *et al.*, 2001; Schwarz, Ames, Audi, Beck, Bollen, Coster, *et al.*, 2001; Herfurth *et al.*, 2002; Raimbault-Hartmann *et al.*, 2002; Blaum and the ISOLTRAP Collaboration, 2003; Sikler, Audi, *et al.*, 2003) vs "relative isobaric distance from stability," derived by fitting a quadratic function to the ensemble of stable nuclides, calculating the isobaric distance from the measured nuclide to this line, and weighting by $10/A^{2/3}$.

between the two. A possible explanation for these discrepencies might be the fact that isomers were neither detectable nor resolvable, causing a systematic bias towards higher masses coupled with a simple underestimation of error bars.

Next, the mass of ^{74}Rb as determined by ISOLTRAP (Herfurth *et al.*, 2002) is compared to MISTRAL (Vieira *et al.*, 2003), showing perfect agreement. While the results of both measurements were limited by statistics, the reliability of ISOLTRAP in the new domain of sub-100-ms measurements is very reassuring.

Figure 5 (bottom) also shows a recent ISOLTRAP measurement of ^{76}Sr by Sikler, Audi, *et al.* (2003), compared to the CSS2 value of Lalleman *et al.* (2001). The questions regarding the systematic error evaluations of the CSS2 measurements would appear to be justified, given the difference of some five standard deviations (and even more in the case of ^{68}Se).

Finally in Fig. 5 (bottom), two comparisons are made with results from ESR-SMS (Falch, 2000) and Q_β results performed at Argonne (Brenner *et al.*, 1998) for $^{150-151}$Er, showing very satisfactory agreement and showing that careful β spectroscopy *can* produce reliable mass measurements.

It is indeed an indication of the great recent progress in this field that in the various situations where masses have been measured by more than one of the techniques reviewed here, the agreement is quite satisfactory. The only disagreements come from CSS2 and the older Q_β measurements in the case of ^{80}Y, from the CSS2 ^{76}Sr and ^{68}Se values, and in some cases the older TOFI measurements.

2. Comparison of measurement uncertainties

Uncertainty is a term that is used to account for the contributions of all experimental errors. Given sufficient statistics, an instrument can be said to make precise measurements when the dispersion of repeated measurements is small. An accurate measurement, however, is not guaranteed by high precision, since the result may

still be incorrect. Measurements using differing techniques, each with their own experimental errors, are used to ensure that precise measurements can be transformed into accurate ones.

The impact of a mass measurement is gauged by two criteria: the accuracy achieved and the distance from stability. As we shall see, these two criteria have up until recently been orthogonal, from a simple statistical argument but also because a more precise measurement generally requires a longer measurement time; something not compatible with the decreasing half-lives encountered the further one goes from stability. Figure 6 is a comparison of these two criteria based on results published since the 1995 mass evaluation for the following programs: SPEG, CSS2, TOFI, ESR-SMS, ESR-IMS, ISOLTRAP, and MISTRAL. Plotted is the (published) relative mass uncertainty versus the quantity "*relative isobaric distance from stability*" derived as follows: a line of (β) stability is determined by fitting a quadratic function to the stable nuclide values of (Z,N). The isobaric distance from the measured nuclide to this line is calculated and then weighted using the function $10/A^{2/3}$ in an attempt at normalization (since the drip lines are reached sooner for light nuclides). The grouping of the data from the various experiments is striking—resulting from concentration on a certain area of the nuclear chart combined with the assignment of a dominating systematic error component. For each experiment there is a general trend of increasing error with distance from stability, due to decreasing statistics from plummeting production cross sections.

SPEG is the most capable of making the first forays into unknown territory. The price to pay for this superior sensitivity comes in obtaining only a moderate measurement uncertainty—from 5×10^{-6} for thousands of events to 5×10^{-5} for tens of events—enough, however, to permit mapping the mass landscape. The farthest point in Fig. 6 for SPEG corresponds to ^{39}Al. Recent developments in detector time resolution have been made in an effort to improve overall precision, but improving the $B\rho$ measurements will require significant work.

The CSS2 measurements (Chartier *et al.*, 1996; Lalleman *et al.*, 2001) would appear to have delivered in terms of reducing uncertainty by increasing the overall time of flight. However, as can be seen from Fig. 5, the error bars of these measurements may well be underestimated, probably due to the ambiguities concerning the total number of turns made by the various ions in the cyclotron. The farthest CSS2 point corresponds to ^{100}Sn.

The ESR-SMS measurements reach very far from stability with accuracies approaching 10^{-7}, but the cooling time necessary to make such measurements excludes nuclides with half-lives less than several seconds. While the ESR-SMS measurements from the 1995 experiment (Radon *et al.*, 2000) seem to be dominated by an uncertainty at the 5×10^{-7} level, the 1997 measurements in the same region (Falch, 2000), performed with an improved data aquisition system and ring/cooler performance, reach as little as 1.5×10^{-7} in many cases. They do scatter over a larger range, however. There is no hint of statistical error increasing with distance from stability (the farthest point corresponds to ^{144}Dy), since the many revolutions of a single stored (and cooled) ion allow the accumulation of a clear signal. [Litvinov *et al.* (2003) have since performed a more detailed analysis of these data and have achieved almost uniform uncertainty of about 2×10^{-7}.] The ESR-IMS measurements, which will allow access to very short half-lives using the isochronous ring mode (Hausmann *et al.*, 2001) have not yet resulted in the same low uncertainty. However, this technique is quite new and these first results are very promising.

Dominating the uncertainty axis are the ISOLTRAP measurements, and the conservative systematic error assignment can be clearly seen with practically all cases falling at 1×10^{-7}. Lack of statistics and isomeric contaminations were responsible for uncertainties above this value, and several recent measurements on Ne, Ar, and Kr (Herfurth *et al.*, 2002; Blaum and the ISOLTRAP Collaboration, 2003) have achieved uncertainties approaching 10^{-8}, even for exotic cases: the farthest ISOLTRAP point corresponds to ^{74}Rb and the most accurate, at 1.4×10^{-8}, to ^{34}Ar. As with all spectrometers, the major uncertainty during on-line runs continues to be the stability of the magnetic field. In the evaluation of most ISOLTRAP measurements with calibration measurements performed only every few hours, the value of $\delta m/m=1\times10^{-7}$, so plainly visible in Fig. 6, has been used as a conservative estimate for systematic error. More frequent calibrations have allowed a reduction of this contribution (Herfurth *et al.*, 2002). Coulomb interaction between ions of different masses stored simultaneously is another source of uncertainty (Bollen *et al.*, 1992). This effect is avoided by loading the trap with only one ion at a time. Electric-field imperfections, e.g., higher-order components and angle with respect to the magnetic-field axis, result in a systematic error proportional to the difference between reference and investigated ion mass. For ISOLTRAP this effect has been quantified in a beautiful campaign of systematic measurements using the ideal ion source: carbon clusters (Blaum *et al.*, 2002). As the mass unit is defined by carbon, the first advantage of using it as a reference ion is that the measurements are directly compared to the mass unit itself. The other crucial advantage is that since the molecular binding energy of the clusters is very small (less than 1 eV per carbon atom), a reference mass is available for every 12 mass units, over the entire nuclear chart. Inevitably, a frequency shift is present, but contributes only 2×10^{-10} per mass unit to the overall uncertainty.

Offering an attractive compromise between going far from stability and preserving good measurement accuracy are the MISTRAL results. The distance from stability of the nuclides measured by MISTRAL is large since the mass numbers are small. Note that ^{11}Li, for which a relative precision of 2.3×10^{-6} was obtained in a recent, preliminary measurement (Lunney, Audi, Bache-

let, *et al.*, 2003), corresponds to a distance-from-stability value of 5.56—off the scale of Fig. 6. The farthest MISTRAL point corresponds to ^{33}Mg. In fact, nuclides must be produced with about the same intensity as the most exotic cases measured by ISOLTRAP (about 1000 per second). The uncertainty of the MISTRAL results is dominated by a systematic error contribution. The Na measurements (Lunney, Audi, Doubre, *et al.*, 2001) revealed a linear deviation from known masses that is, for the moment, explained by the fact that the ions injected from the reference ion source and from ISOLDE do not see exactly the same magnetic field. It turned out that the deviation also changed with time, which caused the experiments to be very lengthy due to the necessity of often repeating the calibration process. While improvements to the beam transport system have practically eliminated the calibration time variation, efforts to eliminate the systematic deviation itself (using magnetic shim coils) have not been successful up to now. For like-mass comparisons, e.g., in the case of using isobars delivered by ISOLDE (Lunney, Monsanglant, *et al.*, 2001) an overall uncertainty of 2×10^{-7} is possible, otherwise the calibration procedure can introduce a contribution of up to 5×10^{-7}.

It is interesting to note that if we were to extrapolate back to stability, using a line following the extreme isobaric distances of SPEG, MISTRAL, and ISOLTRAP, the relative uncertainty would correspond to about 1×10^{-10}. This is, in fact, the accuracy of Penning trap measurements reported for stable nuclides (described in Sec. II.E.1).

3. Complementarity of the different measurement programs

All of the present measurement programs play an important role in the overall scheme of mass determinations. The metrological aspect of mass determinations is the primary reason. This aspect itself has two components: the high precision required for the measurement and the fact that reference masses are required, since absolute measurements are impossible (see below). Thus there is always the need for independent checks of results using different techniques. Finally, another general argument is the one of simple numbers: there are so many masses that require measurement, it is simply impossible for any one experiment to measure everything—even if all nuclides could be produced at any one installation.

The various programs are complementary not only for the differing regions of the nuclear chart where they are exploited but also for the accuracy that is possible, closely correlated with the sensitivity attained (as illustrated in Fig. 6). Techniques going the furthest from stability provide only modest precision but for more precision measurements that follow, it is always more convenient to have at least a rough idea of where to look and not to grope blindly, losing valuable measurement time. The complement is that mass values measured with greater precision (even if not as far from stability) are indispensible for calibrating the data of lesser precision.

Finally, each of the direct programs discussed in this section has its niche. SPEG plays the all-important role of pathfinder. Going the furthest from stability, the SPEG masses give us the first glimpse of what exciting phenomena might be on the exotic nuclear horizon. While the quenching of the $N=20$ shell closure has been known for many years, the newer SPEG values of Sarazin *et al.* (2000) now indicate a similar occurrence at $N=28$. Calibration of such measurements is an extremely delicate procedure, however.

The ESR-SMS technique is notable for the sizable measurement domain—with extremely good precision—making possible a very detailed mapping of a large region. This is extremely useful for drawing conclusions about nuclear structure from a systematic study (e.g., see Novikov *et al.*, 2002). No other technique is able to gather such a large harvest of data. The price to pay, however is the long time that has been required for analysis of this plethora of data. Calibration ions are interspersed but the situation is similar to SPEG in the sense that multidimensional correlations are possible (in this case there is also the question of charge state, eliminated in the SPEG analysis). Experiments are currently in progress at GSI's fragment separator facility for the production of exotic neutron-rich nuclides, which have now been injected into the ESR and measured (Litvinov and Scheidenberger, 2002). This will open up a broad physics avenue for both the ESR mass measurement programs.

The ESR-IMS program is very important for the very short-lived species placing it in direct competition with MISTRAL. For the moment at least, the IMS accuracy is inferior to that of MISTRAL; however, a great advantage can be had in the large volume of measurements. The sensitivity of the IMS approach also seems superior to that of MISTRAL. In order to reach the very-short-lived nuclides and fully exploit its measurement speed, MISTRAL will have to improve its sensitivity to the point where nuclides produced at a rate of less than 10 per second can be measured.

ISOLTRAP is simply the most accurate technique that exists. In addition to the all-important role of sprinkling accurate mass data all over the chart, thereby assuring a plentiful supply of references for the other techniques, the subfield of nuclear physics that requires the ultimate in mass accuracy—weak-interaction studies—has become the exclusive domain of the trapped-ion measurement technique.

E. The future of mass spectrometry

1. The Penning trap

Due to its wide applicability (including short-lived nuclides) and superior performance, the Penning trap is at the heart of most of the new mass measurement projects for exotic nuclides (see below) and therefore warrants some additional comment. The reader is also referred to recent reviews by Werth *et al.* (2003) for precision measurements in general and Bollen (2001) for details on "what Penning traps can provide."

The strength of the Penning trap lies not only in its long observation time, allowing very high resolving power, but also in the fact that the trapping volume is extremely small, about 1 cubic centimeter. When superconducting solenoids are used, the field homogeneity over such a small volume is of superior quality, allowing the mass to be determined with little perturbation. The use of ion cooling also ensures that the same initial conditions are established for both the radioactive and reference ions.

The resolving power in Penning trap mass spectrometry depends on the time of observation T_{obs} of the ion motion. As described by Bollen (2001), the linewidth Δf_c (FWHM) with which the cyclotron frequency of an ion with charge-to-mass ratio q/m stored in a homogeneous magnetic field can be determined is approximately given by $\Delta f_c \approx 1/T_{obs}$. For the resolving power one obtains $R=m/\Delta m=f_c/\Delta f_c \approx f_c \times T_{obs}$. Thus the resolving power can be increased by lengthening the observation time of the ions but with a limitation from the half-life. The statistical uncertainty with which the cyclotron frequency can be determined is inversely proportional both to the resolving power R and to the square root of the number of detected ions N: $(\delta m/m)_{stat} \approx R^{-1} \times N^{-1/2}$. Note that increasing the resolving power simply by increasing the cyclotron frequency is possible either with a stronger field or using higher charge states.

Stable nuclides are important for nuclear physics since they are used for calibration purposes, so the accuracy of their masses must be beyond question. The Penning trap has now been established by several groups as providing the most accurate mass values ever:[12] The University of Washington group confines single ions in a liquid-helium-cooled trap within a pressure-stabilized cryostat and recently published a mass for ^{16}O with an uncertainty of 1.6×10^{-10} (Van Dyck *et al.*, 2001). Using a similar instrument, but with a different type of detection scheme, the MIT group measures masses in pursuit of a more accurate value for the fine-structure constant, and Rainville *et al.* (2001) and Bradley *et al.* (1999) have reported masses for ^{23}Na, ^{85,87}Rb, and ^{133}Cs with uncertainties of $1-2\times10^{-10}$. Stockholm's SMILETRAP (Fritioff *et al.*, 2001a, 2002), a clone of ISOLTRAP but using highly charged ions, recently obtained a 3.2×10^{-10} uncertainty for ^{4}He (Fritioff *et al.*, 2001b) compared to 5.5×10^{-10} from a recent measurement by the Mainz Penning trap (Brunner *et al.*, 2001). The SMILETRAP group has also recently published a measurement of the ^{76}Ge–^{76}Se double-beta-decay Q value in which both nuclides were determined with an uncertainty less than 1.5×10^{-9} (Douysset *et al.*, 2001). Harvard's TRAP spectrometer (Gabrielse *et al.*, 1999) at CERN used simultaneous confinement of protons and antiprotons, cooled by a simultaneously trapped electron cloud, to compare these fundamental baryon masses for a precision test of CPT conservation at a level of 9×10^{-11}. Even though the trapped species are stable and can be observed for long periods,[13] TRAP and SMILETRAP deserve special mention since they have overcome the adverse conditions of an accelerator facility to achieve (near) record accuracy. Finally, the lowly electron has had its mass value improved, thanks to a Penning trap in Mainz—not, in fact, by a direct measurement of a lone trapped electron but one of the g factor of an electron bound to a stripped ^{12}C ion (Beier *et al.*, 2002).

Though there are developments planned to improve it, ISOLTRAP still relies on the destructive time-of-flight technique (the above instruments, with the exception of SMILETRAP and the Mainz trap, measure the different eigenfrequencies using a tuned circuit that detects the signal induced in the trap electrodes by the circulating ion). The time-of-flight technique requires the somewhat cumbersome protocol of performing an entire measurement cycle (accumulation, transfer, cooling, cleaning, transfer, excitation, extraction, detection) for each frequency point. The high resolving power that can be brought to bear in cases where isomers may be present requires not only a long excitation time but also limiting the occupation of the trap to only one ion. As all measurements are sequential—and must be interspersed with reference scans—the time required for getting one mass can be extremely long.

2. Stopping and cooling of ions using gas cells

Ion cooling is a subject that is naturally associated with trapping since isolating a particle at rest inevitably requires shedding a large amount of energy. The lower velocities of ions trapped in three dimensions make the storage-ring techniques of stochastic and electron cooling less interesting for nuclear physics, since they require longer cooling times. Buffer-gas cooling is a technique that is extremely rapid, universally applicable, and has long been used with trapped ions [for a review on trapped-ion cooling, see Itano *et al.* (1995)]. The use of buffer-gas cooling for the collection of ions into traps is relatively new (see Moore and Lunney, 1995; Lunney and Moore, 1999) and newer still is the application of gas cells for stopping high-energy beams produced from fragmentation (see Savard *et al.*, 2002).

Though the interaction of an ion beam with a reservoir of cold gas produces a thermal equilibrium, there is a side effect of diffusion, which is counteracted by having the ion-gas interaction take place inside a confining field. In the case of low-energy (ISOL) beams, the incoming beam is decelerated and injected into a radio-

[12]In a recent review, Barber and Sharma (2003) include an informative figure showing mass measurement accuracy versus time, starting with the work of Thompson and Aston, that corresponds to a progression of roughly an order of magnitude per decade.

[13]Typically measurements are made over one night, since underground trains and elevators cause too much disturbance during the day—see the comments on the work of Cornell *et al.* (1989) by Gabrielse (1990) and their reply (Cornell *et al.*, 1990).

frequency quadrupole ion guide. The moderate gas load is pumped away differentially and the cooled beam is extracted (and bunched, if necessary). In addition to the ISOLTRAP beam-buncher system mentioned above (Herfurth, Dilling, Kellerbauer, Bollen, *et al.*, 2001), a similar system has been successfully brought into operation at JYFL for laser spectroscopy studies (Nieminen *et al.*, 2001, 2002). A beam cooler for negative ions has also been tested at the HRIBF in Oak Ridge by Liu *et al.* (2002). Similar systems are under development for use at GANIL (Delahaye *et al.*, 2001) and for MISTRAL (Henry *et al.*, 2003) as well as a "second-generation" beam cooler at Michigan State University (Schwarz, Bollen, *et al.*, 2003).

In the case of high-energy fragments, higher (almost atmospheric) pressures are used where the supersonic effects of gas flow play an important role. The ions are also guided using adapted electric-field geometries before being injected into the type of Paul-trap cooler used with ISOL beams. At Louvain-la-Neuve, extensive nuclear spectroscopy studies are now possible using such a high-pressure gas cell system, combining a chemically selective laser ion source and sextupole ion guide (Kudryavtsev *et al.*, 1998, 2003). Important tests have also been achieved at ANL by Maier *et al.* (2001) and Clark, Barber, *et al.* (2003) for the CPT program, at MSU by Baumann *et al.* (2002), and at GSI by Engels *et al.* (2001).

Stopping reaction residues produced at high energies in a gas followed by efficient and clean delivery to a Penning trap in cold bunches at low and precise energy gives us, as the title from the recent paper of Savard *et al.* (2002) reads, "the best of both worlds."

3. Future mass measurement projects

There are six new proposed mass measurement projects, most of which are scheduled for data taking within the next few years. Due to the superior performance capabilities of Penning traps, all but one of these projects will employ a Penning trap in conjunction with differing production schemes, with the result that most are complementary in character. The SHIPTRAP project at GSI (Dilling, Ackermann, *et al.*, 2001; Marx *et al.*, 2001; Sikler, Ackermann, *et al.*, 2003) will be dedicated to transuranium (especially superheavy) elements and will stop the residues of fusion-evaporation reactions in a gas cell and transfer them into a Penning trap. A similar project is underway for the Munich Accelerator for Fission Fragments (MAFF) facility at the FRM-II reactor near Munich (Kester *et al.*, 2002; Habs *et al.*, 2003). MAFFTRAP (Szerypo *et al.*, 2003) will have a neutron-rich hunting ground inaccessible to all the others, save for the JYFL trap (Szerypo *et al.*, 2002; Kolhinen *et al.*, 2003) which will exploit the *chasse gardée* of the refractory neutron-rich nuclides that are the fruit of the very special IGISOL (Ion Guide Isotope Separator On-Line) production technique. The LEBIT (Low-Energy Beam Ion Trap) project, coupling a high-field Penning trap to a gas cell, is now under construction at Michigan State (Bollen, 2001; Schwarz, Baird, *et al.*, 2003). This mass-measurement program will benefit from the powerful fragmentation production mechanism and have a rich selection of measurement candidates, both proton- and neutron-rich. As such, it will complement the (fusion-evaporation) Canadian Penning Trap program. The proposed TITAN (Trapped Ions at TRIUMF for Atomic and Nuclear Physics) facility (Dilling *et al.*, 2003) may become a rival to ISOLTRAP, with the potential advantage of using highly charged ions to achieve higher resolving powers given the same statistics. A complementary project is the WITCH spectrometer (Beck *et al.*, 2003), now being installed at ISOLDE for beta-decay studies. WITCH uses a Penning trap to prepare radioactive species for measuring the energy spectrum of the recoil ions after the decay and as such, will be capable of determining beta-end-point energies. The only new project not based on a Penning trap is one under development at GSI using an electrostatic mirror trap (Wollnik and Casares, 2001) connected to a gas cell in which reaction residues separated from the fragment separator are deposited (Scheidenberger *et al.*, 2001).

This leaves the community of nuclear and astrophysicists requiring accurate mass data of nuclides very far from stability in a very good position. The current situation is excellent, and the future is chock full of new, promising projects. Theory, so dependent on such data, will benefit greatly, as Sec. III will attest.

F. Evaluation of nuclear masses

The Atomic Mass Evaluation (AME; Audi and Wapstra, 1993, 1995; Audi *et al.*, 1993) is often referred to as the "mass table," implying a simple compilation of experimental results, perhaps requiring an average here or there where more than one value might exist. This is not so! The many direct (Sec. II.C) and indirect (Sec. II.B) methods described above result in the measurement of *connections* between masses, and not absolute values. As such, the transition from a new mass measurement to a readjusted mass value is far from straightforward. The AME serves as a coordinated network that is able to check by how much or how little a new mass value may change the myriad connected masses. In cases where this poses a problem, i.e., where a conflict arises, evaluation requires a critical review and objective judgement as to whether all sources of error may have been correctly accounted for (see also Wapstra and Audi, 2002).

To illustrate the underlying complexity of the mass network, one part of the connection diagram that accompanies the atomic mass evaluation is shown in Fig. 7 [taken from Audi and Wapstra (1993), where the nuclear chart is depicted using five such panels]. The graph is plotted $N-Z$ versus A, and the Q_α (Q_β) connections appear as horizontal (vertical) lines while the isotopic chains are spread over diagonals. The nuclide ^{133}Cs is discussed here as an example. In the 1993 evaluation, information was provided by 13 measurements, based on three different techniques: (i) Q values for two reactions: $^{133}\mathrm{Cs}(n,\gamma)^{134}\mathrm{Cs}$, $^{133}\mathrm{Cs}(\gamma,n)^{132}\mathrm{Cs}$; (ii) mea-

surements by ISOLTRAP of ^{226}Ra, ^{125,127,128,129,130,131}Cs and ^{140,141,142}Ba, for which it was used as a reference; and (iii) the electron-capture Q value ^{133}Ba$(EC)^{133}$Cs. In this particular case, all measurements were in agreement, providing a mass value of 132.905 447(3) u (see Appendix A for the definition of u).

From a general point of view, values that are compatible with those derived using completely different techniques not only give confidence but, as stated in the evaluation: "...are important for turning precise values into accurate ones." This statement is an important corollary of the law of measurement: precision is necessary but not sufficient for accuracy. In the case of ^{133}Cs, two new Penning trap measurements from MIT were published by Bradley *et al.* (1999) using $C_5H_6^+$ and CO_2^+ as references. The mass value is now 132.905 451 931(27) u, much more precise than the previous one and both values are completely in agreement, meaning they are, in fact, accurate.

The starting point of the 1993 evaluation (Audi *et al.*, 1993) was a set of 5220 experimental data connecting 2417 different nuclides and including 368 identified isomeric states [see also Audi (2001) for a detailed description of the evaluation process]. Analyzing the inconsistencies and carefully checking the validity of the published data led to the rejection of 186 ($\sim$4%) doubtful links. Furthermore, about 13% of the data were superseded by much more accurate ones. After preaveraging the identical links, a set of 1447 links interconnecting 813 *primary* masses (primary links are shown as solid lines in Fig. 7) are subject to a least-squares adjustment. The influence of each datum on the primary masses is calculated by means of the *flow-of-information matrix* (Audi *et al.*, 1986). For the above ^{133}Cs example, the main contributions were 34% for the (n,γ) reaction, 22% for the (γ,n), and 13% for the ISOLTRAP ^{226}Ra measurement. The Q_{EC} value and Cs/Ba ISOLTRAP measurements each contributed only a few percent. The χ^2 distribution was then carefully checked and all values deviating by more than two standard deviations were scrutinized.

The flow-of-information matrix is a powerful tool. It provides the various influences (or weights) of a particular datum on a given mass value and, more generally, enables the evaluators to examine inconsistencies. For example, the errors of the published data comprising the AME95 are underestimated by about 17%, and the responsibility for this is shared equally between direct and indirect techniques (Audi, 2001).

In addition to these primary masses, in the 1993 evaluation, 1604 *secondary* masses were directly determined by as many single links (shown as dotted lines in Fig. 7). As can be seen in Fig. 7, some of them belong to long chains (e.g., Q_α series) and are attributed a high secondary degree (up to 13) reflecting their distance from the network of primaries. Not only ground states but isomeric states must be carefully checked. A recent example illustrating both the linking phenomenon and the isomeric problem is ^{150}Ho (see Fig. 7). This nuclide is linked to 19 others via experimental Q values including

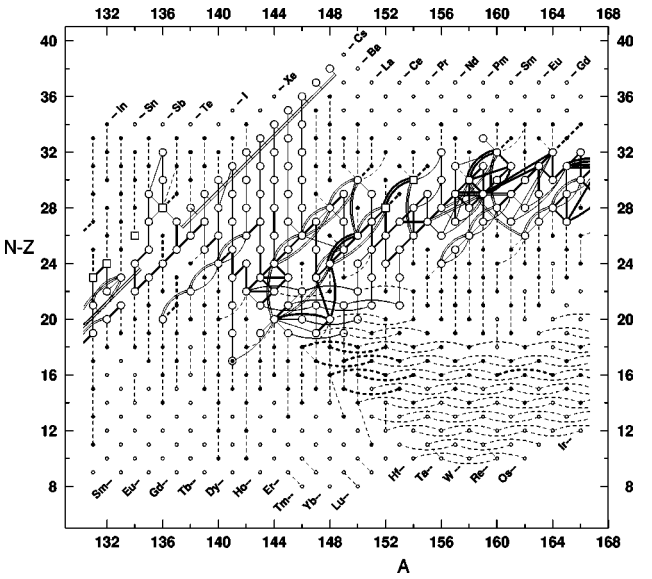

FIG. 7. Part of the multitude of reaction and decay energy input-data links between the various nuclides of the chart from the Atomic Mass Evaluation of 1993 (Audi and Wapstra, 1993).

alpha-decay chains up to ^{174}Au and ^{170}Pt. An experimental Q value for ^{150}Ho in the 1993 AME caused such a rupture of the mass surface that it was rejected in the 1995 AME, leaving no link between the decay chains and known nuclides. The problem was probably caused by an isomeric state fed by a decay sequence. ^{150}Ho was subsequently produced at the ISOLDE facility and the high resolving power of the ISOLTRAP spectrometer was brought to bear to ensure that no isomeric contamination was present (Beck *et al.*, 2000). All the previously unassigned masses could consequently be assigned. (A deviation of over 800 keV also justified the rejection of older values for ^{150}Ho.)

The unambiguous assignment of ground and isomeric states is a delicate task. In the past, isomers were evaluated by the NSDD (Nuclear Structure and Decay Data network). In 1997, a first attempt was made at integrating the data on isomers with the AME and the result was published as NUBASE (Audi *et al.*, 1997).[14]

It is important to notice that the AME deals with *atomic* masses and not *nuclear* masses. The main reason for this is that the overwhelming majority of existing data have been obtained either by indirect methods, measuring mass differences between atoms, or by mass spectrometry (including ISOLTRAP and MISTRAL), generally using singly-charged ions. Fully ionized atoms are not only difficult to produce but also difficult to preserve since they readily acquire electrons. It is only very recently that *nuclear* masses could be measured, mainly due to the use of the in-flight separation production mode [for example, by SPEG (Chartier *et al.*, 1998) or ESR (Radon *et al.*, 1997)]. A comparison of theoretical

[14]The mass values published in the 1997 NUBASE were in fact those of the 1995 AME.

masses to evaluated masses must therefore take into account the *atomic* binding energy. More details about the connection between atomic and nuclear masses, and the atomic mass unit itself, are given in Appendix A.

III. THEORY

It will be recalled from Sec. I that in this review our interest in theory is semiempirical, in the sense that we would like to use theory to determine the masses of unmeasured nuclei by extrapolating from the mass data. Most of the so-called "mass formulas" that we consider are global, i.e., their parameters are fitted to essentially all measured masses, and they are intended to be applicable to all bound nuclei. Actually, hardly any of the models we discuss can be described by simple formulas, and it would be more precise to speak of "semiempirical mass algorithms," the results usually being expressed in tabular form. We shall for the most part confine our attention to global mass formulas for which complete mass tables have been published. However, we briefly consider local mass formulas, i.e., simple algebraic formulas expressing the mass of any given unknown nuclide directly in terms of the masses of known neigboring nuclides.

Actually, in saying that semiempirical theories are used for extrapolating from the mass data out to unknown nuclei, it should be recognized that an even greater leap from the mass data is possible: extrapolation out to homogeneous or infinite nuclear matter (INM). Two forms of this can be recognized. The first is defined as the limit of an ordinary nucleus with an infinite number of nucleons, and with the Coulomb force switched off; without this latter fiction the energy per nucleon would diverge. Although this system is purely hypothetical, it is of enormous theoretical interest in that, being the simplest many-body nuclear system, it serves as a test bench for theoretical methods of deriving nuclear properties from the real two- and three-nucleon forces: the first task of nuclear many-body theory is to derive the properties of uncharged INM, as inferred semiempirically from the properties of real nuclei, from the basic forces between nucleons. The second form of INM, on the other hand, has a real existence, being found in the interior of neutron stars. It consists not only of neutrons and protons but also of electrons, the latter assuring rigorous charge neutrality, from which it follows that the problem of the divergent Coulomb energy simply does not arise. As we shall see, there is still some residual ambiguity in the inferred properties of both kinds of INM, and further mass measurements, combined with reliable semiempirical theories, can be expected to be of significance in such diverse areas as the nuclear many-body problem and the study of neutron-star interiors.

The very first attempt to account theoretically for nuclear binding energies was the 1935 "semiempirical mass formula" (*halbempirisch*) of von Weizsäcker (1935), which we describe in a slightly updated version in Sec. III.A. This formula, inspired by the liquid-drop model of the nucleus, is the macroscopic mass formula *par excellence*, but we shall see that it works remarkably well, accounting for all but a small part of the variation in the binding energy. The nearly 70 years of effort that have already been devoted to elucidating the residual effects are characterized primarily by attempts to establish the coexistence of drop-model aspects on the one hand and microscopic effects such as shell-model and pairing corrections on the other.

We have already pointed out in Sec. I how the shell model and liquid-drop model, despite being mutually exclusive at first sight, can indeed be reconciled and subsumed into a unified framework, the generalized independent-particle model. However, the most direct way of implementing this framework, the Hartree-Fock method, is computationally very demanding, and for many years the scene was dominated by the hybrid "macroscopic-microscopic" (euphonically abbreviated as "mic-mac") approach, which simply decreed that the two aspects of nuclear structure must cohabit, with microscopic corrections grafted onto the liquid-drop model. Like many arranged marriages, this worked fairly well, but some serious ambiguities arose from the decision to ignore the common origin that drop-model and shell-model aspects must have in the Hartree-Fock framework. There is thus a certain need to replace the mic-mac approach to the nuclear mass formula with a Hartree-Fock approach, although it is only with the new millenium that it has become possible to construct full-fledged Hartree-Fock mass formulas. But since the exact way in which the mic-mac approach fuses the drop-model and shell-model aspects is most easily understood as an approximation to the Hartree-Fock method, we shall violate the historical order of development and discuss this method (Sec. III.B) before describing the mic-mac approach (Sec. III.C). Some other global approaches to the mass formula are then described in Sec. III.D, while local approaches are dealt with in Sec. III.E. Finally, in Sec. III.F, we attempt to assess the outstanding problems of the currently available mass formulas, and look at promising trends to explore in the future.

Throughout this section we shall work in terms of the nuclear internal energy E rather than the binding energy $B \equiv -E$.

A. The von Weizsäcker mass formula

We take a slightly generalized form of the original expression of von Weizsäcker (1935), writing it as

$$E = a_{vol}A + a_{sf}A^{2/3} + \frac{3e^2}{5r_0}Z^2A^{-1/3} + (a_{sym}A + a_{ss}A^{2/3})I^2, \tag{9}$$

where $I=(N-Z)/A$ is the *charge-asymmetry parameter* of the given nucleus. This is the form given by Bethe and Bacher (1936), aside from the surface-symmetry term a_{ss}, which was introduced by Myers and Swiatecki (1966) [actually, the present form is slightly more general than that of Myers and Swiatecki (1966), in that we release their constraint of imposing the condition $a_{ss}/a_{sf} = -a_{sym}/a_{vol}$]. On the other hand, since we are

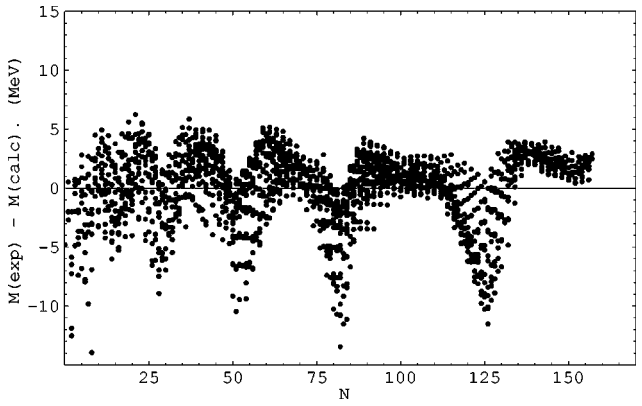

FIG. 8. Deviations from experiment of the von Weizsäcker mass formula (9), shown as a function of neutron number N.

concerned here only with the macroscopic aspects, we omit the pairing effects that von Weizsäcker took into account.

The two leading terms correspond to a spherical liquid drop, with the term a_{sf} representing a surface-tension contribution. The third term denotes the Coulomb energy of the spherical drop, assuming the charge Ze to be uniformly distributed, and with the radius given by $R=r_0A^{1/3}$, a constant value of the *charge-radius constant* r_0, implying the same density for all nuclei; this contribution must be taken into account explicitly, since the Coulomb force, being of infinite range, is not saturated. One also allows the specifically nuclear terms, both volume and surface, to depend not only on the total number of nucleons but also on the neutron-proton composition. To a good approximation this dependence can be expected to be an even function of the charge-asymmetry parameter I, since $M_n \simeq M_p$ and nuclear forces are more or less charge symmetric.

We have fitted the mass formula (9) to the 1768 *measured* nuclides with $N,Z \geqslant 8$ given in the 1995 Audi-Wapstra tables (Audi and Wapstra, 1995),[15] finding an rms error of 2.97 MeV, which is to be compared with the first column of Table I in Appendix D for all the modern mass formulas. This corresponds to a rms fractional error in the binding energy of each nucleus of only 0.4%, a remarkable result, given that nearly 2000 data points are being fitted by just five parameters. Nevertheless, the graph of the residual errors (Fig. 8) shows clearly the importance of the shell effects omitted in Eq. (9); less apparent is the neglected even-odd pairing effect. The values of the five fitted parameters are shown in the first column of Table II in Appendix D.

We see now how the von Weizsäcker formula (9) permits a trivially easy extrapolation from the mass data to the limit of uncharged infinite nuclear matter: we take the limit $A \to \infty$ and switch off the Coulomb term by setting the electron charge e equal to zero. The resulting energy per nucleon is then

$$e_\infty(\rho_0, I) = a_{vol} + a_{sym} I^2, \tag{10}$$

with the two parameters taking the values determined above from the mass fit. Actually, this refers to INM with a neutron/proton ratio given by $I=(\rho_n-\rho_p)/\rho$, where ρ_n and ρ_p refer to the neutron and proton densities, respectively, and $\rho=\rho_n+\rho_p$, the total density; the parameter a_{vol} thus represents the energy per nucleon of charge-symmetric INM. Furthermore, since the nuclei whose masses are being extrapolated are in their ground states, we must presume the corresponding INM to be at its equilibrium density $\rho_0=(3/4\pi)r_0^{-3}$; we show this quantity for convenience in the fourth line of Table II. (A more complete treatment, as, for example, in Sec. III.C, shows that the equilibrium density of INM will depend to some extent on the asymmetry parameter I.)

Thus, while they are characteristic of the liquid-drop model, the three parameters a_{vol}, a_{sym}, and ρ_0 (or r_0) of the von Weizsäcker mass formula (9) can also be interpreted in terms of INM. Now all the global mass formulas that we consider here (Secs. III.B, III.C, and III.D) can be extrapolated to INM, and in all cases the resulting energy per nucleon can be expressed in the form of Eq. (10). However, the values of the parameters will be seen to vary somewhat from one mass formula to another: it is impossible to infer the properties of INM from nuclear masses in a model-independent way. Nevertheless, the values extracted from the von Weizsäcker formula are not markedly different from those inferred from much more sophisticated models. The two remaining parameters, the *surface coefficient* a_{sf} and the *surface-symmetry coefficient* a_{ss}, can be interpreted in terms of what is referred to as semi-infinite nuclear matter. See, for example, Swiatecki (1951), Moszkowski (1970), and Farine *et al.* (1980).

B. Microscopic approaches

We are concerned above all in this subsection with the nonrelativistic Hartree-Fock approach, an approach that is microscopic in the sense that it is based on a solution of the Schrödinger equation with specified forces between all nucleons, albeit with a model wave function. However, we shall see that the forces that have to be used in such an approach are effective interactions, and not the real forces implied, for example, by nucleon-nucleon scattering. Nevertheless, it must be possible in principle to derive *ab initio* not only the binding energies of all nuclei but also all other nuclear properties as well from the basic nucleonic interactions, and it is therefore natural to ask at the outset, before adopting any model-based approaches, just how far towards a viable mass formula it is possible to go with such a "fundamentalist" approach. We can say right away that the answer is "not very far," but we shall nevertheless begin this subsection with a summary of the enormous amount of work that has already been done along these lines, simply in order to set the stage for the discussion of the more successful model-based approaches. We shall also briefly describe in this subsection the relativistic Hartree approach,

[15]Note particularly that we omit all nuclei marked with a # sign, since this indicates that the given value is based on systematics.

which is promising but has not yet been fully developed as a mass formula.

1. Realistic nucleonic interactions and the nuclear many-body problem

The "fundamentalist" approach to nuclear theory was initiated in the 1950s by Brueckner and co-workers, and since then a tremendous effort has been expended in pursuing different possible avenues. Two main types of calculation can be discerned, as follows.[16]

(a) Nonrelativistic methods. These calculations assume that the nucleus is described by a nonrelativistic Schrödinger equation,

$$H\Psi = E\Psi, \tag{11}$$

where

$$H = -\frac{\hbar^2}{2M}\sum_i \nabla_i^2 + \sum_{i>j} V_{ij} + \sum_{i>j>k} V_{ijk}. \tag{12}$$

Here V_{ij} and V_{ijk} are potentials representing the real two-nucleon (N-N) and three-nucleon (N-N-N) interactions, respectively.

The basic problem in solving Eq. (11) for more than two nucleons lies in the strong short-range repulsion of the real N-N force, which makes ordinary perturbation theory quite impractical, even if still formally possible. Diagonalizing the matrix of the exact Hamiltonian (12) in a basis of shell-model states is equally impractical on account of the prodigious dimensionality that would be required, although with an effective force in a restricted basis shell-model diagonalization serves as a promising semiempirical approach to the determination of nuclear masses (see Secs. III.D.1 and III.F). A more feasible way of solving Eq. (11) is through Brueckner-Bethe-Goldstone theory, which was originally developed for handling the highly singular forces that were in vogue during the 1950s; for reviews of the early work see Day (1967) and Bethe (1971). As a fundamental theory of nuclear binding energies this framework had only limited success for finite nuclei, and in recent years it has been used primarily for the somewhat simpler problem of INM (see, for example, Baldo *et al.*, 2000; Lejeune *et al.*, 2000; Zuo *et al.*, 2002a, 2002b). However, the early work of Kuo and Brown (Kuo and Brown, 1966, 1968; Brown and Kuo, 1967; Kuo, 1967), applying Brueckner-Bethe-Goldstone theory to finite nuclei has led to the development of realistic effective forces suitable for the shell-model diagonalizations to which we have just alluded. In the meantime the most successful *ab initio* nonrelativistic calculations of finite nuclei have been based rather on the Green's-function Monte Carlo method (Wiringa *et al.*, 2000; Pieper *et al.*, 2001), but the complexity increases rapidly with mass number A, and it seems that for the foreseeable future the limit is $A=12$ (Wiringa, 2001). [For a very recent brief review see Barrett *et al.* (2003).]

(b) Brueckner-Dirac methods. Here the nucleons are treated fully relativistically, being represented by Dirac spinors. The degrees of freedom associated with the exchange of the mesons responsible for the nucleonic interactions are taken into account explicitly; moreover, the meson parameters are fitted to the N-N scattering data and to measured meson properties (for a review see Machleidt, 1989). When fully developed this approach should be at least as reliable as the nonrelativistic methods. The present situation is that although INM seems to be correctly saturated with this method, the available finite-nucleus results are somewhat unsatisfactory (Fritz *et al.*, 1993; Navrátil *et al.*, 2001).

All these "fundamentalist" approaches are of the greatest interest, since they address what is surely the basic question of nuclear theory, namely, the understanding of the properties of complex nuclei in terms of the actual forces between nucleons, but it is quite clear that we shall have to wait many years before a viable mass formula is found in this way. Nevertheless, such calculations should in the meantime be able to serve at least as a qualitative guide in developing the more phenomenological approaches based on the shell model that we describe below. Indeed, as long ago as 1958 many-body theory had reconciled the validity of the shell model with the short-range character of nuclear forces (Gomes *et al.*, 1958), thereby underpinning these more phenomenological approaches.

2. Mean-field models with phenomenological interactions

Since the *ab initio* approaches that we have just described are quite inadequate for our present purposes, the best that can be done is to be guided by the success of the independent-particle model and assume, at least in the beginning, that all nucleons move in some single-particle field that is not necessarily spherically symmetric. We shall suppose, however, that the shape of this field is time independent, although if the field is not spherically symmetric it will of necessity rotate, simply by virtue of angular momentum conservation, giving rise thereby to rotational spectra (Mottelson, 1962). It will be seen in the following how the adoption of this picture renders both the nonrelativistic and relativistic forms of nuclear many-body theory tractable. The appearance of shell-model features in such an approach is, of course, ensured from the outset; we shall see that saturation, the most characteristic of the drop-model features, can emerge as well. Two main categories of mean-field calculations can be recognized, as follows.

(a) Nonrelativistic Hartree-Fock method. This is a variational method, with a trial wave function having the form of a Slater determinant $\Phi = \det\{\phi_i(x_i)\}$, this being a properly antisymmetrized product of single-particle wave functions $\phi_i(x_i)$. Since a model wave function of the form of Φ can never be identical to the exact wave function Ψ of Eq. (11), whatever the choice of $\phi_i(x_i)$, it

[16]We are not including here the very recent calculations (Kaiser *et al.*, 2002a, 2002b) based on chiral perturbation theory, which work directly in terms of pion exchanges between nucleons, rather than in terms of nucleonic interactions. While very promising, this method has so far been confined to INM and has yet to be applied to finite nuclei.

follows that the expectation value $\langle\Phi|H|\Phi\rangle$ will always be higher than the exact eigenenergy E of Eq. (11). We shall thus have to replace the exact Hamiltonian H by an effective Hamiltonian if the Hartree-Fock method is to give the exact energy E. Hence we write in place of Eq. (12)

$$H^{\text{eff}} = -\frac{\hbar^2}{2M}\sum_i \nabla_i^2 + \sum_{i>j} v_{ij}^{\text{eff}}, \tag{13}$$

in which v_{ij}^{eff} is some effective nuclear force that does not have to fit the N-N scattering data, and that will in fact be softer than one that does. One way in which this force can be determined, particularly appropriate to the present context of nuclear masses, is to optimize the fit of the expectation values

$$E_{HF} = \langle\Phi|H^{\text{eff}}|\Phi\rangle \equiv \int d^3\mathbf{r}\ \mathcal{E}(\mathbf{r}) \tag{14}$$

to all the measured values of E [the quantity $\mathcal{E}(\mathbf{r})$ is the energy-density functional].

For a given force the development of the method proceeds by minimizing E_{HF} with respect to arbitrary variations in the unknown single-particle functions $\phi_i(x_i)$, which are then given as eigensolutions to the so-called Hartree-Fock equation, a single-particle Schrödinger equation of the form

$$\left(-\frac{\hbar^2}{2M}\nabla^2 + U\right)\phi_i = \epsilon_i\phi_i, \tag{15}$$

where U is a single-particle field that in general is nonlocal, deformed, and spin dependent, but ultimately is determined uniquely by the effective force. However, this field depends explicitly on the single-particle functions $\phi_i(x_i)$ themselves, so that Eq. (15) must be solved reiteratively. Once self-consistent solutions $\phi_i(x_i)$ have been determined, E_{HF} can be calculated.

Provided the effective force, unlike the Coulomb force, is not of infinite range and has a short-range repulsion, INM will be saturated, i.e., have a finite density and energy per nucleon. Thus both drop-model and shell-model aspects emerge automatically and on an equal footing in this picture, so that a much more unified approach to the mass formula is offered than is possible with the hybrid mic-mac methods (Sec. III.C).

A particularly suitable form of effective force is the ten-parameter Skyrme form (Vautherin and Brink, 1972; Beiner *et al.*, 1975; Tondeur *et al.*, 1984; Brack *et al.*, 1985; Chabanat *et al.*, 1997, 1998):

$$\begin{aligned} v_{ij} = {} & t_0(1+x_0P_\sigma)\delta(\mathbf{r}_{ij}) + t_1(1+x_1P_\sigma)\frac{1}{2\hbar^2} \\ & \times\{p_{ij}^2\delta(\mathbf{r}_{ij}) + \text{H.c.}\} + t_2(1+x_2P_\sigma)\frac{1}{\hbar^2}\mathbf{p}_{ij}\cdot\delta(\mathbf{r}_{ij})\mathbf{p}_{ij} \\ & + \frac{1}{6}t_3(1+x_3P_\sigma)\rho^\gamma\delta(\mathbf{r}_{ij}) \\ & + \frac{i}{\hbar^2}W_0(\boldsymbol{\sigma_i}+\boldsymbol{\sigma_j})\cdot\mathbf{p}_{ij}\times\delta(\mathbf{r}_{ij})\mathbf{p}_{ij}, \end{aligned} \tag{16}$$

where $\mathbf{p}_{ij}$ is the momentum conjugate to $\mathbf{r}_{ij}$, and $P_\sigma = \frac{1}{2}(1+\boldsymbol{\sigma_1}\cdot\boldsymbol{\sigma_2})$ is the two-body spin-exchange operator. All terms here are formally of zero range, although the momentum dependence of the t_1 and t_2 terms simulates a finite range; the last term is a two-body spin-orbit term. The t_3 term is density dependent, ρ being the local nucleonic density: $\rho = \rho_p + \rho_n$, where ρ_p and ρ_n are the local proton and neutron densities, respectively.

With Skyrme forces the single-particle equation (15) takes the form

$$\begin{aligned} \Big\{ & -\boldsymbol{\nabla}\cdot\frac{\hbar^2}{2M_q^*(\mathbf{r})}\boldsymbol{\nabla} + U_q(\mathbf{r}) + V_q^{coul}(\mathbf{r}) \\ & - i\mathbf{W}_q(\mathbf{r})\cdot\boldsymbol{\nabla}\times\boldsymbol{\sigma}\Big\}\phi_{i,q} = \epsilon_{i,q}\phi_{i,q}, \end{aligned} \tag{17}$$

in which i labels all quantum numbers, and q denotes n (neutrons) or p (protons).[17] All the field terms are now local, essentially because one has been able to introduce position-dependent effective masses M_q^*, one for each of the two types of charge. Actually, at any point in the nucleus these two effective masses are determined entirely by the local densities, according to

$$\frac{\hbar^2}{2M_q^*} = \frac{2\rho_q}{\rho}\frac{\hbar^2}{2M_s^*} + \left(1-\frac{2\rho_q}{\rho}\right)\frac{\hbar^2}{2M_v^*}, \tag{18}$$

in which M_s^* and M_v^* are the so-called isoscalar and isovector effective masses, respectively, quantities that are determined entirely by the Skyrme-force parameters. The precise expressions for these two quantities, and for all those appearing in Eq. (17), as well as for E_{HF}, can be found in Tondeur *et al.* (2000).[18]

Most of the nuclear Hartree-Fock calculations that have been performed use Skyrme forces, although the Gogny group uses forces that are explicitly finite range (Dechargé and Gogny, 1980). While the latter may be regarded as more realistic, the essential nonlocality of the single-particle fields complicates the calculations considerably. Until very recently no Hartree-Fock effective force had been fitted to more than ten or so nuclei, all spherical (including all the known doubly-magic nuclei), presumably because of the computer-time limitations that arose in the past with deformed nuclei (see,

[17] Although Eq. (17) is generally used for both spherical and deformed nuclei, we have neglected several small terms that rigorously vanish only for spherical nuclei: see Engel *et al.* (1975). These terms originate in certain terms appearing in the energy functional, as defined in the second term of Eq. (14), so it could be said that Eq. (17) is still exact, but corresponds to a *slightly* modified energy functional rather than to the original Skyrme force (16). Whether one should take the force or the functional as the starting point is an open question, discussed in Sec. III.F.

[18] Note that in Eq. (2) of Tondeur *et al.* (2000) the kinetic-energy contribution to the energy density was unfortunately omitted. The full formalism is presented correctly by Farine *et al.* (2001).

for example, Patyk *et al.*, 1999). However, it is now possible to fit to the masses of all nuclei (Sec. III.B.4).

(b) Relativistic Hartree method. As in the Dirac-Brueckner method, nucleons are represented by Dirac spinors, and the mesons mediating the nucleonic interactions are taken into account explicitly. However, their sole effect is to generate a mean field in which the nucleons move, and since no two-body (or three-body) forces appear explicitly there are no exchange terms, so we are dealing with a Hartree, rather than a Hartree-Fock, theory. Unlike the Dirac-Brueckner method, the meson parameters are determined by fitting directly to the properties of finite nuclei, rather than to those of the N-N system. In this sense the method, also known as the relativistic mean-field (RMF) method, resembles the nonrelativistic Hartree-Fock method. A further similarity lies in the fact that here too infinite nuclear matter will be saturated, so that again both drop-model and shell-model aspects emerge automatically with equal status. However, the RMF method has the important merit of being Lorentz invariant, a feature that allows the spontaneous appearance of a spin-orbit term in the field. Thus in the event of a contradiction between this method and the nonrelativistic Hartree-Fock method, there would be good reasons for preferring the former.

So far the basic meson-parameter set of this method has not been fitted to the properties of more than ten nuclei. However, using a parameter set determined in this way, the masses (and other properties) of over a thousand nuclei have been calculated (Lalazissis *et al.*, 1999). Unfortunately, the rms error of 2.6 MeV is unacceptable for astrophysical purposes; moreover, only even-even nuclei were calculated. But even if this means that no RMF mass formula can be said to be available at the present time, Lalazissis *et al.* (1999) can still serve as a useful guide to the behavior of the spin-orbit field far from stability. It also provides an extensive bibliography to the RMF method.

3. Correlations

Even when the Slater determinant Φ satisfies the Hartree-Fock equations (15), it can never be identical to the exact nuclear wave function Ψ. Thus we must expect nuclear properties to show features that cannot be accounted for within the Hartree-Fock framework, although it will always be possible to express them in terms of a configuration mixing of Slater determinants; such irreducible deviations from the mean-field picture are referred to as correlations.

(a) Pairing of like nucleons. These are the most widespread and conspicuous correlations in nuclear ground states, involving the tendency of like nucleons in time-reversed single-particle states to couple to zero total angular momentum. Their most obvious manifestation lies in the characteristic even-odd effect in binding energies, but they also account for the spherical shape of many open-shell nuclei: a nucleus with even one nucleon outside doubly-closed shells would be deformed in the pure Hartree-Fock picture.

The simplest way to introduce pairing correlations into the Hartree-Fock framework is as follows. After each Hartree-Fock iteration, in the basis of single-particle states thereby generated, one applies the BCS method (borrowed from the theory of superconductivity) to the pairing interaction, which usually, but not invariably, is chosen to be distinct from the Hartree-Fock effective interaction: see, for example, Chap. 8 of Preston and Bhaduri (1975) or Chap. 6 of Ring and Schuck (1980). This so-called HF-BCS procedure can be cast in variational form (Vautherin, 1973), but the treatment of pairing is only approximate, in the sense that the pairing matrix elements are treated as constants and are not subjected to the variation of the single-particle functions $\phi_i(x_i)$. While acceptable for nuclei close to the stability line, this procedure leads to the presence of an unphysical neutron gas outside nuclei that are close to the neutron drip line, essentially because of the continuum of neutron single-particle states: see, for example, Dobaczewski *et al.* (1984, 1996). This problem is avoided in the Hartree-Fock-Bogolyubov (HFB) method, which is fully variational, with single-particle and pairing aspects treated simultaneously and on the same footing: see Chap. 7 of Ring and Schuck (1980) and also Mang (1975) and Goodman (1979).

(b) Wigner effect. Even when pairing between like nucleons, i.e., nn and pp pairing ($T=1$, $|T_z|=1$ in isospin language) is correctly taken into account, Hartree-Fock and other mean-field calculations systematically underbind nuclei with $N=Z$ by about 2 MeV. This problem is strikingly evident in the mass tables of Aboussir *et al.* (1995), which were based on the approximation to the Hartree-Fock method to be described in Sec. III.C.4, with nn and pp pairing included. Actually, the effect is also conspicuous in the older mic-mac approaches, and it was in this framework that Myers and Swiatecki (1966) stressed that the effect was highly localized, dying out rapidly as $|N-Z|$ increases from zero. They accordingly proposed an additional term in their mass formula with the form

$$E_W = V_W \exp(-\lambda|N-Z|/A), \tag{19}$$

in which V_W is negative and $\lambda \gg 1$.

Since Wigner's supermultiplet theory, based on SU(4) spin-isospin symmetry, gives rise to a similar sharp cusp for nuclei with $N=Z$ (Wigner, 1937; see also Van Isacker *et al.*, 1995), the term became known as the Wigner term. But the cusp of supermultiplet theory arises from repulsive terms that are proportional to $|N-Z|$, which become increasingly important as one moves away from the $N=Z$ line, in contrast to the observed, highly localized, phenomenon. Fortunately, a more direct description of the observed effect seems to be available in terms of $T=0$ neutron-proton pairing, the contribution of which rapidly vanishes as N moves away from Z (Satula *et al.*, 1997; Satula and Wyss, 1997, 2000).

This is not to say that the supermultiplet description is incorrect, but the increasing contribution that it implies away from the $N=Z$ line entails an inconvenient en-

tanglement with the mean-field contributions. Since, furthermore, SU(4) symmetry implies a fixed relation between $T=1$ and $T=0$ pairing (see, for example, Van Isacker and Juillet, 1999), it would seem to be preferable, at least for mass-formula purposes, to regard the two kinds of pairing as being independent and treat them phenomenologically, without reference to the supermultiplet description, even if this description does lie at a somewhat deeper level, embracing not only $T=1$ and $T=0$ pairing but also mean-field features. [A similar comment still holds even if the SU(4) symmetry is replaced by pseudo-SU(4) symmetry (Van Isacker *et al.*, 1999), which is more appropriate for *jj* coupling, as opposed to *LS* coupling.]

Nevertheless, $T=0$ pairing is a more complex phenomenon than $T=1,|T_z|=1$ pairing. For example, while the latter is dominated by the two nucleons coupling to a total angular momentum of $J=0$, in the former one can have $J=1,3,\ldots$. There is also the question of the competing $T=1$ neutron-proton (i.e., $T_z=0$) pairing. As a result no global mass formula constructed so far includes $T=0$ pairing explicitly, phenomenological representations like that of Eq. (19) having been judged more convenient.

We pointed out above that all the Skyrme forces presented until recently had been fitted to no more than ten or so nuclei, including all the known doubly-magic nuclei. But among these latter were the three $N=Z$ nuclei ^{16}O, ^{40}Ca, and ^{56}Ni, and since the Wigner effect was not taken into account in the fits the resulting Hartree-Fock effective interactions will be to some extent distorted.

4. The Skyrme–Hartree-Fock mass formulas

The first complete mass table to be based on the Hartree-Fock method, the HFBCS-1 mass formula, was constructed in the year 2000 by the Brussels-Montreal group (Goriely *et al.*, 2001). It was followed by two more Hartree-Fock mass formulas, HFB-1 (Samyn *et al.*, 2002) and HFB-2 (Goriely *et al.*, 2002), both constructed by the same group. In all three cases a Skyrme force of the form (16) was taken, with pairing correlations represented by a δ-function pairing force,

$$v_{pair}(\boldsymbol{r}_{ij})=V_{\pi q}\delta(\boldsymbol{r}_{ij}). \tag{20}$$

In the first mass formula, HFBCS-1, pairing was treated in the BCS approximation, but the full HFB approach was adopted in HFB-1 and HFB-2.

The following points are common to all three mass formulas (see also Tondeur *et al.*, 2000):

(i) The single-particle states were expanded in a harmonic-oscillator basis limited to $21\hbar\omega$, where $\hbar\omega=41.0A^{-1/3}$ MeV is the oscillator strength.

(ii) The pairing-strength parameter $V_{\pi q}$ was allowed to be different for neutrons and protons, and also to be slightly stronger for an odd number of nucleons ($V^{-}_{\pi q}$) than for an even number ($V^{+}_{\pi q}$), i.e., the pairing force between neutrons, for example, depends on whether N is even or odd. Without this "staggered pairing" device (Nayak and Pearson, 1995), optimizing the pairing-strength parameters to the absolute masses would have led to even-odd differences that were systematically too large. The problem presumably originated in the fact that Hartree-Fock solutions to odd-A and odd-odd nuclei do not satisfy time-reversal symmetry, so that in principle states that are time-reversal invariant should be projected out of these solutions. None of the presently available Hartree-Fock mass formulas do this, whence the need to make the pairing force slightly stronger for an odd number of nucleons. The point is further discussed by Tondeur *et al.* (2000), but note that their statement that the last odd nucleon does not perturb the field generated by the even-even core is wrong. More recently, a much more thorough examination of the question of odd nuclei has been made by Duguet *et al.* (2002a, 2002b), and it is to be hoped that the ideas developed there will be incorporated in future mass formulas.

(iii) The finite size of the proton was taken into account in calculating both the charge radius and the energy, the proton's charge being assumed to be Gaussian-distributed with an rms radius of 0.8 fm.

(iv) The Coulomb exchange energy is calculated using the Slater approximation, as in Eq. (3b) of Tondeur *et al.* (2000), for example. This leads to a slight underbinding, which amounts to about 1.5 MeV in the case of ^{208}Pb (Meyer *et al.*, 1986). This error can be partially absorbed into the parameters of the Skyrme force by the data fit, but the compensation cannot be exact, given that the latter force conserves isospin, while the Coulomb force does not. The residual error is not expected to be significant, and is certainly very much smaller than that arising from the neglect of vacuum polarization (see Sec. III.B.5).

(v) A correction was made for the spurious center-of-mass motion, using the method of Butler *et al.* (1984).

(vi) In the case of deformed nuclei the spurious rotational energy associated with the violation of angular momentum conservation that is inevitable in mean-field theories,

$$E_{rot}=\frac{\hbar^2}{2\mathcal{I}}\langle\hat{J}^2\rangle, \tag{21}$$

is subtracted from the total computed energy; here $\hat{J}^2$ represents the usual angular momentum operator, and $\mathcal{I}$ is the moment of inertia, calculated as described by Tondeur *et al.* (2000).

a. The HFBCS-1 and HFB-1 mass formulas

The first two Hartree-Fock mass formulas, HFBCS-1 and HFB-1, have the following additional features in common. (i) A Wigner correction term of the form of Eq. (19) was included. (ii) The spectrum of single-particle states entering the pairing calculation was cut

off at an energy of $+\hbar\omega$. (iii) With 16 force parameters in all, a single constraint was applied before fitting: the isoscalar and isovector effective masses were set equal, $M_s^*=M_v^*(=M^*)$, the quality of the mass fit being rather insensitive to changes of M_v^* over a wide range of values (Pearson and Goriely, 2001).

With 15 remaining degrees of freedom, an rms error of $\sigma=0.718$ MeV was found for the HFBCS-1 fit to the same data set as the one to which Eq. (9) was fitted—1768 measured masses from the 1995 AME (Audi and Wapstra, 1995); the mean error was $\bar{\epsilon}=0.102$ MeV (Table I).[19] For the force parameters corresponding to the HFBCS-1 fit, the original paper (Goriely *et al.*, 2001) should be consulted; this set is labeled MSk7.

When this same force, MSk7, was run in the HFB code under exactly the same conditions, the fit to the data became unacceptably bad. The force thus had to be refitted to the data, and it will be seen from Table I in Appendix D that the final fit is only slightly inferior to that of the HFBCS-1 mass formula, σ having risen from 0.718 to 0.740 MeV. However, with the force refitted to the data (parameter set BSk1), it was found that on extrapolating to the unknown regions of the nuclear chart lying beyond the data there was a fairly close agreement with the HFBCS-1 mass predictions. Not surprisingly the maximum deviations were found close to the neutron drip line, but they never exceed 2 MeV for $Z\leqslant 110$, or 5 MeV for superheavies up to $Z=120$. For the neutron-separation and beta-decay energies the deviation between the two formulas is usually much smaller, and we note that it is these, rather than the absolute masses, that are relevant to the *r* process. Given the inherent uncertainty that arises in extrapolating a highly phenomenological effective interaction from the data out to the region of the nuclear chart close to the neutron drip line, it seems that as far as mass formulas, and especially the *r* process, are concerned the HFBCS method serves as a good approximation to the HFB method, provided the force is refitted to the data. (The difficulties that might be expected for highly neutron-rich nuclei when pairing is treated in the BCS approximation, as discussed in Sec. III.B.3, seem to be confined to the charge radii of highly neutron-rich nuclei, being systematically a little larger for HFBCS-1 than for HFB-1.)

In saying that the HFBCS-1 and HFB-1 fits were achieved with just 15 parameters (actually, the fits to x_1 and γ were made only roughly), one must not forget that there are four parameters relating to the moment of inertia (Tondeur *et al.*, 2000). While these parameters were determined in fact from the experimental values of the moments of inertia they are masslike, in the sense that they could have been determined in the mass fits, in principle. It might thus be helpful to say that each of these two fits involved 15+4 parameters.

[19]The actual fit was made to the 1888 measured masses with $N,Z\geqslant 8$ given in the unpublished Audi-Wapstra file mass_exp.mas95, but 120 of these experimental masses, marked by a ♦ in the published tables (Audi and Wapstra, 1995), are not "recommended," being inconsistent with local systematics.

b. Impact of new data: the HFB-2 mass formula

After the above two Hartree-Fock mass formulas were constructed, an extensive preliminary version of a new AME (Audi and Wapstra, 2001) became available. This new compilation contained 2135 measured masses of nuclei with $N,Z\geqslant 8$, but since 15 of the nuclei that originally appeared in the 1995 compilation (Audi and Wapstra, 1995) had now been removed, there were actually 382 "new" nuclei, out of which 337 were located in the proton-rich region of the nuclear chart and 45 in the neutron-rich. In addition to showing the rms errors σ and the mean deviations $\bar{\epsilon}$ of the various mass formulas for the 1768 masses of the 1995 compilation, Table I also gives the corresponding errors for the new data.

Actually, the errors shown in the first six columns of Table I do not take account of the experimental errors of the mass measurements, which are specified in the AME's (Audi and Wapstra, 1995, 2001). However, as many neutron-rich new masses suffer a large experimental error, a better assessment of the validity of a given mass formula can be had from Möller's "model" standard deviation σ_{mod}, shown in column 7 for the 382 "new" nuclei; we also show the model mean error $\bar{\epsilon}_{mod}$ (see Appendix B).

In the last column of Table I in Appendix D and in Fig. 13 we show the ratio R of the model error σ_{mod} of the 382 "new" nuclei to the rms error σ for the 1995 compilation (there is negligible difference between σ and σ_{mod} for the 1768 nuclei of the 1995 compilation). It will be seen that both of the above Hartree-Fock formulas extrapolate rather badly to the new data. The problem with the two previously published formulas lies in a tendency to overbind both highly neutron-rich and highly proton-rich nuclei, particularly the $Z\simeq 82$ isotopes and $N\simeq 110$ isotones. Goriely *et al.* (2002) have shown that these problems have a twofold origin: (a) the prescription for the cutoff of the spectrum of single-particle states over which the pairing force acts; (b) the form of the Wigner term. We now discuss each of these two points, and then on that basis describe the formulation of the improved mass formula, HFB-2.

Both BCS and Bogoliubov calculations will diverge if the space of single-particle states over which a δ-function pairing force is allowed to act is not truncated. Making such a cutoff is, however, not simply a computational device but an essential part of the physics, since the pairing interaction between two nucleons is really a long-range phenomenon mediated at least in part by the exchange of surface phonons (Barranco *et al.*, 1999; Giovanardi *et al.*, 2002). To represent such an interaction by a δ-function force is thus legitimate only to the extent that all high-lying excitations are suppressed, although how exactly the truncation of the pairing space should be made will depend on the precise

nature of the real, long-range pairing force.[20] Since this is badly known one has considerable latitude in making the cutoff, and Goriely *et al.* (2002) exploited this ignorance to optimize the cutoff prescription to the mass data (more precisely, to the subset of spherical nuclei).

Now in both the HFBCS-1 and HFB-1 formulas the spectrum of single-particle states admitted to the pairing calculation was cut off at a single-particle energy of $\hbar\omega = 41.0A^{-1/3}$ MeV, which means that as one moves towards the neutron drip line the available spectrum for neutrons above the Fermi energy E_F is narrowed, while that for protons is widened; the opposite situation will prevail as one moves towards the proton drip line. An alternative, and physically more plausible, scenario is that the height of the spectrum above the Fermi energy is constant, at least for a given mass number A. Goriely *et al.* (2002) found that this latter scenario did indeed lead to an improved mass fit, the optimum cutoff height above the Fermi energy being 15 MeV for all nuclei. Actually, the same physical insight that suggests a constant cutoff height above the Fermi energy also suggests that the pairing spectrum of single-particle states should be cut off at a certain depth below the Fermi energy as well. A slight improvement was in fact found in this way, and the final cutoff prescription that was adopted in the HFB-2 mass formula was for the spectrum to be confined between $E_F \pm 15$ MeV.

As for the Wigner term, Goriely *et al.* (2002) made two modifications. First, it was found that a slight improvement resulted from replacing the exponential form of Eq. (19) with a Gaussian form. Second, a significant improvement in the mass fit could be obtained by adding a second Wigner term that was linear in $|N-Z|$ and was confined to light nuclei. The complete Wigner term that was adopted thus had the form

$$E_W = V_W \exp\left\{-\lambda\left(\frac{N-Z}{A}\right)^2\right\} + V'_W|N-Z|\exp\left\{-\left(\frac{A}{A_0}\right)^2\right\}, \tag{22}$$

in place of the form of Eq. (19). The form of this second Wigner term is characteristic of SU(4) spin-isospin symmetry, but it could simply be simulating some other physical feature that has been omitted from the model, conceivably the $T=1$ np pairing [see Satula and Wyss (2002) for a further discussion]. In any case, the optimal value of the cutoff parameter A_0 is 28, which means that the second term rapidly becomes negligible with increasing A.

Varying all 18 parameters, i.e., the 10 Skyrme parameters, 4 pairing parameters, and 4 Wigner parameters, the 2135 measured masses of the new compilation (Audi and Wapstra, 2001) were fitted with an rms error of 0.674 MeV, a significant improvement in the fits to the "new" nuclei being obtained (see Table I in Appendix D). For the 1842 masses with $A \geqslant 56$ the rms error of the HFB-2 formula falls to 0.622 MeV, with a mean error -0.006 MeV; note that only 14 parameters are involved in fitting this subset of the data.

Since the parameters of the new mass formula HFB-2 have been fitted to all of the available data it is impossible to make a direct assessment of its predictive power, or "extrapolatability," i.e., the reliability of its extrapolations. However, the reliability of the underlying model was tested by refitting the parameters to the original 1768 measured masses of the 1995 compilation (Audi and Wapstra, 1995) and then inspecting the predictions of this modified version of the mass formula HFB-2, labeled HFB-2′, for the "new" data. We see from the fourth line of Table I that the new model leads to a drastic improvement over the mass formula HFB-1, adding thereby to the credibility of HFB-2. (The total number of parameters can be expressed as $18+4$, as compared with $15+4$ in the case of HFBCS-1 and HFB-1.) (Strictly speaking, we should say that there are $19+4$ parameters in HFB-2, if we include the pairing cutoff as a free parameter.)

The differences between the predictions of the HFB-2 mass formula on the one hand and the HFBCS-1 and HFB-1 mass formulas on the other become particularly striking when expressed in terms of the shell-model gaps $\Delta(N_0)$ for the various magic neutron numbers N_0, defined in Eq. (3a). In Figs. 9(a)–9(d) we show for all three Hartree-Fock mass formulas how the gaps at $N_0 = 50$, 82, 126, and 184 vary with Z. It will be seen that while the HFB-1 neutron-shell gaps follow closely those of the HFBCS-1 mass formula, those of the HFB-2 mass formula tend to follow a more distinctive trend. While all three mass formulas agree fairly closely at the stability line (as they should), the HFB-2 neutron-shell gaps tend to become smaller and smaller relative to those of the HFBCS-1 and HFB-1 mass formulas as Z decreases, i.e., as the neutron drip line is approached. Looking at the different magic numbers in turn, we see that for all three Hartree-Fock mass formulas the $N_0 = 50$ gap is strongly quenched as the neutron drip line is approached [Fig. 9(a)], while for $N_0 = 82$ the quenching of all three Hartree-Fock gaps is weaker than in the case of $N_0 = 50$, but is stronger for HFB-2 than for the other mass formulas [Fig. 9(b)]. This trend continues at $N_0 = 126$, for which the HFB-2 gap is quite unquenched, while for the other two Hartree-Fock mass formulas the gaps are actually enhanced towards the neutron drip line [Fig. 9(c)]. Finally, at $N_0 = 184$ there is hardly any gap at all for HFB-2, while for HFBCS-1 and HFB-1 it becomes quite strong as the neutron drip line is approached [Fig. 9(d)].

Only the pairing-cutoff prescriptions that have been adopted can account for these striking differences between the HFBCS-1 and HFB-1 mass formulas on the one hand and the HFB-2 formula on the other: the two

[20]The need for a cutoff does not arise if one uses a finite-range pairing force in the BCS or Bogoliubov calculations, but it is doubtful that the usual choice of a simple static energy-independent force such as the Gogny force (Dechargé and Gogny, 1980) is much closer to the complicated underlying reality than is the "truncated δ-function" representation.

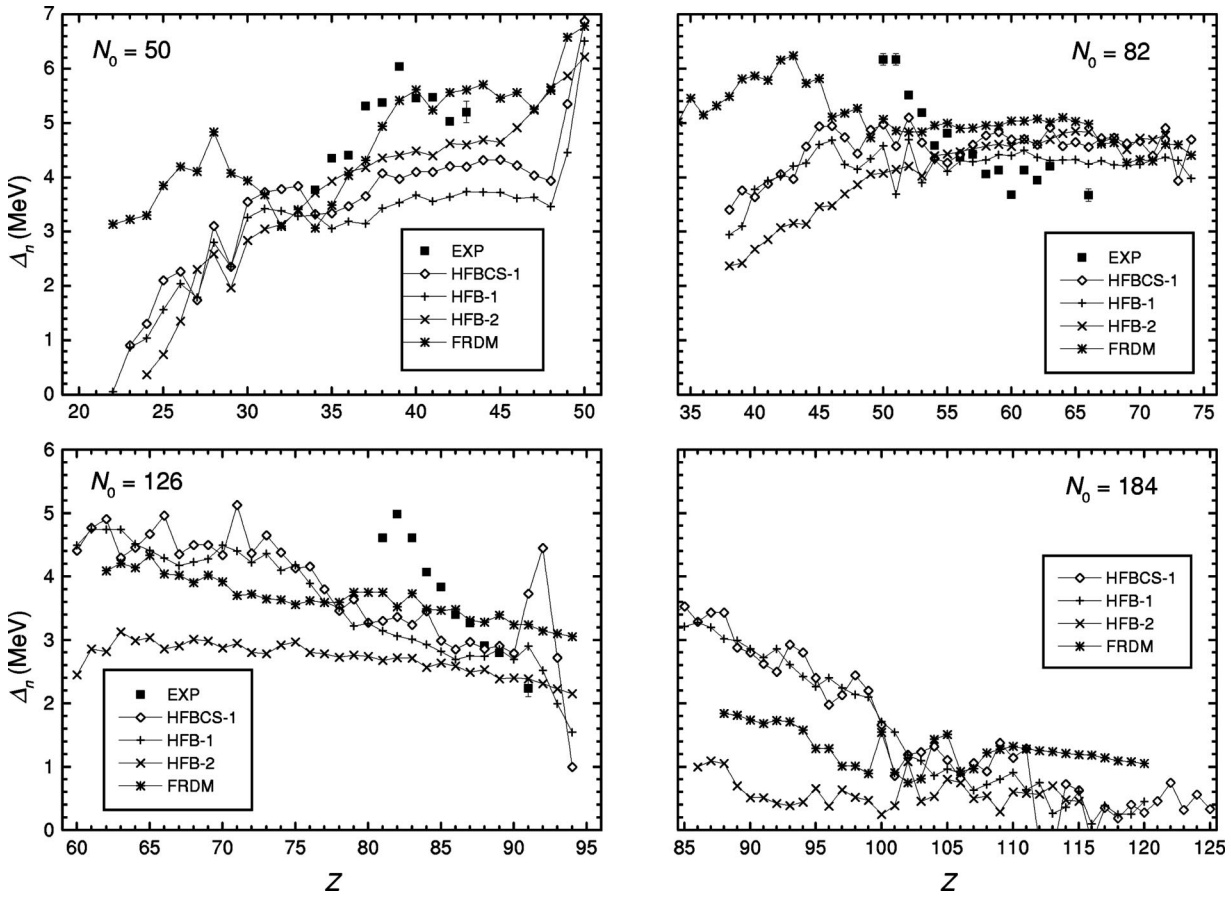

FIG. 9. Neutron-shell gaps as a function of Z for the four mass tables HFBCS-1, HFB-1, HFB-2, and FRDM for $N_0=50$, 82, 126, and 184. The experimental gaps are calculated with mass data from Audi and Wapstra (2001).

former formulas use the same prescription, while the HFB-2 formula uses a different one, and this factor seems to be more important than the replacement of the HFBCS method by the HFB method (assuming always that the force is refitted to the data).[21] To understand what happens, we first note that with the new prescription the available single-particle spectrum is narrower than before for nuclei close to the stability line, which accounts for the fact that the pairing parameters resulting from the data fit are larger. But for highly neutron-rich nuclei the single-particle spectrum entering the neutron-pairing calculation is *wider* than that with the old prescription, so that for these nuclei the neutron pairing will be strongly enhanced, with the result that the neutron-shell gaps are weakened.

The possibility of one or another of the canonical neutron magic numbers being quenched for large neutron excesses can influence the *r* process (Chen *et al.*, 1995; Pearson *et al.*, 1996; Kratz *et al.*, 2000). But the extent to which such quenching actually occurs depends, among other things, on the pairing-cutoff prescription, as we have already seen. Significantly, the prescription leading to the stronger quenching is the one favored by the new mass data (Audi and Wapstra, 2001), as far as the global fits are concerned, but the relatively small number of mass data that bear directly on the shell gaps for large neutron excesses are far less conclusive. For $N_0=50$ (as well as for $N_0=20$ and 28, as one sees in Fig. 2) there can be no doubt that quenching does indeed set in as the neutron drip line is approached, but for $N_0=82$ and 126 the available mass data do no more than suggest that this might be happening: there is a serious need in the case of these two magic numbers to push the measurements to lower Z values.

It could very well turn out that new measurements of this sort will show that the $N_0=82$ and 126 shells are not quenched, and confirm that HFB-2 has the wrong pairing-cutoff prescription. Since of all the different prescriptions that were considered it was the one adopted in HFB-2 that led to the best global mass fit, this could only mean that more sophisticated models of the pairing cutoff would have to be examined, e.g., a dependence on the neutron or proton excess. Thus besides the need for more data there is clearly a serious need for a better and more microscopic theory of pairing to serve as a guide in formulating the pairing-cutoff prescription. But regardless of future developments, one very important lesson of the HFB-2 experience must surely survive: the acqui-

[21]Allusions to "Bogolyubov-enhanced quenching," as in Pearson *et al.* (1996), for example, are thus highly misleading and were inspired by an inadequate understanding of the situation.

sition of new mass data can have implications for nuclei lying far away on the nuclear chart, much closer to the neutron drip line.

Finally, we point out that whatever defects in the three Hartree-Fock mass formulas may be revealed far from the stability line in the future, they already conspicuously fail to reproduce well established data much closer to the stability line: we are referring to the inability of these mass formulas to reproduce the sharp maxima displayed by each of the $N_0=50$, 82, and 126 shell gaps in Figs. 9(a), 9(b), and 9(c), respectively. As can be seen in Fig. 2, every neutron-shell gap, including $N_0=20$ and 28, is strongest when the corresponding proton number is magic (in the case of $N_0=50$ the maximum occurs when Z has the "semi-magic" value of 40).[22] This is the phenomenon of *mutually enhanced magicity* discussed extensively by Zeldes *et al.* (1983); we shall return to this question in Sec. III.B.5.

5. General comments on Skyrme–Hartree-Fock mass formulas

a. Macroscopic parameters

For the forces corresponding to the above three Hartree-Fock mass formulas, MSk7, BSk1, and BSk2, respectively, we show in Table II of Appendix D the values of the macroscopic parameters defined in Eq. (9). The first five parameters relate to infinite nuclear matter and are given analytically in terms of the Skyrme-force parameters (Tondeur *et al.*, 2000), while the last two relate to semi-infinite nuclear matter, and were calculated by Farine (2001). Generally speaking, the values of these parameters for the three Hartree-Fock fits are quite similar to those obtained with the drop-model fit of Eq. (9). The biggest difference is for r_0; this can be understood in part as a result of the neglect by Eq. (9) of both Coulomb exchange and the diffuseness of the charge distribution. This constant is of crucial importance in obtaining correct nuclear radii: see Sec. III.B.5.c. Because of its importance we now deal with the symmetry coefficient a_{sym} under a separate heading.

b. Symmetry coefficient

All three Skyrme–Hartree-Fock mass formulas give values of a_{sym} clustering around 28 MeV, which is somewhat higher than for the drop-model fit of Eq. (9); by way of partial compensation in fitting the same data the surface-symmetry coefficient a_{ss} is more negative for the Hartree-Fock fits than for the drop-model fit. Similar values for a_{sym} are found with the approximation to the Hartree-Fock method to be described in Sec. III.C.4, and we conclude that the value of 28 MeV is quite robust within the framework of Skyrme forces. However, the mic-mac formula of the finite-range droplet model (see Sec. III.C.3) gives a comparable fit to the same data with a value for a_{sym} in the range of 32–35 MeV. Clearly, we need some independent determination of a_{sym}. Fundamental theory is unhelpful on this point, nuclear-matter calculations based on modern realistic nucleonic interactions giving values in the range 28–30 MeV (Engvik *et al.*, 1997; Zuo *et al.*, 1999), while calculations based on chiral perturbation theory (Kaiser *et al.*, 2002a) yield 33.8 MeV.

However, a sensitive experimental determination of a_{sym} that is quite independent of mass fits is possible, in principle, through the measurement of the neutron-skin thickness of finite nuclei, $R_n^{rms}-R_p^{rms}$, where R_n^{rms} is the rms radius of the neutron distribution and R_p^{rms} that of the point proton distribution. Taking an experimental value of 0.14 ± 0.04 fm for the case of ^{208}Pb (Hoffmann *et al.*, 1980) led Tondeur *et al.* (1984) to the value of $a_{sym}=29\pm2$ MeV, which does give a slight advantage to the Skyrme value, but is hardly conclusive. Moreover, a more recent measurement (Starodubsky and Hintz, 1994) of the same quantity gave 0.20 ± 0.04 fm, which implies a somewhat higher value of a_{sym}. Both of these experiments involved nucleon-nucleus scattering and were very difficult, but a newly proposed method based on parity-violating electron-nucleus scattering is promising (Horowitz *et al.*, 2001).

In a completely different approach, a relationship between the neutron radius R_n^{rms} of finite nuclei and the radii of neutron stars has been pointed out (Brown, 2000; Horowitz and Piekarewicz, 2001a, 2001b; Typel and Brown, 2001); one can speculate that astronomical observations might shed light on the value of a_{sym}. Another property of neutron stars that is related to a_{sym} is their rate of neutrino cooling (Lattimer *et al.*, 1991, 1994; Yakovlev *et al.*, 2001). In Appendix C, we discuss the possibility that the minimum possible mass of a neutron star depends strongly on a_{sym}.

In any case, all these different ways of determining R_n^{rms} and a_{sym} have the potential to rule out a Skyrme-force representation on nuclear masses (without necessarily ruling in any other); the implications of such a finding for mass formulas are discussed in Section III.F.

c. Charge radii

Performing a Hartree-Fock calculation on a nucleus automatically yields a unique value for the rms charge radius, so that a comparison with the measured values provides an independent test of the validity of the model. For the 523 nuclei listed in the 1994 data compilation (Nadjakov *et al.*, 1994) the rms error for the three Hartree-Fock mass formulas is 0.024, 0.025, and 0.028 fm, respectively (for further details see Buchinger *et al.*, 2001). It should be stressed that this good agreement was achieved without any further parameter adjustment; r_0 is particularly important in this respect.

d. Incompressibility of nuclear matter

The incompressibility K_{vol} of symmetric infinite nuclear matter for each of the forces of the three

[22]Note that, in the cases of $N_0=20$ and 28, a large part of the enhancement at $Z=20$ and 28, respectively, probably comes from the Wigner effect. However, the weaker peak of the $N_0=28$ gap at $Z=20$ will be remarked.

Hartree-Fock mass formulas is shown in Table II. All three forces are in excellent agreement with the experimental value extracted from breathing-mode measurements (Youngblood *et al.*, 1999, 2002; Lui *et al.*, 2001), 225–240 MeV. However, this agreement may be somewhat fortuitous, since it has been shown (Farine *et al.*, 1997) that with a suitable generalization of the Skyrme force it is possible to change K_{vol}, along with the breathing-mode energies, while maintaining the mass fit (at least to a restricted set of mass data).

e. Effective masses

Table III in Appendix D shows the values (at the equilibrium density ρ_0 of symmetric nuclear matter) of the isoscalar and isovector effective masses, M_s^* and M_v^*, respectively, for the forces MSk7, BSk1, and BSk2. In each of the three cases we see that $M_s^*/M \simeq 1.0$, which is precisely the condition on conventional Skyrme forces that must be satisfied for the density of single-particle states in the vicinity of the Fermi surface to be correct (Barranco and Treiner, 1981),[23,24]

It may indeed appear plausible that to obtain good nuclear masses, especially for open-shell nuclei, a necessary condition is that one have the correct density of single-particle states near the Fermi surface, whence the condition $M_s^*/M \simeq 1.0$ [for forces of the form of Eq. (16)]. We shall return to this question below, but first we note that all INM calculations of M_s^*/M with realistic forces indicate a value of 0.6–0.9 at the density ρ_0 (Brueckner and Gammel, 1958; Friedman and Pandharipande, 1981; Wiringa *et al.*, 1988; Zuo *et al.*, 1999). This significantly lower range of values for M_s^*/M is also confirmed experimentally, both through the spacing of the deepest single-particle states in light nuclei (these states have not been measured in heavier nuclei; Mahaux *et al.*, 1985) and through measurements of the giant isoscalar quadrupole resonance (Bohigas *et al.*, 1979). However, there is no contradiction between these two sets of values of M_s^*/M, since Bertsch and Kuo (1968) and Bernard and Van Giai (1980) have shown that one can obtain reasonable single-particle level densities in finite nuclei with the INM values of M_s^*/M, i.e., of 0.6–0.9, provided one takes into account the coupling between single-particle excitation modes and surface-vibration random-phase approximation modes. Since the good agreement with measured single-particle level densities found by Barranco and Treiner (1981) was obtained without making these corrections, it must be supposed that the resulting error is being compensated by the higher value of M_s^*/M, i.e., $M_s^*/M \simeq 1.0$, which may thus be regarded as a phenomenological value that permits considerable success with straightforward Hartree-Fock, or other mean-field calculations, without any of the complications of Bertsch and Kuo (1968) and Bernard and Van Giai (1980).

All published Skyrme forces such as those of the Lyon group (Chabanat *et al.*, 1997, 1998) with M_s^*/M in the range 0.7–0.9 give a poor agreement with the mass data in the case of open-shell nuclei; see, for example, Figs. 1–4 of Chabanat *et al.* (1998). The Skyrme force MSk5* (Farine *et al.*, 2001), with $M_s^*/M = 0.8$, likewise conforms to the above conjecture that a good mass fit requires $M_s^*/M \simeq 1.0$, since the rms error for the masses of the 416 spherical nuclei to which it was fitted is an unacceptably high 1.141 MeV. Nevertheless, unpublished work of S. Goriely shows that mass fits almost as good as that of the HFB-2 mass formula (Goriely *et al.*, 2002) are possible with $M_s^*/M = 0.8$, provided the pairing cutoff is adjusted appropriately, an rms error of 0.686 MeV having been obtained for the complete data set of 2135 masses. We stress that in this new mass fit the Fermi levels and the immediately adjacent single-particle levels are in good agreement with experiment, but elsewhere the single-particle spectrum is too widely spaced, as expected. This latest calculation thus shows that the coupling between the mass fit and the fit to single-particle levels can be broken by exploiting the degree of freedom associated with the pairing cutoff.

As for the isovector effective mass M_v^*, this was constrained in forces MSk7 and BSk1 to be equal to M_s^*, but, with this constraint being released, it falls to $0.86M$ in the case of force BSk2. Although the quality of the mass fit is rather insensitive to small changes in M_v^* (Pearson and Goriely, 2001), this result agrees remarkably well with the value of 0.83 inferred from the INM calculations of Zuo *et al.* (1999) with modern realistic nucleonic interactions (see especially their Fig. 9). In principle, one can measure M_v^*/M directly from the integrated cross section for electric dipole photoabsorption, since M/M_v^* is the factor by which the Thomas-Reiche-Kuhn sum rule is enhanced. The analysis of Berman and Fultz (1975) leads to $M_v^*/M = 0.83 \pm 0.08$, while other measurements (Leprêtre *et al.*, 1976) are consistent with the lower limit of 0.75. Successful calculations of the position of the giant dipole resonance (Myers *et al.*, 1977; Krivine *et al.*, 1980) were performed with $M_v^*/M = 0.7$, but equally good results have been obtained with $M_v^*/M = 1.05$ (Goriely and Khan, 2002). The point is that the position of the giant dipole resonance does not determine M_v^*/M uniquely, and statements to the contrary (Farine *et al.*, 2001; Tondeur *et al.*, 2000) are wrong.

f. Stability of infinite nuclear matter

Table III also shows the Landau G_0 and G_0' parameters of the three Hartree-Fock forces, as defined by Van Giai and Sagawa (1981). All three forces satisfy the condition that these parameters must be larger than -1 in order to ensure the stability of symmetric nuclear matter against spin and spin-isospin flips, respectively

[23]This condition can be relaxed for Skyrme forces of a more general form than that of Eq. (16): see Farine *et al.* (2001); Onsi and Pearson (2002).

[24]Note that the density of single-particle states in nuclei not very far from the stability line is determined largely by M_s^*/M: see Eq. (18).

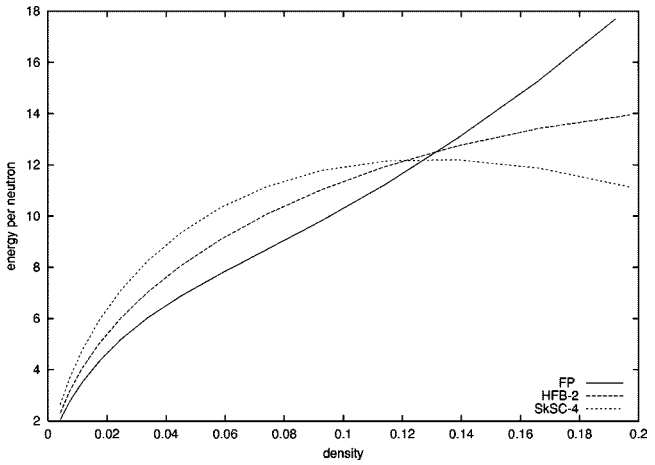

FIG. 10. Energy per neutron (MeV) of neutron matter as a function of density (neutrons/fm^3): FP, the calculations of Friedman and Pandharipande (1981); HFB-2, the force BSk2; SkSC4, the force of ETFSI-1.

(Bäckman *et al.*, 1975). However, the overall agreement with the actual experimental values of around 0 and 1.80 for G_0 and G_0', respectively (Borzov *et al.*, 1984), is less than satisfactory; attempts to improve the agreement inevitably have an adverse effect on the mass fit.

Given the relevance of mass formulas to the *r* process, there is an obvious interest, in the case of those based on the Hartree-Fock method, for the effective interactions to be compatible with the known astrophysical constraints associated with the highly neutron-rich environment in which this process occurs. Following Rayet *et al.* (1982), we consider the extent to which the foregoing effective forces conform to the known properties of neutron matter, i.e., purely neutronic infinite nuclear matter. Of course, it is much more difficult to infer the properties of this system from those of real nuclei than it is those of charge-symmetric INM, but one property can be asserted with certainty: the existence of neutron stars tells us that neutron matter must be stable. Beyond that, the calculations on neutron matter performed with realistic nucleonic forces by Friedman and Pandharipande (1981) should serve as a reliable guide, the solid curve labeled FP in Fig. 10 shows the energy per neutron given by these calculations as a function of the density. More recent calculations of neutron matter (Cugnon *et al.*, 1987; Wiringa *et al.*, 1988; Akmal *et al.*, 1998) give very similar results, at least up to the equilibrium density ρ_0 of symmetric INM, beyond which Skyrme forces are not expected to be relevant. It will be seen that force BSk2, the force of the HFB-2 mass formula, conforms reasonably well to the FP curve, remaining stable up to a density of at least ρ_0; forces MSk7 and BSk1 are indistinguishable from BSk2 in this respect. On the other hand, force SkSC4 (Aboussir *et al.*, 1992), the Skyrme force of the ETFSI-1 mass formula (see Sec. III.C.4), can be seen to lead to an unphysical collapse of neutron matter at subnuclear densities and is thus to be rejected.

Whether or not a given Skyrme force is compatible with the stability of neutron matter up to nuclear equilibrium densities depends critically on the corresponding value of the symmetry coefficient a_{sym}: stability is assured for 28 MeV or higher, while collapse is inevitable for 27 MeV or less. Remarkably, fitting Skyrme forces to nuclear masses drives a_{sym} down very close to the collapse point [in the case of SkSC4 only two values of a_{sym} were tried, 30 and 27 MeV, and the latter certainly gives the better mass fit (Aboussir *et al.*, 1992)]. Insofar as a Skyrme-force fit is valid, it seems that if a_{sym} were a fraction of an MeV smaller then either neutron stars would not exist at all, or at the very least they would be much denser than they actually are.

Another unphysical instability to which neutron matter is prone when calculated with Skyrme forces is a spin flip into a ferromagnetic state that has no energy minimum and would collapse indefinitely (Kutschera and Wójcik, 1994). It is essential that the density ρ_{frmg} at which this occurs be greater than the equilibrium density ρ_0, beyond which the Skyrme form of force is invalid anyway, and irrelevant to ground-state properties. The last line of Table III in Appendix D shows that this condition is satisfied for all three forces.

A systematic study of the conditions that must be satisfied by Skyrme forces against the various kinds of instability of nuclear matter has been given by Margueron *et al.* (2002). Actually, their conditions are probably excessively stringent, since they apply for all densities up to $4\rho_0$, even though one would expect the Skyrme form to break down at lower densities.

g. Mutually enhanced magicity

A striking feature of all three Hartree-Fock mass formulas is the strong underbinding of the doubly-magic nuclei ^{48}Ca, ^{132}Sn, and ^{208}Pb, and their immediate neighbors formed by adding or removing not more than one nucleon of each kind (the presently quoted mass of ^{48}Ni does not display this difficulty, while the only other known doubly-magic nuclei have $N=Z$, and these have been compensated by the phenomenological Wigner term). There are 27 such nuclei, and in the case of both HFB formulas their mean error (experiment $-$calculated) is -1.31 MeV, as compared to 0.040 MeV for the complete set of 1768 data points in the case of HFB-1 and 0.000 MeV (to three decimals) for the 2135 data points in the case of HFB-2. For HFBCS-1 the effect is smaller but still significant, the mean error for the 27 nuclei being -0.731 MeV, to be compared with 0.102 MeV for the complete fit.

It is particularly to be noted that there is no tendency for singly-magic nuclei to be underbound, so the problem of the doubly-magic nuclei cannot simply be attributed to problems arising in the neutron and proton shells separately. Rather, these difficulties are related to the long-standing problem of "mutually enhanced magicities" that we mentioned in connection with neutron-shell strength at the end of Sec. III.B.4. These nuclei, lying close to doubly closed shells, and with no interactions between valence nucleons to consider, should be the simplest of all nuclei to describe within the

Hartree-Fock framework, and it is natural to wonder whether there may not be some fundamental limitation in conventional Skyrme forces of the form of Eq. (16), as suggested by Zeldes *et al.* (1983). If the problem does indeed lie here then the much better fit that has been obtained for all the other nuclei, i.e., for the open-shell nuclei, can only mean that the error in the Skyrme force is compensated by a skewing of the pairing parameters.[25] However, the trouble may not lie with the form (16) of the Skyrme force but elsewhere: since the open-shell nuclei are much more numerous and dominate the fit, it could be that an inadequate treatment of pairing (e.g., an inexact projection of particle number), or the total omission of some other kind of correlation, is being compensated by a skewing of the Skyrme-force parameters, with repercussions on the doubly magic nuclei and their immediate neighbors. But in neither case will we have the correct Skyrme force, and the extrapolation to INM will be distorted.

h. Vacuum polarization and other charge-related effects

To our knowledge no mass formula has ever considered the vacuum polarization induced by the nuclear charge, even though in ^{208}Pb, for example, it adds about 4 MeV to the total energy (Samaddar *et al.*, 1986). A similar, but even larger, effect comes from the Coulomb correlations studied by Bulgac and Shaginyan (1999).

i. Compatibility of Skyrme–Hartree-Fock method with relativistic mean-field theory

Since the spin-orbit field appears spontaneously in the relativistic mean-field method, in a Lorentz-invariant way, it is of interest to see to what extent the spin-orbit field generated by the Skyrme–Hartree-Fock method conforms to the RMF form. Insofar as both methods fit their parameters to the data, the two methods will clearly agree close to the stability line, but it remains to be seen to what extent the spin-orbit fields given by the two methods will continue to agree on extrapolating to the drip lines, i.e., to what extent the spin-orbit fields have the same isospin dependence in the two methods.

Now for a Skyrme force of the form of Eq. (16) the spin-orbit field for nucleons of charge type q is given approximately by

$$\mathbf{W_q}=\frac{1}{2}W_0\boldsymbol{\nabla}(\rho+\rho_q)=\frac{3}{4}W_0\boldsymbol{\nabla}\left\{\rho\pm\frac{1}{3}(\rho_n-\rho_p)\right\}, \quad (23)$$

where the upper sign corresponds to $q=n$, the lower to $q=p$. (There are also some spin-current terms, but since they are weak we do not consider them in the following qualitative argument.) But in RMF theories the spin-orbit field can depend on $(\rho_n-\rho_p)$ only through the ρ boson [see, for example, Eq. (5) of Sharma *et al.* (1995)], and in view of the relatively weak coupling of this boson to the nucleon field it was suggested (Reinhard and Flocard, 1995; Sharma *et al.*, 1995; Rutz *et al.*, 1997) that the spin-orbit field would have a much weaker isospin dependence in RMF models than in Skyrme-force models. Thus, it was argued, an RMF model and a Skyrme-force model that give comparable high-quality fits to the data might diverge when extrapolated far from the stability line. In fact, in view of the importance of the spin-orbit field for the determination of single-particle states, this was expected to be the principal difference between Skyrme-force and RMF methods, and it seemed that the former should fall into disfavor, since a theory that has manifest Lorentz invariance is certainly to be preferred to one that does not, other things being equal.

However, in the case of the Skyrme force it is fairly easy to see that the isospin dependence arising from the second term of Eq. (23) cannot be very large. In the first place we note that even at the neutron drip line the magnitude of $\frac{1}{3}(\rho_n-\rho_p)$ cannot exceed 10% of the first term ρ. Second, both of these terms are acted on by the gradient operator, and since the profiles of the neutron and proton distributions are nearly everywhere parallel it follows that the isospin-dependent term in Eq. (23) can make a nonzero contribution only over very restricted regions of the nucleus. Exact Hartree-Fock calculations (Pearson, 2001) confirm this qualitative argument and show that the extrapolations to nuclei far from the stability line given by Skyrme–Hartree-Fock mass formulas, such as those described above, are consistent with what could be expected from a complete RMF mass formula that had been well fitted to the data (see also Onsi *et al.*, 1997; Nayak and Pearson, 1998).

C. Macroscopic-microscopic approaches

1. The Myers-Swiatecki mass formula of 1966

The first systematic graft of microscopic corrections onto the liquid-drop model was made in the 1966 mass formula of Myers and Swiatecki (1966). Shell effects were regarded as a manifestation of the "bunching" of the single-particle spectrum, i.e., of the deviation of this spectrum from a strictly uniform one of equidistant levels. A simple algebraic representation of this bunching was found, and the crucial physical assumption was made that it must vanish with increasing deformation, it being believed that the single-particle spectrum must then tend towards uniformity.[26] As for the drop-model contribution, this was taken to be given essentially by Eq. (9), with the constraint on a_{ss} already noted and some simple modifications, notably to allow for departures from the spherical symmetry implied by Eq. (9). Pairing was taken into account simply by adding to the calculated energy a term $11A^{-1/2}$ MeV in the case of odd-odd nuclei, and subtracting the same term for even-

[25]This, rather than the failure to project states of well-defined time reversibility, could account for the "staggering" of the pairing forces of all three Hartree-Fock mass formulas.

[26]This same approximate approach was adopted by Lattimer *et al.* (1977) to estimate shell effects beyond the neutron drip line in decompressing neutron matter.

even nuclei. A Wigner term of the form of Eq. (19) was included. The total energy thus found was minimized with respect to the deformation of the nucleus.

The development of this mass formula marked a significant step forward, with the rms discrepancy between experimental and calculated masses being around 1 MeV (no precise figure was given), much better than what we found above for the pure drop-model expression (9). Moreover, even if the predictions for ground-state quadrupole moments were only moderately successful, it should be remembered that without shell corrections all nuclei would be spherical in the ground state. However, fission barriers were systematically too low, the discrepancy becoming steadily worse with increasing Z.

2. The Strutinsky theorem

The next major advance, the Strutinsky theorem (Strutinsky, 1967, 1968), made possible a much more rigorous approach to the problem of making shell corrections to a purely macroscopic model. At a very early stage (Strutinsky, 1967) it was found that the Strutinsky theorem implied that fission barriers could in certain cases be double humped, a feature that would account for a certain number of previously incomprehensible experimental results. More generally, it became clear that the assumption made by Myers and Swiatecki (1966) of vanishing shell effects at large deformations was wrong.

Myers and Swiatecki (1982) have shown how the Strutinsky method can be understood in an intuitively appealing way as a generalization of their algebraic bunching procedure (Myers and Swiatecki, 1966). More microscopically, it can also be derived as an approximation to the Hartree-Fock method, as follows. If $\tilde{\rho}$ is any smooth diagonal approximation to the Hartree-Fock density matrix ρ_{HF}, then an expansion of $E[\rho_{HF}]$ in powers of $\delta\rho \equiv \rho_{HF} - \tilde{\rho}$ leads, as shown by Bunatian *et al.* (1972), to the Strutinsky theorem,

$$E_{HF} \equiv E[\rho_{HF}] \simeq E[\tilde{\rho}] + \sum_i n_i \tilde{\epsilon}_i - \mathrm{tr}\,\tilde{h}\tilde{\rho} + O(\delta\rho)^2. \tag{24}$$

Here $\tilde{h} \equiv h[\tilde{\rho}]$ is the smoothed single-particle Hamiltonian approximating the exact single-particle Hamiltonian $h[\rho_{HF}]$, the $\tilde{\epsilon}_i$ are the corresponding eigenvalues, and the n_i are the appropriate occupation numbers; all the shell-model bunching effects arise in the sum.

The choice of $\tilde{\rho}$ is arbitrary, and in the present application we must suppose it to correspond to the liquid-drop model. Thus we simply take the term $E[\tilde{\rho}]$ as being given by the appropriate drop-model expression, e.g., Eq. (9), without specifying $\tilde{\rho}$ explicitly. As for the single-particle Hamiltonian $\tilde{h}$, this must have the same form as in Eq. (15), whence a choice must be made for the field U. In principle, this is determined by $\tilde{\rho}$, but we cannot determine this latter quantity uniquely from the drop-model expression for $E[\tilde{\rho}]$, there being no way to invert this expression to extract $\tilde{\rho}$. The choice for the field U is thus ambiguous, and the best that one can do in practice is to be guided by considerations of physical plausibility and convenience. Once this choice has been made, the determination of the $\tilde{\epsilon}_i$ is straightforward, involving just the numerical solution of the single-particle Schrödinger equation (note that the field U contains a spin-orbit component, and is deformed in general). With the single-particle states thus determined, the pairing contribution can be calculated with the BCS method, whence one finds the occupation numbers n_i appearing in Eq. (24). The term

$$E_{s.p.} \equiv \sum_i n_i \tilde{\epsilon}_i \tag{25}$$

can now be calculated, and there remains only the last term of Eq. (24) to deal with. Formally, this corresponds to a smoothed version of the sum in the preceding term,

$$\mathrm{tr}\,\tilde{h}\tilde{\rho} \equiv \widetilde{\sum_i} n_i \tilde{\epsilon}_i \equiv \tilde{E}_{s.p.}, \tag{26}$$

but this cannot be evaluated explicitly in the present case since $\tilde{\rho}$ is not specified.

Strutinsky's own procedure (Strutinsky, 1967, 1968) for handling this problem begins by writing the single-particle spectrum as

$$g(\epsilon) = \sum_i n_i \delta(\epsilon - \tilde{\epsilon}_i), \tag{27}$$

whence

$$E_{s.p.} = \int_{-\infty}^{\infty} \epsilon g(\epsilon)\, d\epsilon. \tag{28}$$

A smoothed version of this can then be generated by replacing each δ function in $g(\epsilon)$ with some smoother function $\tilde{g}(\epsilon)$ peaked at the appropriate value of ϵ. Then

$$\tilde{E}_{s.p.} = \int_{-\infty}^{\infty} \epsilon \tilde{g}(\epsilon)\, d\epsilon. \tag{29}$$

The simplest choice for the smoothed function $\tilde{g}(\epsilon)$ is the normalized function

$$\tilde{g}(\epsilon) = \frac{1}{\gamma\sqrt{\pi}} \sum_i n_i \exp\{-(\epsilon - \tilde{\epsilon}_i)^2/\gamma^2\}, \tag{30}$$

where γ is some smoothing parameter that clearly should be at least as large as the average spacing of major shells. In practice a slightly more elaborate smoothing procedure is adopted [see, for example, Sec. 12.4 of Preston and Bhaduri (1975)], but the foregoing suffices to illustrate the principle of the method. In particular, one sees that the procedure will be meaningless unless $\tilde{E}_{s.p.}$ is stable against fairly wide variations in the smoothing parameter γ. Figure 20 of Bolsterli *et al.* (1972) shows that this so-called *plateau condition* can indeed be satisfied moderately well for nuclei lying close to the stability line, but because of problems associated with the continuum it may be impossible to find plateaus in the case of nuclei lying close to the neutron drip line [see, for example, Nazarewicz *et al.* (1994) for a guide to the literature on this point].

This is a second source of ambiguity arising in the use of the Strutinsky theorem to calculate shell corrections to the liquid-drop model, but unlike the first source, associated with the choice of single-particle field, this one can be avoided, since the Strutinsky smoothing procedure that we have just described, referred to as the *standard averaging method* by Nazarewicz *et al.* (1994), can be replaced by more reliable procedures. The first of these is a semiclassical method, being based on the Wigner-Kirkwood expansion (Jennings *et al.*, 1975) [see also Dutta and Pearson (1987)]; other smoothing methods have been developed by Vertse *et al.* (1998, 2000).

Unfortunately, none of these elegant smoothing methods has ever been exploited in a full-scale mass formula. Rather, the several generations of mass formulas based on one form or another of the liquid-drop model that have been developed over the last 30 years or so by the Los Alamos and Berkeley groups all use Strutinsky's "standard averaging method" to implement the Strutinsky theorem. These different mass formulas are all direct descendants of Myers and Swiatecki (1966), and are distinguished mainly by successive improvements to the macroscopic part. We shall deal here only with the latest (1995) and most refined member of this family, as follows.

3. The finite-range droplet model

The name of this mass formula, finite-range droplet model (FRDM), applies, strictly speaking, only to its macroscopic part, but is used to designate the complete model, which includes Strutinsky shell corrections, BCS pairing corrections, and a Wigner term. Since this model has become not only the *de facto* standard for mass formulas but also the usual point of reference for experimentalists, we have adopted it as a sort of yardstick in this review, and must thus give it a detailed critical examination. Fuller details and an extensive guide to the earlier literature are given with the tabulation of Möller *et al.* (1995); an earlier version appeared in 1988 (Möller *et al.*, 1988).[27]

a. Macroscopic term

The original liquid-drop expression of Eq. (9) was generalized in three distinct stages. The first of these consisted of the replacement of the drop model by the so-called "droplet model" (Myers and Swiatecki, 1969, 1974), the second, the introduction of finite-range surface effects (Möller and Nix, 1981), while the third stage consisted of the addition of a purely phenomenological exponential compressibility term (Treiner *et al.*, 1986).

[27]Möller *et al.* (1995) also describe a so-called "finite-range liquid-drop" model, FRLDM. This is less sophisticated than the FRDM and gives a poorer fit to the mass data, but is of interest to the extent that it is still being used in fission-barrier calculations (Möller and Iwamoto, 2000).

To understand the generalizations introduced by the droplet model we rewrite Eq. (9) for the total macroscopic energy as a sum of volume, surface, and Coulomb terms,

$$E_{mac}=E_{vol}+E_{sf}+E_{coul}, \tag{31}$$

and look at the modifications of each of these three terms in turn. We shall confine our discussion initially to spherical nuclei, and indicate later how deformations are taken into account in the model (Myers and Swiatecki, 1974).

The essentially new feature introduced into the volume, or bulk, term is to allow the incompressibility of infinite nuclear matter to be finite, rather than make it infinite, as was implicitly the case with Eq. (9), so that a finite nucleus will be squeezed under the influence of its surface tension and dilated under the influence of the Coulomb force. It is thus convenient to express the central, or bulk, density $\rho^c=\rho_n^c+\rho_p^c$ in terms of a dilatational variable $\epsilon=(\rho_0-\rho^c)/3\rho_0$, where ρ_0 is the equilibrium density of symmetric INM. Then introducing also the central asymmetry variable $\delta=(\rho_n^c-\rho_p^c)/\rho^c$ (we shall see below that this is not exactly equal to I in a finite nucleus), Eq. (10) for the energy per nucleon generalizes to

$$\begin{aligned} E_{vol}/A &\equiv e_\infty(\rho^c,\delta) \\ &= a_{vol}+\frac{1}{2}K_{vol}\epsilon^2 \\ &\quad +(a_{sym}-L\epsilon)\delta^2+\cdots . \end{aligned} \tag{32}$$

Here our a_{sym} is the same coefficient that is denoted J in Myers and Swiatecki (1969) and in subsequent papers of these authors, while L is a density-symmetry coefficient determining the equilibrium density of asymmetric INM according to

$$\rho_{eq}=\rho_0\{1-(3L/K_{vol})I^2\}. \tag{33}$$

Turning now to the surface term, we see that the main new feature is a degree of freedom allowing the neutron and proton surfaces to separate, as certainly happens with real nuclei. To pursue this, one defines a neutron-skin thickness

$$\theta_n\equiv R_n-R_p=\frac{2}{3}r_0(I-\delta)A^{1/3}, \tag{34}$$

where R_n and R_p are equivalent sharp radii of the neutron and proton distributions, respectively, and the charge-radius constant $r_0=(4\pi\rho_0/3)^{-1/3}$. We suppose now that the surface energy can depend on the neutron-proton composition only to the extent that there is a nonvanishing neutron-skin thickness. Because of the approximate charge symmetry of nuclear forces and the near-equality of the neutron and proton masses, only even powers of θ_n can be involved, and one writes, working only to first order in small quantities,

$$\begin{aligned} E_{sf} &= 4\pi R^2\left\{\sigma+\frac{Q}{4\pi r_0^2}\left(\frac{\theta_n}{r_0}\right)^2\right\} \\ &= (1+2\epsilon)a_{sf}A^{2/3}+\frac{4}{9}Q(I-\delta)^2A^{4/3}, \end{aligned} \tag{35}$$

where $a_{sf}=4\pi r_0^2\sigma$ is the usual surface coefficient, and Q is the surface-stiffness coefficient introduced in Myers and Swiatecki (1969).[28]

If we now use the same approximation for the Coulomb energy as was made in Eq. (9), i.e.,

$$E_{coul}=\frac{3}{5}\frac{e^2Z^2}{R_p}, \tag{36}$$

and minimize the total macroscopic energy E_{mac} with respect to ϵ and δ, we find

$$\delta=\frac{I+(9e^2/40r_0Q)Z^2A^{-5/3}}{1+(9a_{sym}/4Q)A^{-1/3}} \tag{37a}$$

and

$$\epsilon=\frac{-2a_{sf}A^{-1/3}+L\delta^2+(3e^2/5r_0)Z^2A^{-4/3}}{K_{vol}}. \tag{37b}$$

Note that in their Eq. (47) for δ Möller *et al.* (1995) make the substitution $Z=A/2$, an approximation that might have implications far from the stability line.

We then find, after considerable algebraic simplification,

$$\begin{aligned}E_{mac}=&\left(a_{vol}+a_{sym}\delta^2-\frac{1}{2}K_{vol}\epsilon^2\right)A\\&+\left(a_{sf}+\frac{9a_{sym}^2}{4Q}\delta^2\right)A^{2/3}\\&+\frac{3e^2}{5r_0}Z^2A^{-1/3}-\frac{9e^4}{400r_0^2Q}Z^4A^{-2}.\end{aligned} \tag{38}$$

Note particularly that this result holds only for the equilibrium values of δ and ϵ, as given by Eqs. (37a) and (37b), respectively. Because of the dependence of ϵ and δ on A and I this expression does not have exactly the same form as Eq. (9), showing that the droplet model is indeed bringing new physics into the mass formula. In fact, the droplet model goes far beyond the original liquid-drop model in that it provides a meaningful framework for the description of dynamic phenomena such as the "breathing mode" (Blaizot, 1980) and the giant dipole resonance (Myers *et al.*, 1977).

Before discussing the remaining refinements, we point out that in the limit of large A Eq. (38) for E_{mac} does go over into the form of Eq. (9), provided we make the identification

$$a_{ss}=\frac{2a_{sf}L}{K_{vol}}-\frac{9a_{sym}^2}{4Q} \tag{39}$$

and neglect all but the leading Coulomb term. This shows that the term in $I^2A^{-1/3}$ in Eq. (9) is not purely a surface-symmetry term but contains a contribution from the volume energy.

But even if the form (9) holds only asymptotically, we see that to this approximation the droplet model can be regarded as expanding the energy per nucleon in powers of $A^{-1/3}$ and I^2. Thus to Eqs. (31) and (38) it is usual to add purely phenomenologically the next two terms in the expansion with respect to $A^{-1/3}$, writing them as $a_{cv}A^{1/3}$ and a_0A^0. In the latest fit (Möller *et al.*, 1995) both these new coefficients are equal to zero, but it should be realized that in the large-A limit there are several terms in E_{vol} and E_{sf} that vary as $A^{1/3}$ and A^0. In any case, since the sharp radius R varies almost as $A^{1/3}$ it follows that the expansion in powers of $A^{-1/3}$ is effectively an expansion in powers of $1/R$. Thus the term $a_{cv}A^{1/3}$ represents a surface energy that varies as $1/R$ and can thus be regarded as a curvature term.

More generally, this expansion converges rather quickly, but since the parameter that determines the rate of convergence of a series must be dimensionless we take it as b/R rather than simply $1/R$, with b being some length. If b were zero then the series would converge infinitely rapidly, i.e., only the volume, or bulk, term would survive. Thus b is a measure of the thickness of the surface region, i.e., the region where we can no longer assume bulk conditions, and the rapidity of the expansion depends on the surface region's being thin compared to the radius. Myers and Swiatecki describe this situation as "thin-skinned" or *leptodermous*. One could also envisage the addition of higher-order surface-symmetry terms, e.g., terms in $I^4A^{2/3}$. Such terms have been shown (Dutta, Arcoragi, Pearson, Behrman, and Farine, 1986) to be necessary to simulate the softening of the surface of highly neutron-rich nuclei that is revealed by more microscopic calculations. However, no full-scale mass formula with the inclusion of such "soft-skinned" or *malacodermous* terms has ever been fitted to the data.

We stress now that Eq. (38) is not the final expression adopted for the total macroscopic energy, even in the original droplet-model paper (Myers and Swiatecki, 1969). Although this paper calculated the variables ϵ and δ with the highly simplified Eq. (36) for the Coulomb energy, exactly as we have done here, a much more sophisticated treatment of the Coulomb energy was adopted in the final expression for E_{mac}. Thus to Eq. (38), the Coulomb dependence of which assumes the simple picture of a uniformly charged classical sphere with a sharp surface, were added a number of correction terms, representing (a) exchange effects, (b) the effect of the surface diffuseness on the Coulomb energy, (c) the redistribution effect, i.e., the tendency of the protons to be repelled outwards, separating to some extent from the neutrons and creating a central depression,[29] and (d) the finite proton size.

[28]Myers and Swiatecki (1969) also admit the presence of surface terms in δ_s^2 and $\delta_s\,\theta_n$, where δ_s is the value of δ in the surface. However, they obtain a result showing that δ_s is proportional to θ_n [their Eq. (3.5)], so their final expression for E_{sf} is equivalent to our Eq. (35).

[29]This redistribution term, as derived by Myers and Swiatecki (1969), is called the *volume redistribution term* in Eq. (40) of Möller *et al.* (1995). However, what this latter reference calls the "surface distribution term" is really nothing physically new but merely the last term of Eq. (38), with Z set equal to $A/2$.

Our discussion of the standard droplet model has so far been limited to spherical nuclei, but Eq. (38) was generalized in Myers and Swiatecki (1974) to take account of deformations: each term except the one in A is multiplied by some correction factor B_i that is a function of the deformation. Also some of the higher-order correction terms that we have mentioned are multiplied by a deformation-dependent B factor, as are some of the terms in Eqs. (37a) and (37b) for δ and ϵ, respectively. In all, there are six of these B functions in the standard droplet model; they have been tabulated by Myers and Swiatecki (1974).

We turn now to the "finite-range" modifications to the original droplet model, the essentially new physics, which consists in taking account of the effect on the surface energy of the finite range of the $N-N$ interaction. Following earlier studies of nucleus-nucleus collisions (Krappe *et al.*, 1979), the new mass model (Möller and Nix, 1981) replaces the term $a_{sf}A^{2/3}$ in Eq. (38) by, to use the notation of the later papers, $a_{sf}B_1A^{2/3}$, where

$$B_1=\frac{A^{-2/3}}{8\pi^2 r_0^2 a^4}\int\int\left(2-\frac{|\boldsymbol{r}-\mathbf{r}'|}{a}\right)\times\frac{\exp(-|\boldsymbol{r}-\boldsymbol{r}'|/a)}{|\boldsymbol{r}-\boldsymbol{r}'|/a}d^3\boldsymbol{r}\,d^3\boldsymbol{r}'. \tag{40}$$

Here the Yukawa and exponential terms have the same range a, and the double volume integral goes over a sharp-surfaced region whose shape is that being assumed for the nucleus in question and whose volume is $V=(4\pi/3)r_0^3A$. This factor B_1 will, of course, be shape dependent, but because it takes account of finite-range effects it will not have the value unity for a spherical shape. The first "finite-range" paper (Möller and Nix, 1981) also introduces a more refined treatment of the Coulomb energy: the term $(3e^2/5r_0)Z^2A^{-1/3}$ is multiplied by a factor B_3 which takes account not only of deformation but also of the diffuseness of the charge distribution, characterized by the diffuseness parameter $a_{den}=b/\sqrt{2}$.

The last major refinement that has been made to the macroscopic term consists of the introduction of the exponential compressibility term (Treiner *et al.*, 1986), which addressed the tendency of the standard droplet model to overestimate the central density (Pearson, 1980, 1982). It might have been thought that including higher-order terms in the leptodermous expansion, beyond the terms $a_{cv}A^{1/3}$ and a_0A^0, would suffice, but Treiner *et al.* (1986) showed that this was not so and that only a term that was exponential in $-A^{1/3}$ would work. Thus Eq. (31) was replaced by

$$E_{mac}=E_{vol}+E_{sf}+E_{coul}+a_{cv}A^{1/3}+a_0A^0-CA\exp(-\gamma A^{1/3})\epsilon, \tag{41}$$

where we show also the curvature and A^0 terms. Equation (37a) for δ remains unchanged, but Eq. (37b) for ϵ becomes

$$\epsilon=\frac{C\exp(-\gamma A^{1/3})-2a_{sf}A^{-1/3}+L\delta^2+\frac{3e^2}{5r_0}Z^2A^{-4/3}}{K_{vol}}. \tag{42}$$

It then turns out that Eq. (38) remains unchanged *at equilibrium*, the effect of the new term only manifesting itself implicitly through ϵ.

b. Shell corrections

A necessary first step in the calculation of shell corrections in any mic-mac mass formula is the specification of the single-particle field U appearing in a single-particle Schrödinger equation of the form of Eq. (15), the eigenvalues of which are the single particle energies ϵ_i required for implementation of the Strutinsky theorem. The FRDM writes

$$U=V_1+V_{s.o.}+V_{coul}, \tag{43}$$

in which the first term is the spin-independent nuclear part, the second the spin-orbit field, and the last term the Coulomb field.

For the first term the model takes the form

$$V_1(\boldsymbol{r})=-\frac{V_0^q}{4\pi a_{pot}^3}\int\frac{\exp(-|\boldsymbol{r}-\boldsymbol{r}'|/a_{pot})}{|\boldsymbol{r}-\boldsymbol{r}'|/a_{pot}}d^3\boldsymbol{r}', \tag{44}$$

in which the volume integral goes over a sharp-surfaced region whose shape is that being assumed for the nucleus in question and whose volume is $V=(4\pi/3)R_{pot}^3$, where

$$R_{pot}=R_{den}+A_{den}-B_{den}/R_{den}, \tag{45}$$

in which A_{den} and B_{den} are fitted parameters, while

$$R_{den}=r_0A^{1/3}(1+\epsilon). \tag{46}$$

It will be seen that this "potential radius" is different from the corresponding quantity involved in Eq. (40) for the macroscopic term. As for the well depth, one writes, with V_s and V_a being fitted parameters,

$$V_0^q=V_s\pm V_a\delta, \tag{47}$$

for $q=p,n$, respectively.

For the quantities ϵ and δ appearing in Eqs. (46) and (47), respectively, the model takes the values given exactly by Eqs. (37b) and (37a), respectively, i.e., the equations of the original droplet model (Myers and Swiatecki, 1969), and not the refined equations used in the macroscopic part of the FRDM itself. Furthermore, the values taken for a_{sf}, a_{sym}, Q, K_{vol}, and L in the calculation of the shell corrections are, because of computer-time limitations (Möller *et al.*, 1995), different from those used in the macroscopic part of the model. There is thus less consistency between the macroscopic and microscopic parts of the calculation than the model is inherently capable of ensuring.

Turning to the spin-orbit field, we have

$$V_{s.o.}(\boldsymbol{r},\boldsymbol{p})=-\lambda^q\frac{\hbar}{4M^2c^2}\boldsymbol{\sigma}\cdot\boldsymbol{\nabla}V_1(\boldsymbol{r})\times\boldsymbol{p}, \tag{48}$$

where

$$\lambda^q = k_q A + l_q , \tag{49}$$

in which k_n, k_p, l_n, and l_p are fitted parameters.

As for the last term in Eq. (43), the Coulomb single-particle field in the FRDM is taken as

$$V_{coul}(\boldsymbol{r}) = \frac{Ze^2}{(4\pi/3)r_0^3 A} \int \frac{d^3\boldsymbol{r}'}{|\boldsymbol{r}-\boldsymbol{r}'|}, \tag{50}$$

in which the volume integral goes over a sharp-surfaced region whose shape is that being assumed for the nucleus in question and whose volume is $(4\pi/3)r_0^3 A$. This term, too, is not fully consistent with the macroscopic part of the model, since a uniform sharp-surfaced distribution is assumed, with surface diffuseness neglected.

As already intimated, the FRDM implements the Strutinsky theorem via the standard averaging method. Further details will be found in Sec. 2.10 of Möller *et al.* (1995), which indicates that in lighter nuclei it was not always possible to satisfy the plateau condition.

In discussing shell-model corrections it will be recalled from Sec. III.B that, in any independent-particle model, energy contributions from spurious rotational and center-of-mass motions will arise. Corrections for these spurious terms will certainly have to be made in any Hartree-Fock calculation, but this is less obvious in the case of mic-mac calculations based on the standard averaging method for implementing the Strutinsky theorem, since it could be argued that the same spurious term arises in both $E_{s.p.}$ and $\tilde{E}_{s.p.}$ terms, so cancelling out. In any case, neither the FRDM nor any other drop-model mass formula makes such a correction, and there is no evidence of any resultant error.

One spurious motion for which the FRDM does make a correction is the zero-point energy of vibrational modes, but it is determined entirely by measured fission lifetimes and thus does not involve any new parameters. We mention in passing that no such term was included in any of the Hartree-Fock mass formulas of Sec. III.B.

c. Pairing corrections

The pairing model adopted in the finite-range droplet model is that of the seniority force, i.e., a pairing force with all matrix elements having the same value, $-G$, treated in the Lipkin-Nogami variation of the BCS method. The most obvious strategy for fitting such a pairing force to the mass data is to adopt some suitable parametrization of G as a function of N,Z, and all deformation parameters β, and fit this directly to the mass data. However, a more circuitous strategy is adopted in the FRDM, with primacy being given to the pairing gap rather than to the effective pairing force; the foundations of this strategy are discussed by Möller and Nix (1992), but it has much older antecedents (Brack *et al.*, 1972). Specifically, the value of G for given N, Z, and β is determined by first postulating an *effective-interaction pairing gap* Δ_G, which represents an average trend over all nuclei of the pairing gap, as deduced from the experimentally observed even-odd differences; the parametrization actually adopted for this quantity is

$$\Delta_{G_n} = \frac{r_{mic} B_s}{N^{1/3}} \tag{51a}$$

and

$$\Delta_{G_p} = \frac{r_{mic} B_s}{Z^{1/3}}, \tag{51b}$$

where B_s is one of the deformation-dependent B_i factors of the droplet model and r_{mic} is a fitting parameter of the model, the only one relating to nn and pp pairing. Then for the given N, Z, and β in question, and for a particular value of r_{mic}, one reads off from these equations the appropriate values of Δ_{G_n} and Δ_{G_p}. At the same time one replaces the actual nucleus by a "smoothed" nucleus with the same N, Z, and β but with a constant level density being assumed, equal to the smoothed density $\tilde{g}$ given by the standard averaging method of the Strutinsky procedure for the actual nucleus in question. For such a smoothed nucleus [known as the "average" nucleus in Möller *et al.* (1995)] the discrete summations of the gap equation reduce to integrals that can be evaluated analytically, whence the value of G corresponding to the given value of Δ_G can be expressed as a simple function,

$$G = G(\Delta_G, \tilde{g}, N_1, N_2, N_{\text{tot}}). \tag{52}$$

Here N_1 and N_2 are labels denoting, respectively, the lower and upper cutoffs on the space of single-particle states in which the pairing force is postulated to act, while N_{tot} is N or Z, as the case may be.

This value of G has been determined for an "average" nucleus from an "average" value Δ_G of the gap and is thus deemed to be appropriate for performing "real" calculations on the "real" nucleus of the given N, Z, and β, using of course the same values of N_1 and N_2 that were taken in Eq. (52). The advantage of this procedure is that it automatically ensures the fluctuations in G necessary to achieve the rather smooth variations of even-odd differences that are observed in reality. In particular, one avoids completely the problem encountered in Sec. III.B that necessitated the introduction of the so-called "staggered pairing." One possible objection to this procedure is that there is no justification for adopting the parametrization (51a) and (51b) beyond the known region of the nuclear chart, with the result that there is no guarantee of a reliable extrapolation.

All this discussion of pairing in the FRDM applies only to nn and pp pairing. There is no np pairing as such, but for odd-odd nuclei a term $\delta_{np} = h/(B_s A^{2/3})$, characterized by the single fitting parameter h, is subtracted from the total energy.

d. Wigner term

Rather than adopt the phenomenologically suggested form (19) for the Wigner term, as in the original mic-

mac mass formula (Myers and Swiatecki, 1966), the finite-range droplet model supposes a form more appropriate to SU(4) symmetry,

$$E_W = V_W\left(|I| + \frac{\delta}{A}\right), \tag{53}$$

where $\delta = 1$ if N and Z are both odd and equal, and vanishes otherwise. We do not know what overall effect this change of parametrization will have had on the fit. [Note particularly that this form of Wigner term does not have a high-A cutoff, unlike the second term of Eq. (22).]

e. Charge-asymmetry term

The finite-range droplet model also has a term of the form $c_a(Z-N)$. An energy term of precisely this form arises from the charge-symmetry-breaking force postulated by Brown *et al.* (2000) to account for the measured energy differences between pairs of mirror nuclei; we find that their fit corresponds to a value of c_a of around 0.56 MeV. However, if a similar term is added to the HFBCS-1 mass formula (Goriely *et al.*, 2001) the optimum value of c_a is very much smaller, $-0.001\,04$ MeV, with a negligible impact on the quality of the mass fit. Since the fit of Brown *et al.* (2000) on mirror nuclei was limited to $A<70$, while the HFBCS-1 fits were made to all nuclei, there is an indication that any charge-asymmetry term should have a considerably more complicated form than the one taken in the FRDM, becoming smaller, rather than bigger, for heavy nuclei.

f. Final fit

We have counted 31 independent mass-related parameters in the finite-range droplet model, as described in the foregoing (the corresponding number for the HFBCS-1 and HFB-1 mass formulas of Sec. III.B is 19, and 22 in the case of HFB-2), but many of these were predetermined by other properties before making the fit to the mass data. Thus the charge-radius constant r_0, and the charge-diffuseness parameter a_{den} were determined by electron-scattering data. Likewise the "finite-range" parameter a was fixed by heavy-ion scattering. Furthermore, all nine parameters relating to the single-particle fields, A_{den}, B_{den}, a_{pot}, V_s, V_a, k_p, l_p, k_n, and l_n were determined from measured systematics of single-particle levels (Bolsterli *et al.*, 1972). We are thus left with the 14 parameters a_{vol}, a_{sf}, a_{sym}, K_{vol}, L, Q, a_{cv}, a_0, C, γ, V_W, r_{mic}, h, and c_a to be determined by the mass data, but since a_{sf}, a_{sym}, K_{vol}, L, and Q take different values in the macroscopic and the microscopic parts of the calculation there were effectively 19 parameters involved in the mass fit. Thus we can say that there are 19+12 parameters involved in the FRDM, as compared to 15+4 for the HFBCS-1 and HFB-1 mass formulas, and 18+4 in the case of HFB-2 (or 19+4, counting the cutoff as a free parameter).

The final fit of the FRDM was made to a data set consisting of 1654 masses with N and $Z \geqslant 8$ [coming from a preliminary version of the 1995 compilation (Audi and Wapstra, 1995)] and 28 fission barriers, and a model error σ_{mod} of 0.669 MeV is quoted for this fit (Möller *et al.*, 1995). For the full 1995 data set of 1768 "recommended" measured masses with N and $Z \geqslant 8$ we find a model error σ_{mod} of 0.667 MeV, while the rms error σ is 0.678 MeV (see Table I in Appendix D).

It is likely that the error would have been even lower if some of the 12 predetermined parameters had been included in the mass fit. This is particularly true in the case of the nine parameters associated with the single-particle fields, given that the single-particle data to which these data were fitted are rather old. We also suspect that some improvement would result from including r_0 in the mass fit, rather than determining it through electron scattering. Indeed, one wonders whether the value adopted by the FRDM for r_0, 1.16 fm, is optimal even from the point of view of electron scattering, given that charge radii calculated in the model tend to be slightly larger than the measured values (Buchinger *et al.*, 2001). [In this respect we recall that the Hartree-Fock mass formulas of Sec. III.B determine r_0 in the mass fit, and nevertheless achieve a better agreement with measured charge radii than does the FRDM (Buchinger *et al.*, 2001); their final value of r_0 is 1.149 fm.] Another way in which the mass fit of the FRDM might conceivably be improved would be to exclude fission barriers from the parameter determination, as was done with the Hartree-Fock mass formulas; as it is, the FRDM parameters might be distorted by the theoretical uncertainties associated with the barriers. Finally, adding "malacodermous" terms to the model (Dutta, Arcoragi, Pearson, Behrman, and Farine, 1986) should also lead to a still better fit.

Less obvious are the implications of the fact that the five parameters a_{sf}, a_{sym}, K_{vol}, L, and Q take different values in the macroscopic and the microscopic parts of the FRDM. Constraining each of these to have the same value in both parts reduces the number of free parameters, so that naively one might expect the quality of the fit to deteriorate. But this is less obvious when one reflects on how the fitting was actually done: the macroscopic and microscopic parts were optimized separately, and the double values for these five parameters simply reflect the fact that the process was truncated before convergence had been achieved. Had reiteration been continued until there was consistency between the two parts the final fit might have been even better than it actually was.

More troubling is the high value found for the charge-asymmetry constant c_a: 0.436 MeV, which is very close to the value of Brown *et al.* (2000), discussed above. If in fact the FRDM value of c_a is unacceptably high, it would be interesting to combine this observation with the fact that charge radii are slightly too large in this same model. Jointly, these two effects could be compensating for a value of the volume-symmetry coefficient a_{sym}, 32.73 MeV in the macroscopic part, 35.00 MeV in the microscopic part, that was too high. However, it is

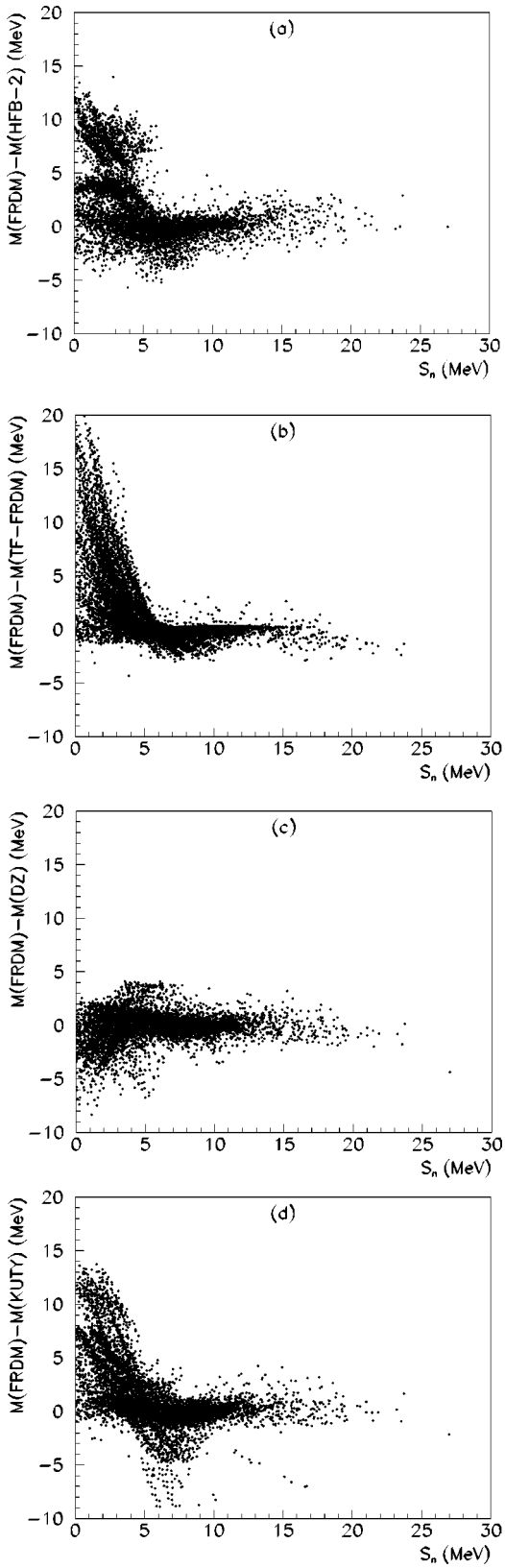

FIG. 11. Differences between FRDM and (a) HFB-2, (b) TF-FRDM, (c) Duflo-Zuker (DZ), (d) Koura *et al.* (KUTY) masses, as functions of S_n.

beyond the scope of this review to see whether one could in this way reconcile the FRDM with the value of close to 28 MeV found in all Skyrme–Hartree-Fock mass formulas.

As for the fit to the 2001 data (Audi and Wapstra, 2001), we see from Table I that the rms error is almost the same as that of HFB-2. However, this latter mass formula was fitted to the newer data, so that it is almost certain that the FRDM would outperform HFB-2 if it were refitted to the same data, even without taking account of the above improvements that we have proposed. But despite the almost identical global fits to the most recent mass data given by the present version of the FRDM and HFB-2, Fig. 11(a) shows that considerable differences between the two formulas emerge on extrapolating to the neutron drip line.

The variation with Z of the neutron-shell gaps given by the FRDM for the magic numbers $N_0=50$, 82, 126, and 184 are shown in Figs. 9(a), 9(b), 9(c), and 9(d), respectively. The observed mutually enhanced magicity is roughly reproduced for $N_0=50$, but not at all for 82 and 126. It will be seen that as the neutron drip line is approached the FRDM gaps behave quite differently from those given by the HFB-2 mass formula, even though these two mass formulas give almost identical global fits to the most recent mass data (Audi and Wapstra, 2001). The lack of any quenching must be a consequence of the parametrization adopted for the single-particle field: pairing cannot initiate any quenching of the shell gaps in the case of the FRDM because of the steady weakening of the pairing gap that the adopted parametrization (51a) imposes as the neutron drip line is approached. However, it is quite conceivable that with different parametrizations for the pairing and single-particle field quenching could have been achieved in the FRDM without any loss in the quality of the fit to the presently available data.

4. The ETFSI approximation

The method known as ETFSI (extended Thomas-Fermi plus Strutinsky integral) offers a much closer approximation to the Hartree-Fock method than does the finite-range droplet model or any of the other drop-model-based methods; see Dutta, Arcoragi, Pearson, Behrman, and Tondeur (1986), Tondeur *et al.* (1987), Pearson *et al.* (1991), Aboussir *et al.* (1992, 1995), and Goriely (2000). It is based entirely on a Skyrme force of the form of Eq. (16), with the constraint of $M^*=M$. The starting point is to calculate the energy of any given nucleus in the fourth-order extended Thomas-Fermi approximation. The resulting energy varies smoothly as a function of N,Z and deformation, so that it constitutes a purely macroscopic term, for which microscopic corrections still have to be added. However, there is a fundamental difference from the earlier mic-mac calculations: a unique single-particle field U can now be generated simply by folding the same Skyrme force over the nucleon distribution determined in the first part of the calculation. There is thus a much closer unity between the two parts of the calculation than in earlier mic-mac calculations, the same Skyrme force underlying both parts. Furthermore, in applying the Strutinsky theorem,

all the ambiguities that we mentioned in relation to smoothing vanish, since the term in $\mathrm{tr}\,\tilde{h}\tilde{\rho}$ of Eq. (24) reduces to an integral over quantities determined in the extended Thomas-Fermi calculation: this is the Strutinsky integral.

It turns out that in its latest form, ETFSI-2 (Goriely, 2000), this method approximates Hartree-Fock so well that the two methods give essentially equivalent results. The rms errors of the respective data fits are virtually identical, and the fitted forces give very similar extrapolations out to the drip lines (note, however, that the fitted forces are *not* identical). Nevertheless, the ETFSI approximation is very much faster[30] and thus was feasible at a time when the Hartree-Fock method itself was not. As far as mass formulas are concerned, the ETFSI approximation has now been made effectively redundant by the Hartree-Fock calculations, but it is still extremely valuable for the far more complicated calculations of fission barriers: ETFSI calculations of some 2000 barriers were recently performed (Mamdouh *et al.*, 1998, 2001).

5. The TF-FRDM approximation

Myers and Swiatecki (1996) have constructed a mass formula based on a different semiclassical approximation, using a force that is finite range and both momentum and density dependent; the momentum dependence involves both a p^2 term and a novel $1/p$ term. This force is purely central, there being no spin-orbit component. Besides the force there are two other significant differences with respect to the ETFSI method. (i) The semiclassical calculation is zeroth-order Thomas-Fermi, rather than fourth-order extended Thomas-Fermi, which means that the nuclear surface is not as well represented as in ETFSI. The effect of this on the quality of the fit to the data is presumably taken up by the parameters, but the compensation might not hold in the unknown regions far from stability to which one will want to extrapolate. (ii) The shell corrections are not calculated self-consistently, as in the Hartree-Fock method (and the ETFSI approximation thereto), but are taken directly from the finite-range-droplet-model calculation, along with the pairing corrections and the deformations, making this much closer to the mic-mac formulas based on the drop model.

There are seven force parameters that were fitted to the mass data, but these relate, of course, just to the macroscopic part. Thus any estimate of the total number of parameters involved in this mass formula must take account of the original FRDM parameters as well, bearing in mind that even though the present model makes use only of the microscopic part of the FRDM, the deformation parameters, for example, depend also on its macroscopic part. Now for the final force emerging in the Thomas-Fermi calculation the corresponding drop-model parameters, a_{vol}, etc., can be calculated, which means that some of these parameters implicitly have three different values in different parts of the model; the Thomas-Fermi value of a_{sym}, for example, is 32.65 MeV, as compared to 32.73 and 35.00 MeV for the macroscopic and microscopic FRDM values, respectively. However, despite all this additional flexibility, the fit to the 1995 data is only slightly better than that given by the FRDM, while the fit to the 2001 data is slightly worse.

In Fig. 11(b), where we plot the differences between the TF-FRDM and FRDM masses as a function of the neutron-separation energy S_n, it will be seen that the Thomas-Fermi-based model has a tendency to bind much more strongly than the latter in the case of highly neutron-rich nuclei, presumably because the Thomas-Fermi-based model is taking account of the malacodermous effects neglected by the FRDM. The question thus arises, which of the two formulas should be believed. Since the microscopic terms are identical in the two models it must be the difference between the macroscopic parts that is leading to the different mass predictions. But the microscopic part of the FRDM is strongly coupled with its macroscopic part, as it should be, so that the more the macroscopic part of the Thomas-Fermi formula differs from that of the FRDM, the more inconsistent it is to use the FRDM microscopic terms in conjunction with the Thomas-Fermi macroscopic term. Thus insofar as the two models lead to different extrapolations far from the stability line, it would seem that one should prefer the original FRDM to the Thomas-Fermi version of the model if one is to avoid internal contradictions.

This difficulty could have been avoided by calculating the microscopic corrections corresponding to the Thomas-Fermi force, exactly as with the ETFSI method. (It would, of course, be necessary also to define a spin-orbit two-body force, which might involve a modification of the original central force. Pairing also would have to be dealt with explicitly.) Then, and only then, would the level of self-consistency be high enough for a meaningful comparison with the ETFSI (and Hartree-Fock) results to be possible. It would be interesting for this Thomas-Fermi approach to be carried through to completion along these lines (particularly if the full fourth-order extended Thomas-Fermi formalism were used), since it is quite possible that the radically different form of force adopted would lead to results different from those given by all the approaches based on Skyrme forces.

D. Other global approaches

1. The Duflo-Zuker mass formula

The approach to the mass formula problem followed by Duflo and Zuker (1995) is more fundamental than

[30]This much greater rapidity comes in large part from the fact that all the quantities that enter the Strutinsky theorem (24) vary smoothly with respect to N, Z, and deformation, thereby making extensive interpolation possible.

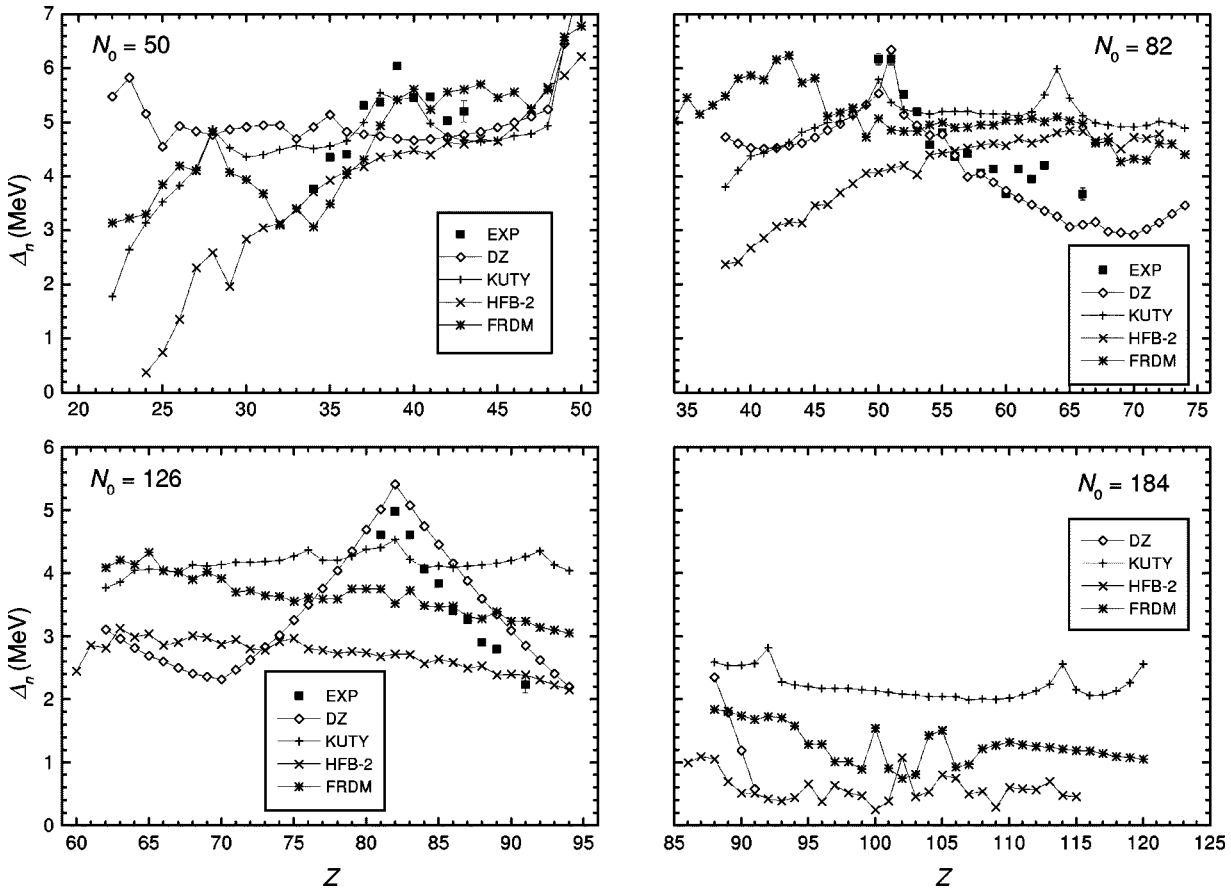

FIG. 12. Neutron-shell gaps as a function of Z for the four mass tables Duflo-Zuker (DZ), Koura *et al.* (KUTY), HFB-2, and FRDM for $N_0=50$, 82, 126, and 184. Experimental gaps calculated with mass data from Audi and Wapstra (2001).

the mic-mac methods, and yet is not strictly microscopic, since no nucleonic interaction appears explicitly. Nevertheless, the starting point is the assumption that there exist effective interactions ("pseudopotentials") smooth enough for Hartree-Fock calculations to be possible. It is then shown that the corresponding Hamiltonian $\mathcal{H}$ [the H^{eff} of Eq. (13)] can be separated into monopole and multipole terms, $\mathcal{H}_m$ and $\mathcal{H}_M$, respectively. The monopole term is entirely responsible for saturation and single-particle properties, serving in principle as a platform for Hartree-Fock calculations, while the multipole term acts as a residual interaction that permits the method to be pushed beyond pure Hartree-Fock by admitting a very general configuration mixing that includes, but is not confined to, pairing and Wigner correlations. It is these monopole and multipole terms, rather than any effective interaction, that are parametrized, the parametrization being formulated through scaling and symmetry arguments in such a way that one takes account of the main features of both saturation and the configuration mixing corresponding to shell-model diagonalizations based on the Kuo-Brown interaction (Kuo and Brown, 1966, 1968; Brown and Kuo, 1967; Kuo, 1967). The magic numbers and the regions of strong deformation both arise naturally in this schema, although in earlier versions they were put in by hand (Abzouzi *et al.*, 1991; Zuker, 1994).[31] A technical limitation of the method is the failure to take account of the spurious center-of-mass and rotational energies, but it does not seem to have affected the results too seriously.

With 28 parameters, the 1768 masses of the 1995 compilation (Audi and Wapstra, 1995) are fitted with an rms error of a mere 0.346 MeV. Similarly, the extrapolations to the new data (Audi and Wapstra, 2001) that have become available since this mass formula was fitted can be seen from Table I to be of high quality. As for the long-range extrapolations, Fig. 11(c) shows that the deviations with respect to the FRDM grow as the neutron drip line is approached, but they are relatively modest, and can take either sign. A closer examination shows that they are related to a much stronger gap for the Duflo-Zuker mass formula at $N_0=184$.

The variation with Z of the neutron-shell gaps given by the Duflo-Zuker mass formula for the magic numbers $N_0=50$, 82, 126, and 184 are shown in Fig. 12. For $N_0=50$ there is a clear-cut disagreement with experiment, with neither the mutually enhanced magicity in the vicinity of $Z=40$ nor the quenching being reproduced. On

[31]These last two papers nevertheless provide some essential insights into the model; important discussions are also to be found in Duflo and Zuker (1999) and Zuker (2003).

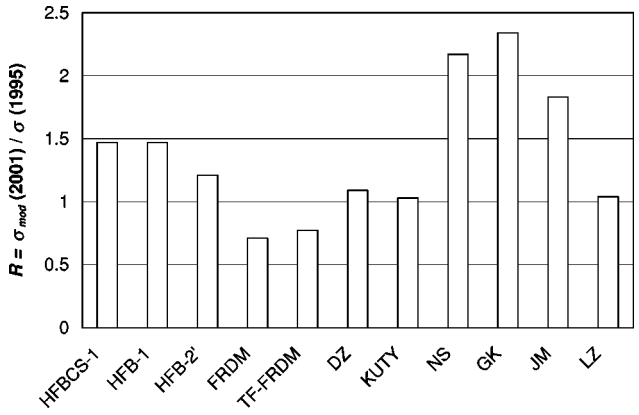

FIG. 13. A comparison of the predictive power of the various models (the quantity R in Table I): DZ, Duflo-Zuker; FRDM, finite-range droplet model; GK, Garvey-Kelson; JM, Jänecke-Masson; KUTY, Koura *et al.*; LZ, Liran-Zeldes; NS, Nayak-Satpathy; TF-FRDM, Thomas-Fermi finite-range droplet model.

the other hand, for both $N_0=82$ and 126 the experimental trends, including the mutually enhanced magicity, are very well reproduced, right up to the incipient onset of quenching. The predicted quenching occurring thereafter is strong for both these magic numbers, but, remarkably, the gaps begin to recover as the neutron drip line is approached still more closely. No other mass formula behaves in this way, and it is not clear whether this represents physical reality or is simply an artifact of an over-restrictive parametrization; no experimental check is available at the present time, of course. On the other hand, the predicted recovery is quite weak, and may not be of much consequence in practical applications, such as to the *r* process.

2. The mass formula of Koura *et al.*

Like the FRDM, the mass formula of Koura *et al.* (2000) has two parts, but the respective parts are not identified with macroscopic and microscopic terms, as such, but rather with general trends on the one hand and fluctuations about these trends on the other hand. In this way, the existence of smoothly varying components in the shell and pairing energies is recognized, but at the price of losing the physical transparency of the macroscopic part of the FRDM. A single-particle field is, of course, an essential feature of the fluctuation part, exactly as in the microscopic part of the FRDM, but there is now no apparent connection with the gross term, so again there seems to be less physics than in the case of the FRDM. Deformation is handled by taking a superposition of translated spherical nuclei. An alternative to the Strutinsky method is used. The quality of the data fit is very similar to that of the FRDM, but far more parameters are involved: 34 parameters are fitted directly to the mass data, while the single-particle field has 81 parameters, none of which are fitted to the mass data.

As for the extrapolations, one sees from Fig. 11(d) that the mass formula of Koura *et al.*, like HFB-2, tends to bind much more strongly than the FRDM as the neutron drip line is approached. The Koura *et al.* gaps likewise follow the same general trends as those of HFB-2, but are definitely stronger.

3. The infinite-nuclear-matter mass formula

The infinite-nuclear-matter (INM) mass formula of Nayak and Satpathy (Nayak, 1999; Nayak and Satpathy, 1999; Satpathy *et al.*, 1999) could, at first sight, be regarded as another mic-mac formula, but one that attempts to graft the shell corrections onto the drop-model part, not by the Strutinsky theorem but rather by the generalized Hugenholtz–Van Hove theorem, which relates the chemical potential of any homogeneous fermion system such as INM to the mean energy per particle of this system. In its original form (Hugenholtz and Van Hove, 1958) the theorem applies only to symmetric INM, but it can easily be generalized to the case of asymmetric INM (Farine, 1981; Satpathy and Nayak, 1983).

To begin our presentation of the INM model we combine Eqs. (2.1-4) and (2.8) of Nayak (1999) to write the energy of a finite nucleus as

$$E^F(A,Z)=A e_\infty(\rho_0,I)+f(A,Z)+\eta(A,Z). \tag{54}$$

In the first term here $e_\infty(\rho_0,I)$ denotes the energy per nucleon in INM, as given by Eq. (10), while the second term takes account of some finite-nucleus effects,

$$f(A,Z)=a_{sf}A^{2/3}+\frac{3e^2}{5r_0}\{Z^2-5(3/16\pi)^{2/3}Z^{4/3}\}A^{-1/3} - \delta(A,Z), \tag{55}$$

the last term of which represents pairing, parametrized as $\Delta A^{-1/2}$. Thus the first two terms of Eq. (54) correspond closely to the von Weizsäcker mass formula given in Eq. (9), except that Nayak and Satpathy omit the surface-symmetry term, but include pairing (and a Coulomb-exchange term). The last term of Eq. (54), $\eta(A,Z)$, then serves as a repository for all the post-1935 physics, containing, among other things, the compression or dilatation of the liquid drop of Eq. (54) (Myers and Swiatecki, 1969), shell effects, and deformation corrections [deformations are, of course, shell driven, but the η terms contain not only the microscopic part of the deformation corrections but also the macroscopic part (Myers and Swiatecki, 1974), the liquid drop of the INM model always being assumed to be spherical]. Without treating any of these effects explicitly, Nayak and Satpathy now claim that their aggregate is so strongly constrained by the Hugenholtz–Van Hove theorem that the residual ambiguity can be removed by the data, permitting thereby an unambiguous extrapolation to the drip lines.

To do this, the INM model (Nayak, 1999; Nayak and Satpathy, 1999; Satpathy *et al.*, 1999) draws a fundamental distinction between the first two terms of Eq. (54), i.e., the von Weizsäcker terms, on the one hand, and the η terms on the other: the former are regarded as "global" and the latter as "local," and it is asserted that local

and global quantities must be independent. Then, after some algebraic manipulation to incorporate the Hugenholtz–Van Hove theorem, Eq. (54) decouples into a pair of equations, one of which involves only η:

$$\eta(A,Z)/A=\frac{1}{2}\left[(1+I)\left(\frac{\partial\eta}{\partial N}\right)_Z+(1-I)\left(\frac{\partial\eta}{\partial Z}\right)_N\right]. \quad (56)$$

This partial differential equation, which is Eq. (2.6) of Nayak (1999), constitutes the backbone of the INM model, even if its implementation requires that it be discretized as the pair of finite-difference equations (2.9) of Nayak (1999):

$$\eta(N,Z)=\frac{N}{A-1}\,\eta(N-1,Z)+\frac{Z}{A-1}\,\eta(N,Z-1),$$
$$\eta(N,Z)=\frac{N}{A+1}\,\eta(N+1,Z)+\frac{Z}{A+1}\,\eta(N,Z+1). \quad (57)$$

But these equations, like Eq. (56), are of first order, and thus can extrapolate and interpolate only smooth trends in the masses, since to reproduce the sharp fluctuations characteristic of shell effects it is necessary (but not sufficient) to include many higher-order derivatives. The model is thus incapable of predicting any shell structure that may lie beyond the data set to which the model is fitted, and it becomes easy to see why the model must predict strong quenching of shell effects (Nayak, 1999). It also follows that if the data had been cut off below $Z=75$, $N=115$, for example, it would have been impossible to predict the doubly magic nature of ^{208}Pb; we have checked this point numerically.

Clearly, Eq. (56) cannot be correct, even though it has been derived from the Hugenholtz–Van Hove theorem. This is a theorem of great generality, holding for any homogeneous fermion system, and it is a necessary condition on any nuclear model that this theorem be satisfied in the INM limit; it is easy to see that all mass formulas based on the liquid-drop model satisfy it, as do those that are based on Hartree-Fock methods. And just because of its great generality the Hugenholtz–Van Hove theorem will hold even for fermion systems in which there is no independent-particle motion [e.g., solid nitrogen at zero temperature (Gomes *et al.*, 1958)], which means that it can tell us nothing new about shell structure, i.e., nothing that is not already present in the existing mass data. Nevertheless, Eq. (56) has unequivocal implications for shell structure: it says that shell structure must be quenched as the drip lines are approached.

How has the Hugenholtz–Van Hove theorem led to a statement concerning a question on which it cannot have anything to say? The problem lies not with the theorem but with the way in which Nayak and Satpathy apply it, specifically with the assumption made in decoupling Eq. (54) that the "local" η quantities are independent of the "global" quantities. This cannot be right: for example, the depth of the shell-model field must depend on the volume parameter a_{vol}, even if it is not determined uniquely by this parameter, while deformability depends on the surface coefficient a_{sf}. More generally, to assert the independence of global and local properties is equivalent to denying the possibility of a self-consistent field, and thus the validity of the Hartree-Fock method (Pearson and Goriely, 2003). In this way the prediction of shell quenching (Nayak, 1999) is built into the INM model at the outset. If the Hugenholtz–Van Hove theorem had been capable of telling us something about shell structure, then the network of equations to which it led would of necessity have contained finite differences of much higher order.

Nevertheless, if the INM model is inherently incapable of predicting shell effects, it may be wondered how it can fit the data so well, including, of course, the known shell structure: the rms error for 1884 masses is 0.401 MeV. The point is that the pair of finite-difference equations (57) form a network of recurrence relations connecting each nucleus with its nearest neighbors. This network is solved over a hexagonal mesh, each containing 58 nuclei, and to start the integration it is necessary to specify four baseline nuclei of known mass. However, by taking different meshes, up to 70 different values of η for a given nucleus can be found, the mean of which is taken as the final value for the nucleus in question. But no matter how many times a given nucleus is calculated, an essential feature of this procedure is that each known nucleus is calculated in terms of other known nuclei. Thus in claiming that the low rms error has been achieved with only five parameters, the global parameters a_{vol}, a_{sym}, a_{sf} and r_0, and the strength of the pairing term, the Nayak and Satpathy papers (Nayak, 1999; Nayak and Satpathy, 1999; Satpathy *et al.*, 1999) do not take into account the large numbers of baseline masses that are required to solve the network of equations. Without these data points (or an equal number of other parameters that serve as initial conditions) it is impossible to solve the network. We do not know the exact number of baseline nuclei that were taken, but since 1884 masses are fitted, and 4 baseline nuclei per block of 58 nuclei are needed, it cannot be less than 130, and from the description of the procedure it is presumably much larger. There will thus be no problem in getting an excellent fit to the mass data, including the observed shell effects, with a model of the form of Eq. (57), even though it is inherently incapable of *predicting* shell effects.

Actually, although its authors present it as a global mass formula, the form of the basic equations of the INM model, Eq. (57), is typical of the local mass formulas of the Garvey-Kelson type (Garvey and Kelson, 1966; Jänecke and Masson, 1988) that we discuss in the next subsection. [Indeed, the Garvey-Kelson formulas are third order and still cannot reliably extrapolate very far (Jänecke and Masson, 1988).] As such, the INM model has all the limitations of local mass formulas: an inability to predict shell effects correctly and a total unsuitability for long-range extrapolations. But even as a local mass formula, making only short-range extrapolations, the large value of the ratio R given in Table I shows that the INM model does not perform very well.

E. Local mass formulas

Often one is confronted with the situation of requiring the mass of a nucleus which, although unmeasured itself, lies fairly close to a considerable number of nuclei of known mass. Such cases arise, for example, in connection with the *rp* process of nucleosynthesis (Schatz *et al.*, 1998) and also when preparing experimental searches for double β decay or $2p$ emission. To handle this situation several simple procedures have been devised to express the unknown mass in terms of the nearby known masses. The actual physics involved in these so-called local mass formulas is often minimal, and it is not expected that novel features such as the onset of a new deformation zone or the occurrence of a new magic number will be predicted. We shall describe in this subsection some of the more familiar of these procedures, and compare their predictions for the new data with the predictions made by the global mass formulas (Table I in Appendix D).

1. Systematic trends

As shown in Fig. 1, the two-neutron separation energy S_{2n} varies in a very regular way with respect to N. The same remark also applies to the variation with respect to Z and A, and likewise to other mass derivatives such as S_{2p}, Q_β, and Q_α. Even when a kink is observed, as for shell closures, similar kinks are seen to occur in neighboring chains.

On the basis of this observation, a straightforward and systematic scheme for interpolation and extrapolation has been developed (Wapstra *et al.*, 1985; Audi and Wapstra, 1993, 1995; Borcea *et al.*, 1993), with the mass assignment to a given unknown nuclide being made in such a way that all the mass-derivative quantities mentioned above vary as smoothly as possible. The assessment of smoothness is usually made visually, but mathematical approaches have also been considered (Borcea and Audi, 1993, 1998). When such smoothness is judged to be well established, extrapolations of up to three or four nuclides can be made. These "values derived from systematic trends," accompanied by appropriately increasing error bars, are published with the evaluated masses, but are distinguished from the experimental data by being labeled with the symbol # (Audi and Wapstra, 1995).

In the course of this procedure it occasionally happens that replacing the quoted experimental value of a particular mass by some other value can lead to a substantial improvement in the overall smoothness of the various mass-derivative quantities. New measurements generally confirm that the original suspicion of an incorrect experimental value was well founded. An example is the case of ^{150}Ho already described in Sec. II.F. Such cases are indicated in the table by both the # and ♦ symbols (Audi and Wapstra, 1995).

The 1995 table provided systematics-based predictions for 368 of the 382 new data given by Audi and Wapstra (2001). The small errors given in Table I demonstrate that these predictions are particularly accurate.

2. Garvey-Kelson relations

Garvey and Kelson (1966) and Garvey *et al.* (1969) developed algebraic relations connecting the masses of neighboring nuclides. The most widely used is the so-called *transverse relation* linking six masses,

$$\begin{aligned} &M(N+2,Z-2)-M(N,Z)+M(N,Z-1)\\ &\quad -M(N+1,Z-2)+M(N+1,Z)\\ &\quad -M(N+2,Z-1)=0, \end{aligned} \tag{58}$$

derived from an independent-particle picture, with spin and isospin independence. It is also assumed that single-particle energies and effective interactions vary smoothly and slowly with A. On the n-rich side, the mass of the $(N+2,Z-2)$ nuclide may be determined with good accuracy if the five others are known. Similarly, on the p-rich side, the mass of the (N,Z) nuclide may generally be calculated.[32] In this way, Eq. (58) was examined in 1087 cases using the 1768 masses published in AME 1995, resulting in a relatively low rms error as can be seen in Table I.

Mass predictions can be made using an iterative procedure, but it is clear that since the number of known masses used in the relation diminishes with each iteration, the error will grow. In the limit of seven iterations, for example, 242 out of the 382 new masses could be calculated with deviations $\sigma_{mod}=0.232$ MeV and $\overline{\epsilon}_{mod}=-0.018$ MeV. A total of 21 iterations was required to reach 340 of these masses, but with the resulting large rms deviation of $\sigma_{mod}=0.717$ MeV (quoted in Table I). Pushing the relation further leads to numerically unstable predictions.

Several other mass formulas based on the Garvey-Kelson relations were developed to try to minimize this loss of convergence in order to extrapolate to the drip lines (Comay *et al.*, 1988; Jänecke and Masson, 1988; Masson and Jänecke, 1988). In Table I, a comparison of the 372 masses predicted by Jänecke and Masson (1988) (JM) to the new mass data shows that they do not surpass the quality of predictions from global approaches.

3. Neural networks

Another manner in which to take advantage of the regularity of the mass surface is the use of neural networks. The first attempts (Gazula *et al.*, 1992; Gernoth *et al.*, 1993) simply used N and Z as input. The output is a "yes" or "no" answer that corresponds to a physical state such as the stability, or a numerical value such as

[32]There are some exclusions around the $N=Z$ line. In particular, nuclei having $N=Z=$odd must not be involved.

the spin, the decay probability (Gernoth and Clark, 1995a), the separation energy, or the mass excess. In the case of atomic masses, the large number of available data is nicely adapted for training the network on one part of the data and testing it on other parts.

One important result concerns the encoding of N and Z. When an analog encoding is used, the neural network misses the shell effects and smoothes the mass surface in a way similar to a pure liquid-drop model, leading to $\sigma \simeq$ a few MeV. When a binary encoding is used, the shell structure is correctly taken into account and the obtained deviations are $\sigma \simeq 1-2$ MeV and $\overline{\epsilon} \simeq 0.4$ MeV when two or three layers are used with typically 300 to 400 parameters. The lowest deviations obtained up to now are $\sigma \simeq 0.7$ MeV and $\overline{\epsilon} \simeq 0.010$ MeV by adding $A = N+Z$ and $N-Z$ values as input and carefully monitoring the training phase. Weighting the mass input with the correponding uncertainties has also been pursued (Gernoth and Clark, 1995b). While the "predicted" masses are, in fact, only interpolated, new schemes have been developed to specifically attack the problem of extrapolation (Mavrommatis *et al.*, 2000; Athanassopoulos *et al.*, 2003), but with deviations of around 1.5 MeV, this approach does not seem too promising. In this field, at least, the human brain would seem to do better than neural networks!

4. The Liran-Zeldes mass formula

Liran (1973) and Liran and Zeldes (1976) developed a semiempirical formula in which the binding energy is expressed as a sum of pairing, deformation, and Coulomb energies. The parameters used in the development of these three terms are fitted separately for each domain delimited by magic N and Z values. The number of parameters to adjust is 11 in the case of diagonal shells, where the major valence shells are the same for neutrons and protons, and 15 in other cases.

Provided there are enough data in the explored region, the extrapolations are rather accurate (see Table I), especially given that the parameters were fitted using only the restricted set of experimental masses known in 1976. The magic numbers are chosen *a priori* and not predicted by the model. In the case of the trans-lead and superheavy regions, this raised the key question of the choice of associated magic proton number. Recently, Liran *et al.* (2000, 2001) tested an older adjustment (Liran, 1973) in which $Z=126$ was chosen over $Z=114$. In the superheavy region, the deviations for the 49 new masses with $N \geqslant 129$ are $\sigma = 0.155$ MeV and $\overline{\epsilon} = -0.001$ MeV. In the trans-lead region, a new partial fit was performed leading to deviations $\sigma = 0.246$ MeV, and $\overline{\epsilon} = -0.001$ MeV, indicating good reliability for mass predictions in these regions. Further improvements are expected from a completely new fit, in particular for the masses near boundaries.

5. Approaches for nuclei around the $N=Z$ line

a. The isobaric mass multiplet equation

The isospin formalism allows for every nuclear state to be assigned an isospin which is part of an isobaric multiplet, all members of which have nearly identical wave functions. The energy differences in a multiplet are very well described by a quadratic formula of isospin projection having three coefficients: the isobaric mass multiplet equation (see Benenson and Kashy, 1979). The coefficients of all measured multiplets have been recently tabulated by Britz *et al.* (1998). Deviations from the quadratic form are relatively small (below the level of 10^{-6}), making it possible to predict proton-rich analog levels, including ground states, to relatively good accuracy. The application of this equation is, of course, limited to those multiplets having known coefficients and will not allow extrapolations for nuclides much beyond $A=100$.

b. Coulomb energy corrections to mirror nuclides

Numerous examples of mass determinations using Coulomb energy differences can be found in the literature, with Brown *et al.* (2002) providing the latest refinements, including the use of Hartree-Fock calculations in order to generate the necessary nuclear structure information for (often unbound) nuclides in the range $A = 41-75$, of interest to the *rp* process. On condition that the mass of the corresponding neutron-rich mirror nuclide is known, the displacement energies can be calculated relatively accurately since they depend mainly on the Coulomb interaction, although isospin symmetry breaking needs to be taken into account.

6. Interacting boson model

This model uses group theory for describing low-lying states of even-even nuclei. Bosons of differing angular momenta are used to model valence nucleons, and they interact through a Hamiltonian containing two-body interactions. The latest version of this model has included the binding energy in the analysis, since it is very sensitive to the Hamiltonian used. It is described by Fossion *et al.* (2002), who use it to analyze the fine structure of the mass surface in particular regions (e.g., Hg) by making local adjustments.

7. Conclusion concerning local formulas

One might have expected that local formulas, while of more limited scope, would be more accurate than the global ones described in Secs. III.B–III.D. Table I shows that this is not the case except for the systematic masses given by Audi and Wapstra (1995), which are far more reliable than all other predictions. Near the $N=Z$ line, the possibility to make use of the isobaric mass multiplet equation, or of data on mirror nuclei, also provides high quality predictions, but for a very limited range of nuclides. While fitted on old data, the Liran-Zeldes mass formula is still competitive.

F. Outstanding problems and future directions

A recent significant development has been the claim of Bohigas and Leboeuf (2002) that considerations of quantum chaos impose a lower limit on the accuracy with which nuclear masses can be predicted. The precise value of this lower limit is somewhat uncertain, but it appears unlikely that global mass formulas could ever predict masses with an rms deviation much smaller than 0.3 MeV.

One mass formula stands out above all others with respect to both the quality of the data fit and the success with which it predicts the new data (Table I): this is the mass formula of Duflo and Zuker (1995), and in fact it performs fairly close to the limit claimed to be imposed by quantum chaos. However, this does not mean that with Duflo-Zuker we have reached the end of history, even as far as mass formulas are concerned. On the contrary, since different mass formulas giving comparable data fits can extrapolate quite differently out to the neutron drip line, it is essential that both the microscopic and mic-mac approaches be developed to the point where they give data fits whose quality is comparable to that of the Duflo-Zuker formula. Only in this way will we have some reasonable handle on the range of uncertainty for long-range extrapolation, although for a given quality of fit to the mass data one would have greater confidence in the long-range extrapolations given by the more microscopic model, simply because nuclear binding energies, along with all other properties, originate ultimately in the basic interactions between the constituent nucleons.[33]

The best microscopic mass formula we have at the present time is HFB-2 (note that because of the phenomenological Wigner terms it cannot be regarded as being fully microscopic), but the quality of its fit to the data is distinctly inferior to that given by the Duflo-Zuker formula. Perhaps the most obvious place to look for improvement over HFB-2 lies in the calculational details of the method itself: numerical accuracy, convergence, and, in the case of deformed nuclei, the removal of the spurious rotational energy. Let us say at once that there is no evidence of any problem of this sort, and that some of the most serious doubts concerning the HFB-2 mass formula lie rather with the treatment of pairing. In the first place, it needs to be asked whether one should take for the pairing force the same interaction that is used in the Hartree-Fock part of the calculation, i.e., the Skyrme force. The Gogny group has always imposed this constraint (Dechargé and Gogny, 1980), and Dobaczewski *et al.* (1984) have adopted the same point of view with regard to the Skyrme force SkP, but there is no compelling evidence for this constraint. Rather, we believe that the "truncated δ function" should provide an adequate representation of the pairing force, but it is essential to admit a possible density dependence confining it to the nuclear surface, and above all to consider more flexible parametrizations of the cutoff. Both these points require a much more thorough phenomenological study than they have so far enjoyed, but it is fairly clear already that the data alone will not be sufficient to discriminate between all the different possibilities: there would always be the fear that future data would repeat the same nasty surprise with which the 2001 data (Audi and Wapstra, 2001) confronted the HFBCS-1 and HFB-1 formulas. Thus an urgent priority is the development of a much better microscopic understanding of pairing that would discriminate between different models that give equally good fits to the data but different extrapolations. Bertsch and Esbensen (1991), Barranco *et al.* (1999), and Garrido *et al.* (1999) serve as welcome steps in this direction.

As for the Skyrme force itself, the most plausible source of improvement would be to add to the form of Eq. (16) a t_4 term, i.e., a term with simultaneous density and momentum dependence. Preliminary studies (Farine *et al.*, 2001) do not suggest that any dramatic reduction of the rms error is possible in this way. Another avenue to explore would be to include a tensor term (we are indebted to F. Weber for this reminder), although the only published studies of such a term (Stancu *et al.*, 1977) are not very promising.

1. Beyond Skyrme forces

It is, of course, always conceivable that there is some fundamental limitation with the Skyrme form, and indeed we have already raised the possibility that this form of force might be incapable of simultaneously fitting masses and an independently determined value of the symmetry coefficient a_{sym}. Also to be borne in mind here is the failure of all three Skyrme–Hartree-Fock mass formulas to represent correctly the phenomenon of mutually enhanced magicity. But going beyond the Skyrme form means that finite-range forces will have to be adopted, and we have already remarked that Hartree-Fock calculations with such forces will be much more complicated than with Skyrme forces. Moreover, if the adopted finite-range forces are purely static, as with the Gogny forces (Dechargé and Gogny, 1980), then the effective mass will be significantly lower than the real nucleon mass, which may spoil the mass fit for open-shell nuclei: the Gogny force has $M_s^*/M=0.67$, which may account for the poor agreement with the experimental masses of spherical open-shell nuclei, as displayed in Fig. 9 of Dechargé and Gogny (1980). It might be possible to rectify this problem with an appropriate pairing cutoff, but otherwise it would be necessary to make the finite-range forces momentum dependent, possibly by resurrecting some forms that have not been used since the pre-Skyrme days of the 1960s; see Davies *et al.* (1966), Tabakin and Davies (1966), Saunier and Pearson (1967), Pearson and Saunier (1968). All in all,

[33]Another reason for preferring microscopic mass formulas is that these give us not only the mass but also the nuclear wave function. This is of especial importance in applications such as to the *r* process of nucleosynthesis, where one needs to be able to calculate β-decay rates, in addition to masses, and it is highly desirable that one use the same model for both.

finite-range forces do not seem to offer a promising approach to the mass-formula problem.

2. Hartree-Fock without forces

The formulation of the Hartree-Fock method as we have described it in Sec. III.B.2 proceeds by first deriving the energy-density functional appearing in Eq. (14), $\mathcal{E}(\mathbf{r})$, from the given effective force v_{ij}^{eff}. The Hartree-Fock equation (15) is then derived from $\mathcal{E}(\mathbf{r})$. Now in principle instead of starting from an effective force one could always begin at the level of the energy-density functional $\mathcal{E}(\mathbf{r})$, postulating a suitable form for it, with a convenient number of adjustable parameters. This approach was adopted long ago by Tondeur (1978a, 1978b), but has to a large extent been eclipsed by explicit use of Skyrme, or Gogny, forces (see, however, footnote 17). Indeed, the range of possible terms that could be included in the energy-density functional is vast, being by no means restricted to terms that correspond to a simple force, but this has the disadvantage of there being no obvious way of eliminating *a priori* all but a manageable number of terms. By contrast, the use of a simple force certainly has an intuitively physical appeal, which no doubt accounts for the popularity of this approach.

However, should certain intrinsic limitations to the use of a force begin to emerge, then one could always have recourse to the energy-density functional approach, adding to the functional that corresponds to the original force just those terms that might be expected to repair the defect that has been encountered. The Skyrme–Hartree-Fock calculations that we have described here might well have reached the point where further progress depends on generalizations along these lines. Recent results of Yu and Bulgac (2003) using the energy-density functional of Fayans *et al.* (2000) are very promising.

3. Beyond Hartree-Fock

Having raised the question of going beyond Skyrme forces, it is natural to envisage going beyond Hartree-Fock. Of course, pairing and Wigner correlations are already taken into account, but the success of the Duflo-Zuker formula as compared to HFB-2 suggests that other types of configuration mixing might be significant. Stevenson *et al.* (2001, 2002); and Rikovska Stone *et al.* (2002) have begun to explore this possibility, evaluating up to third order a perturbation series the leading term of which is just the usual Hartree-Fock expression. While this procedure will certainly give rise to correlations that are not included in the kind of Hartree-Fock calculations that we have described here, it is not clear to what extent the essential pairing and Wigner correlations are embraced. Only very preliminary results, obtained with a density-dependent separable effective interaction, have been published so far.

In principle, another way of going beyond Hartree-Fock would be to diagonalize the matrix of the effective Hamiltonian (13) in a basis of shell-model states, fitting the parameters of the effective interaction to the known masses. However, implementing such a program explicitly as the basis of a global mass formula is totally impractical at the present time, but some of the general features that would arise in such calculations have already been included in the Duflo-Zuker mass formula.

Nevertheless, it is worth noting that shell-model diagonalization has already been used to calculate the nuclei of the *sd* shell (Retamosa *et al.*, 1997; Caurier *et al.*, 1998) and of the *fp* shell (Caurier *et al.*, 1999). Such calculations are completely microscopic, but can at the present time be implemented only locally, because of computer limits on the dimensionality of the basis. These calculations, when compared to experiment, fare no worse than the other microscopic or mic-mac models, but do no better either. In fact, the known shell quenching at $N=20$ can be reproduced only by introducing intruder orbits. Clearly, these shell-model calculations are too limited at the present time for predicting masses far from stability if provisions for irregular behavior must be prescribed in advance.

In order to overcome limitations of conventional shell-model calculations, the so-called Monte Carlo shell model has been developed by Otsuka (2001; Otsuka, Utsuno, *et al.*, 2001). The many-body problem is solved by a judicious selection of basis states, using the stochastic quantum Monte Carlo diagonalization method, which are then used in a shell-model calculation. For the present, encouraging results have been obtained for light nuclides, including an interesting interpretation for shell quenching at $N=20$ (Otsuka, Fujimoto, *et al.*, 2001).

4. Possible improvements to the mic-mac approach

We have already indicated several obvious ways in which the finite-range droplet model could achieve a still better fit to the mass data: inclusion of malacodermous terms, optimization of r_0 and the parameters of the single-particle potential to the mass data, exclusion of fission barriers from the fits, closer attention to the charge-asymmetry term, and a more general Wigner term, possibly of the form of Eq. (22) (the first term of this seems to be essential). The extrapolations would likewise have greater credibility if the standard averaging method of Strutinsky were replaced by more modern methods (Jennings *et al.*, 1975; Dutta and Pearson, 1987; Vertse *et al.*, 1998, 2000), and if the parameters a_{sf}, a_{sym}, K_{vol}, L, and Q were constrained to keep the same values in the microscopic and macroscopic parts of the calculation. Above all, it must be remembered that all the pairing-related ambiguities that have beset the Hartree-Fock mass formulas are just as likely to be in play in the mic-mac formulas; in particular, it will be essential to release the constraints (51a) and (51b) that were imposed on the FRDM's pairing gaps.[34]

[34]Actually, in seeking a better mic-mac formula one could take the formula of Koura *et al.*, rather than the FRDM, as the

But whatever developments the future holds, there remains the question of which of the presently available mass formulas should be used in practical applications. While one formula, namely, Duflo-Zuker, gives a significantly better data fit than all the others, the safest procedure to adopt in practical applications, such as to the *r* process, would probably be to examine the implications not only of the Duflo-Zuker formula, but also of the FRDM and HFB-2. The better the agreement among the three approaches the greater one's confidence in the predictions.[35]

IV. CONCLUSION

In Sec. II we described the new techniques of high sensitivity and accuracy that are enabling an extremely fine mapping of an ever-widening mass landscape. While it is sobering that the difficult task of producing pure beams of exotic nuclides allows steps towards the drip lines to be taken at a rate of barely one nucleon per decade, there is hope in the next-generation initiatives EURISOL (Vervier, 2003), the Rare Isotope Accelerator (RIA; Savard, 2003; Sherrill, 2003), and the future GSI fragmentation facility (Henning, 2003), which plans to include *two* new storage rings for mass measurements (Geissel *et al.*, 2003). These programs plan for aggressive research and development in production and handling techniques in order to increase beam intensities by three orders of magnitude in the next ten years. We have also described the continuing efforts of the Atomic Mass Evaluation, which provides an enormous service to nuclear science, both experimental and theoretical.

Nevertheless, Fig. 4 makes it clear that only about a quarter of all the possible nuclei lying between the drip lines have already had their masses measured. Less apparent from this figure is the near certainty that many of the remaining nuclei will stay unmeasured for the foreseeable future. This is particularly true in the case of the heavy, highly neutron-rich, nuclei, the masses of which are required for a full understanding of the *r* process of stellar nucleosynthesis. There is thus a great need for a reliable "mass formula," as one continues to call any semiempirical theory, however complicated, that permits extrapolation from the data out to the unknown regions of the nuclear chart. Recent developments in this area are reviewed in Sec. III, where we make it clear that the present situation is somewhat unsatisfactory, in that different mass formulas giving acceptable fits to the mass data will nevertheless diverge strongly in their extrapolations out to the neutron drip line.

Even if one were to give greatest credibility to the most microscopic of the available mass formulas, HFB-2 (Goriely *et al.*, 2002), considerable ambiguity would remain, as we have pointed out, especially with regard to pairing. Future progress would be helped enormously by the development of better theories of pairing, but at least as important is the acquisition of more mass data, further and further from the stability line. Indeed we recall how the new mass data of 2001 (Audi and Wapstra, 2001) diagnosed flaws in the earlier Hartree-Fock mass formulas, HFBCS-1 and HFB-1, and led directly to the development of the HFB-2 formula, with its radically different behavior in the highly neutron-rich region. There is no reason to believe that new data acquired in the future will not lead to equally radical revisions of the mass extrapolations.

Particularly valuable would be new masses relating to the shell gaps at magic neutron numbers, since we have seen how sensitive these quantities are to the choice of pairing model. Furthermore, regardless of its relevance to the development of suitable mass models, a knowledge of masses at magic neutron numbers, and of a possible quenching of the shell gaps, is of vital importance for understanding the *r* process. But *any* new mass would be useful, since the more one accumulates data and fits them correctly, the less will be the ambiguity in the extrapolation to the ever-diminishing number of unknown nuclei. However, despite the experimental progress reported here, the masses of many exotic nuclei of interest will certainly remain unmeasured for many years to come, and in the meantime it will be essential to sustain the interplay between experiment and theory that we have described.

ACKNOWLEDGMENTS

We wish to acknowledge valuable communications with O. Bohigas, G. Bollen, A. Bulgac, J. Dobaczewski, S. Goriely, J. Jänecke, P. Leboeuf, A. Lejeune, R. Machleidt, G. Martinez-Pinedo, W. Nazarewicz, M. Samyn, C. Scheidenberger, T. Tachibana, P. Van Isacker, R. B. Wiringa, R. Wyss, and A. Zuker. P. Möller is thanked for extensive discussions on his method for calculating model errors, and for sending us his code. M. Farine is thanked for performing the semi-infinite nuclear matter calculations. We are indebted to G. Audi and A. H. Wapstra for making available to us the 2001 preliminary version of their new AME, and C.T. and D.L. thank particularly G. Audi for his invaluable help in clarifying many delicate points. R. C. Nayak and H. Koura are thanked for sending us files of their respective tables. J.M.P. expresses his appreciation of the many years of collaboration with F. Tondeur. J.M.P. was partially supported by NSERC of Canada. D.L. and C.T. were supported by IN2P3 of France.

starting point, but since the physical content of its different terms is less transparent than in the case of the FRDM, it is less obvious how to go about making improvements, except by adding still more terms, and thus still more parameters.

[35]In this context one might be tempted to use the measured abundances of *r*-process nuclides to discriminate between the different mass formulas. However, one would have to make sure that there was no residual ambiguity associated with the astrophysical conditions under which nucleosynthesis occurs.

APPENDIX A: RELATION BETWEEN ATOMIC AND NUCLEAR MASSES

As mentioned in Sec. II.F, the masses given in the Atomic Mass Evaluation (Audi and Wapstra, 1993, 1995) are indeed atomic and not nuclear masses, the relation between the two being given by

$$M^{AME}(N,Z) \equiv M_{at}(N,Z) = M(N,Z) + Zm_e - B_{el}(Z), \tag{A1}$$

where $M_{at}(N,Z)$ is the atomic mass, m_e is the electron mass, and $B_{el}(Z)$ is the total binding energy of the electrons.

Of course, not only the masses but all the energy differences tabulated in the AME are also expressed in terms of atomic masses, and thus are not exactly equal to their nuclear counterparts. As an example, the tabulated binding energy $B^{AME}(N,Z)$ is different from the nuclear binding energy $B(N,Z)$ as defined by Eq. (1):

$$B^{AME}(N,Z) = \{NM_n + ZM_H - M_{at}(N,Z)\}c^2 = B(N,Z) - ZB_{el}(Z=1) + B_{el}(Z), \tag{A2}$$

where M_H is the mass of the hydrogen atom.

In order to derive the nuclear quantities from the tabulated (atomic) ones, the value of $B_{el}(Z)$ has to be calculated, and its uncertainty may be much larger than that of the experimental atomic mass itself. The electron binding energy ranges from 13.6 eV for H up to more than 700 keV for U. Calculations have been made by Huang *et al.* (1976) for all elements from $Z=2$ to 106.[36]

As first proposed by Foldy (1951), $B_{el}(Z)$ can be fitted by a power law. The old formula used by Seeger and Howard (1975) and Myers (1976),

$$B_{el}(Z) = 14.33\ Z^{2.39}\ \text{eV}, \tag{A3}$$

deviates from the tabulation of Huang *et al.* (1976) by nearly 100 keV at the upper limit of $Z=106$. A better approximation may be obtained by using

$$B_{el}(Z) = 14.4381\ Z^{2.39} + 1.554\,68\times10^{-6}\ Z^{5.35}\ \text{eV}, \tag{A4}$$

which provides a rms error over the entire range of tabulated masses of 150 eV, although considerably larger errors can be expected for extrapolation to the superheavy region.

Atomic masses are expressed either in mass units or in energy units. The atomic mass unit u is defined as 1/12 of the mass of the neutral ^{12}C atom; its most recently determined value (Mohr and Taylor, 2000) is $u = 1.660\,538\,73\times10^{-27}$ kg $= 931.494\,014$ MeV/c^2, with an experimental uncertainty of 0.08 ppm. Such precision is impossible in direct absolute-mass measurements and was obtained, in fact, from a determination of Avogadro's number N_A, defined as the number of atoms in 12 g of ^{12}C, whence

$$u = 10^{-3}/N_A\ \text{kg}. \tag{A5}$$

Ultimately, the atomic mass unit is defined in terms of the standard kilogram. This is, in fact, the last of the three fundamental quantities whose standard is an actual artifact rather than an invariant property of nature: the standard second is defined in terms of the frequency of a certain spectral line; the standard meter is defined relative to the standard second through the velocity of light, for which an exact value has been attributed and frozen: $c = 299\,792\,458$ m s^{-1}; as for the standard kilogram, it resides in Sèvres, close enough to smoggy Paris that its definition includes a cleaning recipe! It has been proposed [see, for example, Mohr and Taylor (2000); Paul *et al.* (2001)] that this mass standard be replaced by the atomic mass unit, i.e., $\frac{1}{12}$ of the neutral ^{12}C atom, essentially by fixing the value of Avogadro's number and using Eq. (A5). The most accurate way of determining N_A consists of effectively counting the atoms in a pure silicon crystal of known mass and volume by measuring the lattice spacing; a precise knowledge of the isotopic composition of the crystal together with the corresponding atomic masses is also required.

In any case, for a given value of the atomic mass unit expressed in kg, there is no ambiguity in the energy equivalent as long as it is expressed in joules. On the other hand, expressing this same energy in electron volts requires a precise definition of the volt: see, for example, Sec. 2 of Cohen and Wapstra (1983).

APPENDIX B: ON MODEL ERRORS

The rms error σ_{rms} with which a model or theory fits a data set $\{M_1, M_2, \ldots, M_i, \ldots, M_n\}$ is widely used as a measure of the validity of that model as a representation of the phenomenon in question. However, the experimental error σ_i with which each data point M_i is measured will itself contribute to σ_{rms}, thereby limiting the usefulness of this quantity as a measure of the validity of the model. Clearly, it would be better to replace σ_{rms} by some other quantity to which the experimental errors do not contribute.

By assuming that the inherent errors of the model follow a Gaussian distribution, Möller and Nix (1988) applied the method of maximum likelihood to obtain a *model standard deviation* given by

$$\sigma_{mod}^2 = \frac{1}{\sum w_i}\sum\ w_i\{(M_i - M_i^{mod})^2 - \sigma_i^2\}, \tag{B1}$$

[36]The accuracy of mass measurements is now so great that QED contributions to electronic binding energies have become relevant for the determination of atomic mass values of stable nuclides: see the recent discussion by Indelicato *et al.* (2001).

where M_i^{mod} is the model prediction for the data point i, and the weighting factor is

$$w_i = \frac{1}{(\sigma_i^2 + \sigma_{mod}^2)^k} \tag{B2}$$

with $k=2$. These two equations are given as Eqs. (42) and (43), respectively, in the paper of Möller and Nix (1988), although these authors write σ_{th}^{2*} in place of σ_{mod}^2. Actually, such a definition of σ_{mod} is intuitively plausible for any positive value of k and furthermore has the convenient property of reducing to the familiar σ_{rms} in the limit of all the experimental errors vanishing. However, the value of σ_{mod} depends on the value chosen for k, and only the analysis of Möller and Nix (1988) leads to a unique result.

These considerations have been extended by Möller *et al.* (1995) to the definition of a *model mean error*,

$$\overline{\epsilon}_{mod} = \frac{1}{\Sigma g_i} \sum g_i (M_i - M_i^{mod}). \tag{B3}$$

This is essentially Eq. (10) of Möller *et al.* (1995), except that we have written $\overline{\epsilon}_{mod}$ in place of μ_{th}^*. The weighting function in Eq. (B3) is

$$g_i = \frac{1}{\sigma_i^2 + \eta^2}, \tag{B4}$$

in which the quantity η^2 is given by

$$\eta^2 = \frac{1}{\sum g_i^2} \sum g_i^2 \{(M_i - M_i^{mod} - \overline{\epsilon}_{mod})^2 - \sigma_i^2\}, \tag{B5}$$

according to Eq. (9) of Möller *et al.* (1995).

Equations (B3) and (B5) are coupled through Eq. (B4), which means that to obtain $\overline{\epsilon}_{mod}$ we have to solve for η as well. The question thus arises, what is the meaning of η? We see from the definition (B5) that it can be interpreted as a "model standard deviation" around the mean error $\overline{\epsilon}_{mod}$, and indeed when the latter is zero we have $\eta = \sigma_{mod}$. For this reason Möller *et al.* (1995) write η^2 as σ_{th}^{2*} again, but in order to avoid all confusion we use a different symbol. In any case, η is a quantity of subsidiary interest and does not reduce to σ_{rms} when all the experimental errors vanish, but rather to $(\sigma_{rms}^2 - \overline{\epsilon}^2)^{1/2}$ (note that in that case $\overline{\epsilon}_{mod}$ still reduces to $\overline{\epsilon}$).

APPENDIX C: MINIMUM MASS OF NEUTRON STARS, AND THE SYMMETRY COEFFICIENT a_{sym}

It is known that binary systems of neutron stars lose energy through gravitational radiation, and it is generally supposed that the end result of this process will be a merger of the two stars. However, 30 years before any neutron star had ever been observed, it was pointed out that there must be a minimum mass $M_{\min}$, below which no neutron star could have a stable existence (Landau, 1938; Oppenheimer and Serber, 1938). It was thus speculated that in a binary system in which one neutron star was initially much lighter than the other, the lighter star could lose so much matter to the heavier that its mass would fall to $M_{\min}$ before an actual merger had taken place. The fate of the binary would then be an explosion of the lighter star rather than a merger of the two (Blinnikov *et al.*, 1984; Colpi *et al.*, 1989, 1991; Sumiyoshi *et al.*, 1998). It is thus a matter of some interest to calculate the actual value of $M_{\min}$. Haensel *et al.* (2002) have discussed the sensitivity of $M_{\min}$ to the equation of state of neutron-star matter; here we wish simply to point out that the symmetry coefficient a_{sym} must play a crucial role.

To see this we adopt an exceedingly simple model of the neutron star: we regard it as an enormous nucleus and represent it by the von Weizsäcker mass formula, Eq. (9), generalized to include gravity. Since this has a nonsaturating character formally identical to that of the Coulomb force, though with opposite sign, we can write for the energy per nucleon

$$\frac{E_{nuc}}{A} = a_{vol} + a_{sf} A^{-1/3} + \frac{3}{5r_0}\left\{\frac{e^2}{4}(1-I)^2 - GM^2\right\} A^{2/3} + (a_{sym} + a_{ss} A^{-1/3}) I^2, \tag{C1}$$

where G is the gravitational constant and M the nucleon mass. For normal nuclei the gravitational correction will be utterly negligible, but for very large values of A in systems consisting entirely of neutrons, $I=1$, we have

$$\frac{E_{nuc}}{A} = a_{vol} + a_{sym} - \frac{3GM^2}{5r_0} A^{2/3}. \tag{C2}$$

The sum of the nuclear terms, $a_{vol} + a_{sym}$, is always positive, but the system will be bound by gravity if the number of neutrons exceeds a certain critical minimum:

$$A \geq \left\{(a_{vol} + a_{sym}) \frac{5r_0}{3GM^2}\right\}^{3/2}. \tag{C3}$$

For the FRDM mass formula, $a_{sym} = 32.7$ MeV (see Table II), we find that the corresponding critical mass is 2.3×10^{29} kg, which is just 0.1 of the mass of a typical neutron star. It is plausible to regard this critical mass as an estimate of $M_{\min}$. For the HFB-2 mass formula, $a_{sym} = 28.0$ MeV, we find a value that is around 36% smaller.

In view of the extreme crudity of our model, little credence can be given to the absolute values of our estimates of $M_{\min}$, but at least we have given reason to believe that $M_{\min}$ should depend sensitively on a_{sym}. And in any case, we see why it is that the ablating star finally explodes: it is blown apart by the repulsive symmetry energy, once the nonsaturating gravitational attraction is no longer sufficient to overcome it.

APPENDIX D: TABLES

TABLE I. The rms error (σ) and mean error ($\overline{\epsilon}$) of fits given by various mass formulas to the masses of the 1995 (Audi and Wapstra, 1995) and 2001 (Audi and Wapstra, 2001) evaluations. Mass formula HFB-2 was fitted to the 2001 compilation, but all others were fitted to the 1995 or earlier evaluations. Errors are also shown for the 382 "new" nuclei appearing in the 2001 compilation with σ_{mod} and $\overline{\epsilon}_{mod}$ denoting errors determined using the analysis prescribed by Möller (Möller and Nix, 1988; Möller *et al.*, 1995; see text). The quantity R is the ratio of σ_{mod} of the "new" nuclei to the rms error of the 1995 compilation and is a measure of the predictive power of the mass formulas fitted to the 1995 data (R is shown graphically in Fig. 13). All errors are in MeV. The last four lines correspond to local relations for which predictions of all 382 "new" masses do not necessarily exist.

	1995 data (1768 nuclei)		2001 data (2135 nuclei)		"New" nuclei (382 nuclei)				
	σ	$\overline{\epsilon}$	σ	$\overline{\epsilon}$	σ	$\overline{\epsilon}$	σ_{mod}	$\overline{\epsilon}_{mod}$	R
HFBCS-1 (III.B.4)	0.718	0.102	0.805	0.180	1.115	0.494	1.056	0.460	1.47
HFB-1 (III.B.4)	0.740	0.040	0.822	0.131	1.123	0.510	1.091	0.494	1.47
HFB-2 (III.B.4)			0.674	0.000	0.769	0.377	0.724	0.356	
HFB-2′ (III.B.4)	0.651	−0.039	0.702	0.058	0.857	0.470	0.789	0.437	1.21
FRDM (III.C.3)	0.678	0.023	0.676	0.072	0.655	0.247	0.485	0.202	0.71
TF-FRDM (III.C.5)	0.662	−0.034	0.655	−0.036	0.655	−0.085	0.511	−0.121	0.77
Duflo-Zuker (1995, 1999) (III.D.1)	0.346	−0.010	0.373	0.009	0.479	0.054	0.378	0.028	1.09
Koura *et al.* (2000) (III.D.2)	0.656	0.012	0.682	0.053	0.755	0.200	0.676	0.163	1.03
Nayak-Satpathy (1999) (III.D.3)	0.359	0.000	0.485	0.047	0.837	0.229	0.779	0.208	2.17
Audi-Wapstra (1995) (III.E.1)					0.317	0.053	0.122	−0.002	
Garvey and co-workers (1966, 1969) (III.E.2)	0.277	−0.010			0.717	0.127	0.653	0.096	2.36
Jänecke-Masson (1988) (III.E.2)	0.247	−0.010	0.319	0.010	0.540	0.070	0.451	0.071	1.83
Liran-Zeldes (1976) (III.E.4)	0.534	−0.005	0.586	−0.036	0.722	−0.226	0.554	−0.253	1.04

TABLE II. Macroscopic parameters of different mass formulas. The quantities in parentheses for the FRDM denote the values used in the microscopic part of the model.

	Eq. (9)	HFBCS-1	HFB-1	HFB-2	FRDM
a_v (MeV)	−15.73	−15.794	−15.805	−15.794	−16.247
a_{sym} (MeV)	26.46	27.95	27.81	28.00	32.73 (35)
r_0 (fm)	1.2185	1.1487	1.1492	1.1487	1.16
ρ_0 (fm^{-3})	0.13196	0.15749	0.15730	0.15749	0.153
K_{vol} (MeV)	∞	231.2	231.3	233.6	240 (300)
a_{sf} (MeV)	17.77	17.4	17.5	17.5	22.92 (22)
a_{ss} (MeV)	−17.70	−28.9	−29.3	−30.9	−82.5 (−95.7)

TABLE III. Nuclear-matter parameters specific to Hartree-Fock mass formulas.

	MSk7 (HFBCS)	BSk1 (HFB-1)	BSk2 (HFB-2)
M_s^*/M	1.050	1.050	1.042
M_v^*/M	1.050	1.050	0.860
G_0	−0.081	−0.079	−0.705
G_0'	0.229	0.220	0.446
ρ_{frmg}/ρ_0	1.47	1.47	1.12

REFERENCES

Aalseth, C. E., F. T. Avignone III, A. Barabash, F. Boehm, R. L. Brodzinski, J. I. Collar, P. J. Doe, H. Ejiri, S. R. Elliott, E. Fiorini, R. J. Gaitskell, G. Gratta, *et al.*, 2002, Mod. Phys. Lett. A **17**, 1475.

Aboussir, Y., J. M. Pearson, A. K. Dutta, and F. Tondeur, 1992, Nucl. Phys. A **549**, 155.

Aboussir, Y., J. M. Pearson, A. K. Dutta, and F. Tondeur, 1995, At. Data Nucl. Data Tables **61**, 127.

Abzouzi, A., E. Caurier, and A. P. Zuker, 1991, Phys. Rev. Lett. **66**, 1134.

Akmal, A., V. R. Pandharipande, and D. G. Ravenhall, 1998, Phys. Rev. C **58**, 1804.

Armbruster, P., 2000, Annu. Rev. Nucl. Part. Sci. **50**, 411.

Arnould, M. and K. Takahashi, 1999, Rep. Prog. Phys. **62**, 395.

Aston, F. W., 1920, Nature (London) **105**, 617.

Aston, F. W., 1933, *Mass Spectra and Isotopes* (Edward Arnold, London) [2nd ed. (Edward Arnold, London, 1942)].

Athanassopoulos, S. T., E. Mavrommatis, K. A. Gernoth, and J. W. Clark, 2003, in *Exotic Nuclei and Atomic Masses (ENAM2001)*, edited by J. Äystö, P. Dendooven, A. Jokinen, and M. Leino (Springer-Verlag, Heidelberg), p. 49.

Audi, G., 2001, Hyperfine Interact. **132**, 7.

Audi, G., O. Bersillon, J. Blachot, and A. H. Wapstra, 1997, Nucl. Phys. A **624**, 1.

Audi, G., W. G. Davies, and G. E. Lee-Whiting, 1986, Nucl. Instrum. Methods Phys. Res. A **249**, 443.

Audi, G., and A. H. Wapstra, 1993, Nucl. Phys. A **565**, 1.

Audi, G., and A. H. Wapstra, 1995, Nucl. Phys. A **595**, 409.

Audi, G., and A. H. Wapstra, 2001, private communication.

Audi, G., A. H. Wapstra, and M. Dedieu, 1993, Nucl. Phys. A **565**, 193.

Auger, G., W. Mittig, A. Lépine-Szily, L. K. Fifield, M. Bajard, E. Baron, D. Bibet, P. Bricault, J. M. Casandjian, M. Chabert, M. Chartier, J. Fermé, *et al.*, 1994, Nucl. Instrum. Methods Phys. Res. A **350**, 235.

Äystö, J., V. Kolhinen, S. Rinta-Antila, S. Kopecky, J. Hakala, J. Huikari, A. Jokinen, A. Nieminen, and J. Szerypo, 2003, *Symmetries in Nuclear Structure* (unpublished).

Bäckman, S.-O., A. D. Jackson, and J. Speth, 1975, Phys. Lett. B **56**, 209.

Bai, Y., D. J. Vieira, H. L. Seifert, and J. M. Wouters, 1998, in *Exotic Nuclei and Atomic Masses ENAM98*, edited by B. M. Sherrill, D. J. Morrissey, and C. N. Davids, AIP Conf. Proc. No. 455 (AIP, Woodbury, NY), p. 90.

Baldo, M., G. Giansiracusa, U. Lombardo, and H. Q. Song, 2000, Phys. Lett. B **473**, 1.

Barber, R. C., and K. S. Sharma, 2003, Nucl. Instrum. Methods Phys. Res. B **204**, 460.

Barillari, D. K., J. V. Vaz, R. C. Barber, and K. S. Sharma, 2003, Phys. Rev. C **67**, 064316.

Barranco, F., R. A. Broglia, G. Gori, E. Vigezzi, P. F. Bortignon, and J. Terasaki, 1999, Phys. Rev. Lett. **83**, 2147.

Barranco, M. and J. Treiner, 1981, Nucl. Phys. A **351**, 269.

Barrett, B. R., B. Mihaila, S. C. Pieper, and R. B. Wiringa, 2003, Nucl. Phys. News **13** (1), 17.

Barton, C. J., D. S. Brenner, N. V. Zamfir, M. A. Caprio, A. Aprahamian, M. C. Wiescher, C. W. Beausang, Z. Berant, R. F. Casten, J. R. Cooper, R. L. Gill, R. Krücken, *et al.*, 2003, Phys. Rev. C **67**, 034310.

Baumann, T., M. J. Chromik, R. R. C. Clement, C. Freigang, P. Heckman, J. P. Seitz, B. M. Sherrill, M. Thoennessen, and E. J. Tryggestad, 2002, Nucl. Phys. A **701**, 282.

Beck, D., F. Ames, G. Audi, G. Bollen, F. Herfurth, H.-J. Kluge, A. Kohl, M. Koenig, D. Lunney, I. Martel, R. B. Moore, H. Raimbault-Hartmann, *et al.*, 2000, Eur. Phys. J. A **8**, 307.

Beck, M., F. Ames, D. Beck, G. Bollen, B. Delauré, J. Deutsch, V. V. Golovko, V. Y. Kozlov, I. S. Kraev, A. Lindroth, T. Phalet, W. Quint, *et al.*, 2003, Nucl. Instrum. Methods Phys. Res. B **204**, 521.

Becker, S., G. Bollen, F. Kern, H.-J. Kluge, R. B. Moore, G. Savard, L. Schweikhard, H. Stolzenberg, and the ISOLDE Collaboration, 1990, Int. J. Mass Spectrom. Ion Processes **99**, 53.

Beier, T., H. Häffner, N. Hermanspahn, S. Karshenboim, H.-J. Kluge, W. Quint, S. Stahl, J. Verdú, and G. Werth, 2002, Phys. Rev. Lett. **88**, 011603.

Beiner, M., H. Flocard, Nguyen Van Giai, and P. Quentin, 1975, Nucl. Phys. A **238**, 29.

Belozyorov, A. V., R. Kalpakchieva, Y. E. Penionzhkevich, Z. Dlouhý, Š. Piskoř, J. Vincour, H. G. Bohlen, M. von Lucke-Petsch, A. N. Ostrowski, D. V. Alexandrov, E. Y. Nikolskii, B. G. Novatskii, *et al.*, 1998, Nucl. Phys. A **636**, 419.

Benenson, W., and E. Kashy, 1979, Rev. Mod. Phys. **51**, 527.

Bennaceur, K., J. Dobaczewski, and M. Płoszajczak, 1999, Phys. Rev. C **60**, 034308.

Berger, J.-F., L. Bitaud, J. Dechargé, M. Girod, and K. Dietrich, 2001, Nucl. Phys. A **685**, 1c.

Berman, B. L., and S. C. Fultz, 1975, Rev. Mod. Phys. **47**, 713.

Bernard, V., and Nguyen Van Giai, 1980, Nucl. Phys. A **348**, 75.

Bertsch, G. F., and H. Esbensen, 1991, Ann. Phys. (N.Y.) **209**, 327.

Bertsch, G. F., and T. T. S. Kuo, 1968, Nucl. Phys. A **112**, 204.

Bethe, H. A., 1971, Annu. Rev. Nucl. Sci. **21**, 93.

Bethe, H. A., and R. F. Bacher, 1936, Rev. Mod. Phys. **8**, 82.

Bianchi, L., B. Fernandez, J. Gastebois, A. Gillibert, W. Mittig, and J. Barrette, 1989, Nucl. Instrum. Methods Phys. Res. A **276**, 509.

Blaizot, J. P., 1980, Phys. Rep. **64**, 171.

Blaum, K., G. Bollen, F. Herfurth, A. Kellerbauer, H.-J. Kluge, M. Kuckein, S. Heinz, P. Schmidt, and L. Schweikhard, 2003, J. Phys. B **36**, 921.

Blaum, K., G. Bollen, F. Herfurth, A. Kellerbauer, H.-J. Kluge, M. Kuckein, E. Sauvan, C. Scheidenberger, and L. Schweikhard, 2002, Eur. Phys. J. A **15**, 245.

Blaum, K., and the ISOLTRAP Collaboration, 2003, private communication.

Blinnikov, S. I., I. D. Novikov, T. V. Perevodchikova, and A. G. Polnarev, 1984, Sov. Astron. Lett. **10**, 177.

Bohigas, O., A. M. Lane, and J. Martorell, 1979, Phys. Rep. **51**, 267.

Bohigas, O., and P. Leboeuf, 2002, Phys. Rev. Lett. **88**, 092502.

Bohr, A., and B. R. Mottelson, 1953, K. Dan. Vidensk. Selsk. Mat. Fys. Medd. **27**, 16.

Bohr, N., 1939, Phys. Rev. **55**, 418.

Bollen, G., 2001, Nucl. Phys. A **693**, 3.

Bollen, G., F. Ames, G. Audi, D. Beck, J. Dilling, O. Engels, S. Henry, F. Herfurth, A. Kellerbauer, H.-J. Kluge, A. Kohl, E. Lamour, *et al.*, 2001, Hyperfine Interact. **132**, 215.

Bollen, G., S. Becker, H.-J. Kluge, M. König, R. B. Moore, T. Otto, H. Raimbault-Hartmann, G. Savard, L. Schweikhard,

H. Stolzenberg, and the ISOLDE Collaboration, 1996, Nucl. Instrum. Methods Phys. Res. A **368**, 675.
Bollen, G., H.-J. Kluge, M. König, T. Otto, G. Savard, H. Stolzenberg, R. B. Moore, G. Rouleau, G. Audi, and the ISOLDE Collaboration, 1992, Phys. Rev. C **46**, R2140.
Bolsterli, M., E. O. Fiset, J. R. Nix, and J. L. Norton, 1972, Phys. Rev. C **5**, 1050.
Borcea, C., and G. Audi, 1993, Rom. J. Phys. **38**, 455.
Borcea, C., and G. Audi, 1998, in *Exotic Nuclei and Atomic Masses ENAM98*, edited by B. M. Sherrill, D. J. Morrissey, and C. N. Davids, AIP Conf. Proc. No. 455 (AIP, Woodbury, NY), p. 98.
Borcea, C., G. Audi, A. H. Wapstra, and P. Favaron, 1993, Nucl. Phys. A **565**, 158.
Borzov, I. N., S. V. Tolokonnikov, and S. A. Fayans, 1984, Sov. J. Nucl. Phys. **40**, 732.
Bosch, F., T. Faestermann, J. Friese, F. Heine, P. Kienle, E. Wefers, K. Zeitelhack, K. Beckert, B. Franzke, O. Klepper, C. Kozhuharov, G. Menzel, *et al.*, 1996, Phys. Rev. Lett. **77**, 5190.
Brack, M., J. Damgaard, A. S. Jensen, H. C. Pauli, V. M. Strutinsky, and C. Y. Wong, 1972, Rev. Mod. Phys. **44**, 320.
Brack, M., C. Guet, and H.-B. Håkansson, 1985, Phys. Rep. **123**, 275.
Bradley, M. P., J. V. Porto, S. Rainville, J. K. Thompson, and D. E. Pritchard, 1999, Phys. Rev. Lett. **83A**, 4510.
Brenner, D. S., 2001, Hyperfine Interact. **132**, 255.
Brenner, D. S., B. D. Foy, C. J. Barton, C. N. Davids, D. Seweryniak, D. Blumenthal, R. L. Gill, N. V. Zamfir, and D. D. Warner, 1998, in *Exotic Nuclei and Atomic Masses ENAM98*, edited by B. M. Sherrill, D. J. Morrissey, and C. N. Davids, AIP Conf. Proc. No. 455 (AIP, Woodbury, NY), p. 102.
Brenner, D. S., C. Wesselborg, R. F. Casten, D. D. Warner, and J.-Y. Zhang, 1990, Phys. Lett. B **243**, 1.
Britz, J., A. Pape, and M. S. Antony, 1998, At. Data Nucl. Data Tables **69**, 125.
Brown, B. A., 2000, Phys. Rev. Lett. **85**, 5296.
Brown, B. A., R. R. C. Clement, H. Schatz, A. Volya, and W. A. Richter, 2002, Phys. Rev. C **65**, 045802.
Brown, B. A., W. A. Richter, and R. Lindsay, 2000, Phys. Lett. B **483**, 49.
Brown, G. E., 1971, *Unified Theory of Nuclear Models and Forces*, 3rd ed. (North-Holland, Amsterdam).
Brown, G. E., and T. T. S. Kuo, 1967, Nucl. Phys. A **92**, 481.
Brown, L. S., and G. Gabrielse, 1986, Rev. Mod. Phys. **58**, 233.
Brueckner, K. A., and J. L. Gammel, 1958, Phys. Rev. **109**, 1023.
Brunner, S., T. Engel, A. Schmitt, and G. Werth, 2001, Eur. Phys. J. D **15**, 181.
Buchinger, F., J. M. Pearson, and S. Goriely, 2001, Phys. Rev. C **64**, 067303.
Bulgac, A. and V. R. Shaginyan, 1999, Phys. Lett. B **469**, 1.
Bunatian, G. G., V. M. Kolomietz, and V. M. Strutinsky, 1972, Nucl. Phys. A **188**, 225.
Butler, M. N., D. W. L. Sprung, and J. Martorell, 1984, Nucl. Phys. A **422**, 157.
Canchel, G., L. Achouri, J. Äystö, R. Béraud, B. Blank, E. Chabanat, S. Czajkowski, P. Dendooven, A. Emsallem, J. Giovinazzo, J. Honkanen, A. Jokinen, *et al.*, 2001, Eur. Phys. J. A **12**, 377.
Caurier, E., G. Martinez-Pinedo, F. Nowacki, A. Poves, J. Retamosa, and A. P. Zuker, 1999, Phys. Rev. C **59**, 2033.
Caurier, E., F. Nowacki, A. Poves, and J. Retamosa, 1998, Phys. Rev. C **58**, 2033.
Chabanat, E., P. Bonche, P. Haensel, J. Meyer, and R. Schaeffer, 1997, Nucl. Phys. A **627**, 710.
Chabanat, E., P. Bonche, P. Haensel, J. Meyer, and R. Schaeffer, 1998, Nucl. Phys. A **635**, 231.
Chartier, M., G. Auger, W. Mittig, A. Lépine-Szily, L. K. Fifield, J. M. Casandjian, M. Chabert, J. Fermé, A. Gillibert, M. Lewitowicz, M. Mac Cormick, M. H. Moscatello, *et al.*, 1996, Phys. Rev. Lett. **77**, 2400.
Chartier, M., W. Mittig, G. Auger, B. Blank, J. M. Casandjian, M. Chabert, J. Fermé, L. K. Fifield, A. Gillibert, A. S. Lalleman, A. Lépine-Szily, M. Lewitowicz, *et al.*, 2001, Hyperfine Interact. **132**, 275.
Chartier, M., W. Mittig, N. A. Orr, J.-C. Angélique, G. Audi, J.-M. Casandjian, A. Cunsolo, C. Donzaud, A. Foti, A. Lépine-Szily, M. Lewitowicz, S. Lukyanov, *et al.*, 1998, Nucl. Phys. A **637**, 3.
Chen, B., J. Dobaczewski, K.-L. Kratz, K. Langanke, B. Pfeiffer, F.-K. Thielemann, and P. Vogel, 1995, Phys. Lett. B **355**, 37.
Clark, J. A., R. C. Barber, C. Boudreau, F. Buchinger, J. A. Caggiano, J. E. Crawford, H. Fukutani, S. Gulick, J. C. Hardy, A. Heinz, J. K. P. Lee, M. Maier, *et al.*, 2003, *in Exotic Nuclei and Atomic Masses (ENAM2001)*, edited by J. Äystö, P. Dendooven, A. Jokinen, and M. Leino (Springer-Verlag, Heidelberg), p. 39.
Clark, J., R. C. Barber, C. Boudreau, F. Buchinger, J. E. Crawford, S. Gulick, J. C. Hardy, A. Heinz, J. K. P. Lee, R. B. Moore, G. Savard, D. Seweryniak, *et al.*, 2003, Nucl. Instrum. Methods Phys. Res. B **204**, 487.
Clark, J. A., K. S. Sharma, and G. Savard, 2003, private communication.
Coc, A., R. Le Gac, M. de Saint Simon, C. Thibault, and F. Touchard, 1988, Nucl. Instrum. Methods Phys. Res. A **271**, 512.
Cocher, S., and I. Hofmann, 1990, Part. Accel. **34**, 189.
Cohen, E. R., and A. H. Wapstra, 1983, Nucl. Instrum. Methods Phys. Res. **211**, 153.
Colpi, M., S. L. Shapiro, and S. A. Teukolsky, 1989, Astrophys. J. **339**, 318.
Colpi, M., S. L. Shapiro, and S. A. Teukolsky, 1991, Astrophys. J. **369**, 422.
Comay, E., I. Kelson, and A. Zidon, 1988, At. Data Nucl. Data Tables **39**, 235.
Cornell, E. A., R. M. Weisskopf, K. R. Boyce, R. W. Flanagan, Jr., G. P. Lafyatis, and D. E. Pritchard, 1989, Phys. Rev. Lett. **63**, 1674.
Cornell, E. A., R. M. Weisskopf, K. R. Boyce, R. W. Flanagan, Jr., G. P. Lafyatis, and D. E. Pritchard, 1990, Phys. Rev. Lett. **64**, 2099.
Cugnon, J., P. Deneye, and A. Lejeune, 1987, Z. Phys. A **328**, 409.
Danared, H., 1995, Phys. Scr. T **59**, 121.
Davids, C. N., P. J. Woods, J. C. Batchelder, C. R. Bingham, D. J. Blumenthal, L. T. Brown, B. C. Busse, M. P. Carpenter, L. F. Conticchio, T. Davinson, J. Deboer, S. J. Freeman, *et al.*, 2001, Hyperfine Interact. **132**, 133.
Davies, K. T. R., S. J. Krieger, and M. Baranger, 1966, Nucl. Phys. **84**, 545.
Day, B. D., 1967, Rev. Mod. Phys. **39**, 719.
Dechargé, J., and D. Gogny, 1980, Phys. Rev. C **21**, 1568.
Dehmelt, H., 1990, Rev. Mod. Phys. **62**, 525.

Delahaye, P., G. Ban, D. Durand, A. M. Vinodkumar, C. Le Brun, E. Liénard, F. Mauger, O. Naviliat, J. Szerypo, and B. Tamain, 2001, Hyperfine Interact. **132**, 479.
Della Negra, S., H. Gauvin, D. Jacquet, and Y. Le Beyec, 1982, Z. Phys. A **307**, 305.
Dilling, J., D. Ackermann, F. P. Heßberger, S. Hofmann, H.-J. Kluge, G. Marx, G. Münzenberg, Z. Patyk, W. Quint, D. Rodriguez, C. Scheidenberger, J. Schönfelder, *et al.*, 2001, Hyperfine Interact. **132**, 495.
Dilling, J., G. Audi, D. Beck, G. Bollen, F. Herfurth, A. Kellerbauer, H.-J. Kluge, D. Lunney, R. B. Moore, C. Scheidenberger, S. Schwarz, G. Sikler, *et al.*, 2001, Hyperfine Interact. **132**, 331.
Dilling, J., P. Bricault, M. Smith, H.-J. Kluge, and TITAN Collaboration, 2003, Nucl. Instrum. Methods Phys. Res. B **204**, 492.
Dobaczewski, J., H. Flocard, and J. Treiner, 1984, Nucl. Phys. A **422**, 103.
Dobaczewski, J., W. Nazarewicz, T. R. Werner, J.-F. Berger, C. R. Chinn, and J. Dechargé, 1996, Phys. Rev. C **53**, 2809.
Douysset, G., T. Fritioff, C. Carlberg, I. Bergström, and M. Björkhage, 2001, Phys. Rev. Lett. **86**, 4259.
Duflo, J., and A. P. Zuker, 1995, Phys. Rev. C **52**, R23.
Duflo, J., and A. P. Zuker, 1999, Phys. Rev. C **59**, R2347.
Duguet, T., P. Bonche, P.-H. Heenen, and J. Meyer, 2002a, Phys. Rev. C **65**, 014310.
Duguet, T., P. Bonche, P.-H. Heenen, and J. Meyer, 2002b, Phys. Rev. C **65**, 014311.
Dutta, A. K., J.-P. Arcoragi, J. M. Pearson, R. Behrman, and F. Tondeur, 1986, Nucl. Phys. A **458**, 77.
Dutta, A. K., J.-P. Arcoragi, J. M. Pearson, R. H. Behrman, and M. Farine, 1986, Nucl. Phys. A **454**, 374.
Dutta, A. K., and J. M. Pearson, 1987, Pramana **29**, 379.
Eddington, A. S., 1920, Nature (London) **106**, 14.
Eddington, A. S., 1926, *The Internal Constitution of the Stars* (Cambridge University Press, Cambridge) (Dover edition, New York, 1959).
Elliott, S. R., and P. Vogel, 2002, Annu. Rev. Nucl. Part. Sci. **52**, 115.
Elsasser, W., 1933, J. Phys. Radium **4**, 549.
Elsasser, W., 1934a, J. Phys. Radium **5**, 389.
Elsasser, W., 1934b, J. Phys. Radium **5**, 635.
Engel, Y. M., D. M. Brink, K. Goeke, S. J. Krieger, and D. Vautherin, 1975, Nucl. Phys. A **249**, 215.
Engels, O., L. Beck, G. Bollen, D. Habs, G. Marx, J. Neumayr, U. Schramm, S. Schwarz, P. Thirolf, and V. Varentsov, 2001, Hyperfine Interact. **132**, 505.
Engvik, L. M. Hjorth-Jensen, R. Machleidt, H. Müther, and A. Polls, 1997, Nucl. Phys. A **627**, 85.
Falch, M., 2000, *Schottky Massenmessungen mit TCAP Datenaufnahmesystem am Experimentierspeicherring der GSI*, Ph.D. thesis (Ludwich Maximilians Universität, München).
Farine, M., 1981, *Calcul des coefficients macroscopiques des formules de masse dans l'approximation de Hartree-Fock*, Ph.D. thesis (Université de Montréal).
Farine, M., 2001, private communication.
Farine, M., J. Côté, and J. M. Pearson, 1980, Nucl. Phys. A **338**, 86.
Farine, M., J. M. Pearson, and F. Tondeur, 1997, Nucl. Phys. A **615**, 135.
Farine, M., J. M. Pearson, and F. Tondeur, 2001, Nucl. Phys. A **696**, 396.
Fayans, S. A., S. V. Tolokonnikov, E. L. Trykov, and D. Zawischa, 2000, Nucl. Phys. A **676**, 49.
Fedosseev, V. N., D. V. Fedorov, R. Horn, G. Huber, U. Köster, J. Lassen, V. I. Mishin, M. D. Seliverstov, L. Weissman, K. Wendt, and the ISOLDE Collaboration, 2003, Nucl. Instrum. Methods Phys. Res. B **204**, 353.
Fogelberg, B., K. A. Mezilev, H. Mach, V. I. Isakov, and J. Slivova, 1999, Phys. Rev. Lett. **82**, 1823.
Foldy, L. L., 1951, Phys. Rev. **83**, 397.
Fossion, R., C. de Coster, J. E. Garcia-Ramos, T. Werner, and K. Heyde, 2002, Nucl. Phys. A **697**, 703.
Franzke, B., K. Beckert, H. Eickhoff, F. Nolden, H. Reich, U. Schaaf, B. Schlitt, A. Schwinn, M. Steck, and T. Winkler, 1995, Phys. Scr. T **59**, 176.
Friedman, B., and V. R. Pandharipande, 1981, Nucl. Phys. A **361**, 502.
Friedman, F. L., and V. F. Weisskopf, 1955, in *Niels Bohr and the Development of Physics*, edited by W. Pauli (McGraw-Hill, New York), p. 134.
Fritioff, T., H. Bluhme, R. Schuch, I. Bergström, and M. Björkhage, 2002, Eur. Phys. J. A **15**, 249.
Fritioff, T., C. Carlberg, G. Douysset, R. Schuch, and I. Bergström, 2001a, Hyperfine Interact. **132**, 231.
Fritioff, T., C. Carlberg, G. Douysset, R. Schuch, and I. Bergström, 2001b, Eur. Phys. J. D **15**, 141.
Fritz, R., H. Müther, and R. Machleidt, 1993, Phys. Rev. Lett. **71**, 46.
Gabrielse, G., 1990, Phys. Rev. Lett. **64**, 2098.
Gabrielse, G., A. Khabbaz, D. S. Hall, C. Heimann, H. Kalinowski, and W. Jhe, 1999, Phys. Rev. Lett. **82**, 3198.
Gamow, G., 1930, Proc. R. Soc. London, Ser. A **126**, 632.
Gan, Z. G., Z. Qin, H. M. Fan, X. G. Lei, Y. B. Xu, J. J. He, H. Y. Liu, X. L. Wu, J. S. Guo, X. H. Zhou, S. G. Yuan, and G. M. Jin, 2001, Eur. Phys. J. A **10**, 21.
Garrido, E., P. Sarriguren, E. Moya de Guerra, and P. Schuck, 1999, Phys. Rev. C **60**, 064312.
Garvey, G. T., W. J. Gerace, R. L. Jaffe, I. Talmi, and I. Kelson, 1969, Rev. Mod. Phys. **41**, S1.
Garvey, G. T., and I. Kelson, 1966, Phys. Rev. Lett. **16**, 197.
Gaulard, C., G. Audi, D. Lunney, M. de Saint Simon, C. Thibault, and N. Vieira, 2003, private communication.
Gazula, S., J. W. Clark, and H. Bohr, 1992, Nucl. Phys. A **540**, 1.
Geissel, H., F. Attallah, K. Beckert, F. Bosch, M. Falch, B. Franzke, M. Hausmann, T. Kerscher, O. Klepper, H.-J. Kluge, C. Kozhuharov, Y. Litvinov, *et al.*, 2001, Nucl. Phys. A **685**, 115c.
Geissel, H., G. Münzenberg, and K. Riisager, 1995, Annu. Rev. Nucl. Sci. **45**, 163.
Geissel, H., H. Weick, M. Winkler, G. Münzenberg, V. Chichkine, M. Yavor, T. Aumann, K. H. Behr, M. Böhmer, A. Brünle, K. Burkard, J. Benlliure, *et al.* 2003, Nucl. Instrum. Methods Phys. Res. B **204**, 71.
Gernoth, K. A., and J. W. Clark, 1995a, Neural Networks **8**, 291.
Gernoth, K. A., and J. W. Clark, 1995b, Comput. Phys. Commun. **88**, 1.
Gernoth, K. A., J. W. Clark, J. S. Prater, and H. Bohr, 1993, Phys. Lett. B **300**, 1.
Ghosh, P. K., 1995, *Ion Traps* (Clarendon, Oxford).
Giovanardi, N., F. Barranco, R. A. Broglia, and E. Vigezzi, 2002, Phys. Rev. C **65**, 041304.

Giovinazzo, J., B. Blank, M. Chartier, S. Czajkowski, A. Fleury, M. J. Lopez Jimenez, M. S. Pravikoff, J.-C. Thomas, F. de Oliveira Santos, M. Lewitowicz, V. Maslov, *et al.*, 2002, Phys. Rev. Lett. **89**, 102501.

Gomes, L. C., J. D. Walecka, and V. F. Weisskopf, 1958, Ann. Phys. (N.Y.) **3**, 241.

Goodman, A. L., 1979, Adv. Nucl. Phys. **11**, 263.

Goriely, S., 2000, in *Capture Gamma-Ray Spectroscopy and Related Topics*, edited by S. Wender, AIP Conf. Proc. No. 529 (AIP, Melville, NY), p. 287.

Goriely, S., 2003, Nucl. Phys. A **718**, 287c.

Goriely, S., and E. Khan, 2002, Nucl. Phys. A **706**, 217.

Goriely, S., M. Samyn, P.-H. Heenen, J. M. Pearson, and F. Tondeur, 2002, Phys. Rev. C **66**, 024326.

Goriely, S., F. Tondeur, and J. M. Pearson, 2001, At. Data Nucl. Data Tables **77**, 311.

Grunder, H. A., 2002, Nucl. Phys. A **701**, 43.

Guerreau, D., 2002, Eur. Phys. J. A **13**, 263.

Habs, D., M. Groß, W. Assmann, F. Ames, H. Bongers, S. Emhofer, S. Heinz, S. Henry, O. Kester, J. Neumayr, F. Ospald, P. Reiter *et al.*, 2003, Nucl. Instrum. Methods Phys. Res. B **204**, 739.

Haensel, P., J. L. Zdunik, and F. Douchin, 2002, Astron. Astrophys. **385**, 301.

Hansen, P. G., A. S. Jensen, and B. Jonson, 1995, Annu. Rev. Nucl. Part. Sci. **45**, 591.

Hardy, J. C., and I. S. Towner, 2001, Hyperfine Interact. **132**, 115.

Hardy, J. C., and I. S. Towner, 2002, Eur. Phys. J. A **15**, 223.

Hausmann, M., J. Stadlmann, F. Attallah, K. Beckert, P. Beller, F. Bosch, H. Eickhoff, M. Falch, B. Franczak, B. Franzke, H. Geissel, T. Kerscher, *et al.*, 2001, Hyperfine Interact. **132**, 291.

Haxel, O., J. H. D. Jensen, and H. E. Suess, 1948, Naturwissenschaften **35**, 376.

Haxel, O., J. H. D. Jensen, and H. E. Suess, 1949a, Naturwissenschaften **36**, 153.

Haxel, O., J. H. D. Jensen, and H. E. Suess, 1949b, Naturwissenschaften **36**, 155.

Haxel, O., J. H. D. Jensen, and H. E. Suess, 1949c, Phys. Rev. **75**, 1766.

Haxel, O., J. H. D. Jensen, and H. E. Suess, 1950, Z. Phys. **128**, 295.

Henning, W. F., 2003, Nucl. Instrum. Methods Phys. Res. B **204**, 725.

Henry, S., C. Bachelet, Z. Djouadi, C. Gaulard, M. de Saint Simon, and D. Lunney, 2003, in *Exotic Nuclei and Atomic Masses (ENAM2001)*, edited by J. Äystö, P. Dendooven, A. Jokinen, and M. Leino (Springer-Verlag, Heidelberg), p. 490.

Herfurth, F., F. Ames, G. Audi, D. Beck, K. Blaum, G. Bollen, A. Kellerbauer, H.-J. Kluge, M. Kuckein, D. Lunney, R. B. Moore, M. Oinonen, *et al.*, 2003, J. Phys. B **36**, 931.

Herfurth, F., J. Dilling, A. Kellerbauer, G. Audi, D. Beck, G. Bollen, H.-J. Kluge, D. Lunney, R. B. Moore, C. Scheidenberger, S. Schwarz, G. Sikler, *et al.*, 2001, Phys. Rev. Lett. **87**, 142501.

Herfurth, F., J. Dilling, A. Kellerbauer, G. Bollen, S. Henry, H.-J. Kluge, E. Lamour, D. Lunney, R. B. Moore, C. Scheidenberger, S. Schwarz, G. Sikler, *et al.*, 2001, Nucl. Instrum. Methods Phys. Res. A **469**, 254.

Herfurth, F., A. Kellerbauer, F. Ames, G. Audi, D. Beck, K. Blaum, G. Bollen, O. Engels, H.-J. Kluge, D. Lunney, R. B. Moore, M. Oinonen, *et al.*, 2002, Eur. Phys. J. A **15**, 17.

Heßberger, F. P., S. Hofmann, D. Ackermann, V. Ninov, M. Leino, G. Münzenberg, S. Saro, A. Lavrentev, A. G. Popeko, A. V. Yeremin, and C. Stodel, 2001, Eur. Phys. J. A **12**, 57.

Heßberger, F. P., S. Hofmann, D. Ackermann, V. Ninov, M. Leino, S. Saro, A. Andreyev, A. Lavrentev, A. G. Popeko, and A. V. Yeremin, 2000, Eur. Phys. J. A **8**, 521.

Hoffmann, G. W., L. Ray, M. Barlett, J. McGill, G. S. Adams, G. J. Igo, F. Irom, A. T. M. Wang, C. A. Whitten, Jr., R. L. Boudrie, J. F. Amann, C. Glashausser, *et al.*, 1980, Phys. Rev. C **21**, 1488.

Hofmann, S., 2002, Eur. Phys. J. A **15**, 195.

Hofmann, S., F. P. Heßberger, D. Ackermann, S. Antalic, P. Cagarda, S. Cwiok, B. Kindler, J. Kojouharova, B. Lommel, R. Mann, G. Münzenberg, A. G. Popeko, *et al.*, 2001, Eur. Phys. J. A **10**, 5.

Hofmann, S., and G. Münzenberg, 2000, Rev. Mod. Phys. **72**, 733.

Horowitz, C. J., and J. Piekarewicz, 2001a, Phys. Rev. Lett. **86**, 5647.

Horowitz, C. J., and J. Piekarewicz, 2001b, Phys. Rev. C **64**, 062802.

Horowitz, C. J., S. J. Pollock, P. A. Souder, and R. Michaels, 2001, Phys. Rev. C **63**, 025501.

Huang, K.-N., M. Aoyagi, M. H. Chen, B. Crasemann, and H. Mark, 1976, At. Data Nucl. Data Tables **18**, 243.

Hugenholtz, N. M., and L. Van Hove, 1958, Physica (Utrecht) **24**, 363.

Indelicato, P., E. Lindroth, T. Beier, J. Bieroń, A. M. Costa, I. Lindgren, J. P. Marques, A.-M. Mårtenson-Pendrill, M. C. Martins, M. A. Ourdane, F. Parente, P. Patté, *et al.*, 2001, Hyperfine Interact. **132**, 349.

Issmer, S., M. Fruneau, J. A. Pinston, M. Asghar, D. Barnoud, J. Genevey, T. Kerscher, and K. E. G. Löbner, 1998, Eur. Phys. J. A **2**, 173.

Itano, W. M., J. Bergquist, J. Bollinger, and D. Wineland, 1995, Phys. Scr. T **59**, 106.

Jänecke, J., and P. J. Masson, 1988, At. Data Nucl. Data Tables **39**, 265.

Jennings, B. K., R. K. Bhaduri, and M. Brack, 1975, Nucl. Phys. A **253**, 29.

Jensen, A. S., P. G. Hansen, and B. Jonson, 1984, Nucl. Phys. A **431**, 393.

Jokinen, A., A. Nieminen, J. Äystö, R. Borcea, E. Caurier, P. Dendooven, M. Gierlik, M. Górska, H. Grawe, M. Hellström, M. Karny, Z. Janas, *et al.*, 2002, EPJdirect4 **A3**, 1.

Jonson, B., 2002, Nucl. Phys. A **701**, 35.

Jonson, B., and A. Richter, 2000, Hyperfine Interact. **129**, 1.

Kaiser, N., S. Fritsch, and W. Weise, 2002a, Nucl. Phys. A **697**, 255.

Kaiser, N., S. Fritsch, and W. Weise, 2002b, Nucl. Phys. A **700**, 343.

Kalpakchieva, R., H. G. Bohlen, W. von Oertzen, B. Gebauer, M. von Lucke-Petsch, T. N. Massey, A. N. Ostrowski, T. Stolla, M. Wilpert, and T. Wilpert, 2000, Eur. Phys. J. A **7**, 451.

Kessler, E. G., Jr., M. S. Dewey, R. D. Deslattes, A. Henins, H. G. Boerner, M. Jentschel, C. Doll, and H. Lehmann, 1999, Phys. Lett. A **255**, 221.

Kester, O., D. Habs, M. Groß, H. J. Maier, P. G. Thirolf, T. Sieber, T. Faestermann, T. von Egidy, and U. Köster, 2002, Nucl. Phys. A **701**, 71.

Kettunen, H., J. Uusitalo, M. Leino, P. Jones, K. Eskola, P. T. Greenlees, K. Helariutta, R. Julin, S. Juutinen, H. Kankaanpää, P. Kuusiniemi, M. Muikku, *et al.*, 2001, Phys. Rev. C **63**, 044315.

Klapdor-Kleingrothaus, H. V., A. Dietz, H. L. Harney, and I. V. Krivosheina, 2001, Mod. Phys. Lett. A **16**, 2409.

Kolhinen, V. S., T. Eronen, J. Hakala, A. Jokinen, S. Kopecky, S. Rinta-Antila, J. Szerypo, and J. Äystö, 2003, Nucl. Instrum. Methods Phys. Res. B **204**, 502.

Köster, U., 2000, *Ausbeuten und Spektroskopie radioaktiver Isotope bei* LOHENGRIN *und* ISOLDE, Ph.D. thesis (Technische Universität, München).

Köster, U., 2002a, Eur. Phys. J. A **15**, 255.

Köster, U., 2002b, Nucl. Phys. A **701**, 441c.

Koura, H., M. Uno, T. Tachibana, and M. Yamada, 2000, Nucl. Phys. A **674**, 47.

Krappe, H. J., J. R. Nix, and A. J. Sierk, 1979, Phys. Rev. C **20**, 992.

Kratz, K.-L., B. Pfeiffer, F.-K. Thielemann, and W. B. Walters, 2000, Hyperfine Interact. **129**, 185.

Krivine, H., J. Treiner, and O. Bohigas, 1980, Nucl. Phys. A **336**, 155.

Kruppa, A. T., M. Bender, W. Nazarewicz, P.-G. Reinhard, T. Vertse, and S. Ćwiok, 2000, Phys. Rev. C **61**, 034313.

Kudryavtsev, Y., M. Facina, M. Huyse, J. Gentens, P. Van den Bergh, and P. Van Duppen, 2003, Nucl. Instrum. Methods Phys. Res. B **204**, 336.

Kudryavtsev, Y., S. Franchoo, J. Gentens, M. Huyse, R. Raabe, I. Reusen, P. Van Duppen, P. Van den Bergh, L. Vermeeren, and A. Wöhr, 1998, Rev. Sci. Instrum. **69**, 738.

Kugler, E., 2000, Hyperfine Interact. **129**, 23.

Kuo, T. T. S., 1967, Nucl. Phys. A **90**, 199.

Kuo, T. T. S., and G. E. Brown, 1966, Nucl. Phys. A **85**, 40.

Kuo, T. T. S., and G. E. Brown, 1968, Nucl. Phys. A **114**, 241.

Kutschera, M., and W. Wójcik, 1994, Phys. Lett. B **325**, 271.

Lalazissis, G. A., S. Raman, and P. Ring, 1999, At. Data Nucl. Data Tables **71**, 1.

Lalleman, A. S., G. Auger, W. Mittig, M. Chabert, M. Chartier, J. Fermé, A. Gillibert, A. Lépine-Szily, M. Lewitowicz, M. H. Moscatello, N. A. Orr, G. Politi, *et al.*, 2001, Hyperfine Interact. **132**, 315.

Landau, L. D., 1938, Nature (London) **141**, 333.

Langevin, M., C. Détraz, D. Guillemaud-Mueller, A. C. Mueller, C. Thibault, F. Touchard, and M. Epherre, 1983, Phys. Lett. **125B**, 116.

Lattimer, J. M., F. Mackie, D. G. Ravenhall, and D. N. Schramm, 1977, Astrophys. J. **213**, 225.

Lattimer, J. M., C. J. Pethick, Madappa Prakash, and P. Haensel, 1991, Phys. Rev. Lett. **66**, 2701.

Lattimer, J. M., K. A. Van Riper, Madappa Prakash, and Manju Prakash, 1994, Astrophys. J. **425**, 802.

Lejeune, A., U. Lombardo, and W. Zuo, 2000, Phys. Lett. B **477**, 45.

Lépine-Szily, A., 2001, Hyperfine Interact. **132**, 35.

Leprêtre, A., H. Beil, R. Bergère, P. Carlos, J. Fagot, A. de Miniac, A. Veyssière, and H. Miyase, 1976, Nucl. Phys. A **258**, 350.

Lima, G. F., A. Lépine-Szily, G. Audi, W. Mittig, M. Chartier, N. A. Orr, R. Lichtenthaler, J. C. Angelique, J. M. Casandjian, A. Cunsolo, C. Donzaud, A. Foti, *et al.*, 2002, Phys. Rev. C **65**, 044618.

Lindroos, M., and the CERN ISOLDE team, the ISOLDE Collaboration, and the REX-ISOLDE Collaboration, 2003, Nucl. Instrum. Methods Phys. Res. B **204**, 730.

Liran, S., 1973, Ph.D. thesis (Jerusalem) (in Hebrew).

Liran, S., A. Marinov, and N. Zeldes, 2000, Phys. Rev. C **62**, 047301.

Liran, S., A. Marinov, and N. Zeldes, 2001, Phys. Rev. C **63**, 017302.

Liran, S., and N. Zeldes, 1976, At. Data Nucl. Data Tables **17**, 431.

Lister, C. J., P. E. Haustein, D. E. Alburger, and J. W. Olness, 1981, Phys. Rev. C **24**, 260.

Litvinov, Y., and C. Scheidenberger, 2002, private communication.

Litvinov, Y., *et al.*, 2003, in preparation.

Liu, Y., J. F. Liang, G. D. Alton, J. R. Beene, Z. Zhou, and H. Wollnik, 2002, Nucl. Instrum. Methods Phys. Res. B **187**, 117.

Lu, X., J. Guo, K. Zhao, Y. Cheng, Y. Ma, Z. Li, S. Li, and M. Ruan, 1998, Eur. Phys. J. A **2**, 149.

Lui, Y.-W., H. L. Clark, and D. H. Youngblood, 2001, Phys. Rev. C **64**, 064308.

Lukyanov, S. M., Y. E. Penionzhkevich, R. Astabatyan, S. Lobastov, Y. Sobolev, D. Guillemaud-Mueller, G. Faivre, F. Ibrahim, A. C. Mueller, F. Pougheon, O. Perru, O. Sorlin, *et al.*, 2002, J. Phys. G **28**, L41.

Lunney, D., G. Audi, C. Bachelet, K. Blaum, G. Bollen, C. Gaulard, S. Henry, F. Herfurth, A. Kellerbauer, A. Lépine-Szily, M. de Saint Simon, H. Simon, *et al.*, 2003, CERN-INTC-2003-007.

Lunney, D., G. Audi, H. Doubre, S. Henry, C. Monsanglant, M. de Saint Simon, C. Thibault, C. Toader, C. Borcea, G. Bollen, and the ISOLDE Collaboration, 2001, Phys. Rev. C **64**, 054311.

Lunney, D., G. Audi, and H.-J. Kluge, 2001, Eds., *Atomic Physics at Accelerators: Mass Spectrometry* (Kluwer Academic, Dordrecht). Also published as volume 132 of the journal Hyperfine Interactions.

Lunney, D., and G. Bollen, 2000, Hyperfine Interact. **129**, 249.

Lunney, D., C. Monsanglant, G. Audi, G. Bollen, C. Borcea, H. Doubre, C. Gaulard, S. Henry, M. de Saint Simon, C. Thibault, C. Toader, N. Vieira, *et al.*, 2001, Hyperfine Interact. **132**, 299.

Lunney, M. D. and R. B. Moore, 1999, Int. J. Mass Spectrom. Ion Processes **190**, 153.

Machleidt, R., 1989, Adv. Nucl. Phys. **19**, 189.

Madsen, N., P. Bowe, M. Drewsen, L. H. Hornekær, N. Kjærgaard, A. Labrador, J. S. Nielsen, J. P. Schiffer, P. Shi, and J. S. Hangst, 1999, Phys. Rev. Lett. **83**, 4301.

Mahaux, C., P. F. Bortignon, R. A. Broglia, and C. H. Dasso, 1985, Phys. Rep. **120**, 1.

Maier, M., C. Boudreau, F. Buchinger, J. A. Clark, J. E. Crawford, J. Dilling, H. Fukutani, S. Gulick, J. K. P. Lee, R. B. Moore, G. Savard, J. Schwartz, *et al.*, 2001, Hyperfine Interact. **132**, 521.

Mamdouh, A., J. M. Pearson, M. Rayet, and F. Tondeur, 1998, Nucl. Phys. A **644**, 389.

Mamdouh, A., J. M. Pearson, M. Rayet, and F. Tondeur, 2001, Nucl. Phys. A **679**, 337.

Mang, H. J., 1975, Phys. Rep. **18**, 325.

Margueron, J., J. Navarro, and Nguyen Van Giai, 2002, Phys. Rev. C **66**, 014303.

Marx, G., D. Ackerman, J. Dilling, F. P. Heßberger, S. Hofmann, H.-J. Kluge, R. Mann, G. Münzenberg, Z. Qamhieh, W. Quint, D. Rodriguez, M. Schädel, *et al.*, 2001, Hyperfine Interact. **132**, 463.
Masson, P. J., and J. Jänecke, 1988, At. Data Nucl. Data Tables **39**, 273.
Mavrommatis, E., S. T. Athanassopoulos, K. A. Gernoth, and J. W. Clark, 2000, Condens. Matter Theor. **15**, 207.
Mayer, M. G., 1948, Phys. Rev. **74**, 235.
Mayer, M. G., 1949, Phys. Rev. **75**, 1969.
Mayer, M. G., 1950, Phys. Rev. **78**, 16.
Mazzocchi, C., Z. Janas, J. Döring, M. Axiotis, L. Batist, R. Borcea, D. Cano-Ott, E. Caurier, G. de Angelis, E. Farnea, A. Faßbender, A. Gadea, *et al.*, 2001, Eur. Phys. J. A **12**, 269.
Meldner, H., 1967, Ark. Fys. **36**, 593.
Meyer, B. S., 1994, Annu. Rev. Astron. Astrophys. **32**, 153.
Meyer, J., J. Bartel, M. Brack, P. Quentin, and S. Aicher, 1986, Phys. Lett. B **172**, 122.
Mitsuoka, S., H. Ikezoe, T. Ikuta, Y. Nagame, K. Tsukada, I. Nishinaka, Y. Oura, and Y. L. Zhao, 1997, Phys. Rev. C **55**, 1555.
Mittig, W., A. Lépine-Szily, and N. A. Orr, 1997, Annu. Rev. Nucl. Sci. **47**, 27.
Mohr, P. J., and B. N. Taylor, 2000, Rev. Mod. Phys. **72**, 351.
Möller, P., and A. Iwamoto, 2000, Phys. Rev. C **61**, 047602.
Möller, P., W. D. Myers, W. J. Swiatecki, and J. Treiner, 1988, At. Data Nucl. Data Tables **39**, 225.
Möller, P., and J. R. Nix, 1981, Nucl. Phys. A **361**, 117.
Möller, P., and J. R. Nix, 1988, At. Data Nucl. Data Tables **39**, 213.
Möller, P., and J. R. Nix, 1992, Nucl. Phys. A **536**, 20.
Möller, P., J. R. Nix, W. D. Myers, and W. J. Swiatecki, 1995, At. Data Nucl. Data Tables **59**, 185.
Monsanglant, C., 2000, *Mesures de masses de haute précision avec* MISTRAL *au voisinage de* ^{32}*Mg,* Ph.D. thesis (Université Paris XI, Orsay).
Moore, R. B., and M. D. Lunney, 1995, in *Practical Aspects of Ion Trap Mass Spectrometry*, edited by R. E. March and J. F. J. Todd (CRC Press, Boca Raton), Vol. II, p. 263.
Morrissey, D. J., 2002, Eur. Phys. J. A **15**, 105.
Moszkowski, S. A., 1970, Phys. Rev. C **2**, 402.
Mottelson, B., 1962, *Proceedings of the International School of Physics Enrico Fermi XV Course* (Academic, New York), p. 44.
Myers, W. D., 1976, At. Data Nucl. Data Tables **17**, 411.
Myers, W. D., and W. J. Swiatecki, 1966, Nucl. Phys. **81**, 1.
Myers, W. D., and W. J. Swiatecki, 1969, Ann. Phys. (N.Y.) **55**, 395.
Myers, W. D., and W. J. Swiatecki, 1974, Ann. Phys. (N.Y.) **84**, 186.
Myers, W. D., and W. J. Swiatecki, 1982, Annu. Rev. Nucl. Part. Sci. **32**, 309.
Myers, W. D., and W. J. Swiatecki, 1996, Nucl. Phys. A **601**, 141.
Myers, W. D., W. J. Swiatecki, T. Kodama, L. J. El-Jaick, and E. R. Hilf, 1977, Phys. Rev. C **15**, 2032.
Nadjakov, E. G., K. P. Marinova, and Y. P. Gangrsky, 1994, At. Data Nucl. Data Tables **56**, 133.
Navrátil, P., J. P. Vary, W. E. Ormand, and B. R. Barrett, 2001, Phys. Rev. Lett. **87**, 172502.
Nayak, R. C., 1999, Phys. Rev. C **60**, 064305.
Nayak, R. C., and J. M. Pearson, 1995, Phys. Rev. C **52**, 2254.
Nayak, R. C., and J. M. Pearson, 1998, Phys. Rev. C **58**, 878.
Nayak, R. C., and L. Satpathy, 1999, At. Data Nucl. Data Tables **73**, 213.
Nazarewicz, W., T. R. Werner, and J. Dobaczewski, 1994, Phys. Rev. C **50**, 2860.
Nieminen, A., P. Campbell, J. Billowes, D. H. Forest, J. A. R. Griffith, J. Huikari, A. Jokinen, I. D. Moore, R. Moore, G. Tungate, and J. Äystö, 2002, Phys. Rev. Lett. **88**, 094801.
Nieminen, A., J. Huikari, A. Jokinen, J. Äystö, P. Campbell, E. C. A. Cochrane, and EXOTRAPS Collaboration, 2001, Nucl. Instrum. Methods Phys. Res. A **469**, 244.
Nolen, J. A., 2002, Eur. Phys. J. A **13**, 255.
Notani, M., H. Sakurai, N. Aoi, Y. Yanagisawa, A. Saito, N. Imai, T. Gomi, M. Miura, S. Michimasa, H. Iwasaki, N. Fukuda, M. Ishihara, *et al.*, 2002, Phys. Lett. B **542**, 49.
Novikov, Y. N., F. Attallah, F. Bosch, M. Falch, H. Geissel, M. Hausmann, T. Kerscher, O. Klepper, H.-J. Kluge, C. Kozhuharov, Y. A. Litvinov, K. E. G. Löbner, *et al.*, 2002, Nucl. Phys. A **697**, 92.
Oganessian, Y., 2002, Eur. Phys. J. A **13**, 135.
Oganessian, Y. T., 2001, Nucl. Phys. A **685**, 17c.
Oganessian, Y. T., V. K. Utyonkov, Y. V. Lobanov, F. S. Abdullin, A. N. Polyakov, I. V. Shirokovsky, Y. S. Tsyganov, G. G. Gulbekian, S. L. Bogomolov, B. N. Gikal, A. N. Mezentsev, S. Iliev, *et al.*, 1999, Phys. Rev. Lett. **83**, 3154.
Oganessian, Y. T., V. K. Utyonkov, Y. V. Lobanov, F. S. Abdullin, A. N. Polyakov, I. V. Shirokovsky, Y. S. Tsyganov, G. G. Gulbekian, S. L. Bogomolov, B. N. Gikal, A. N. Mezentsev, S. Iliev, *et al.*, 2002, Eur. Phys. J. A **15**, 201.
Oinonen, M., P. Baumann, P. Dendooven, Y. Fujita, M. Górska, H. Grawe, Z. Hu, Z. Janas, A. Jokinen, R. Kirchner, O. Klepper, A. Knipper, *et al.*, 1999, Eur. Phys. J. A **5**, 151.
Onsi, M., R. C. Nayak, J. M. Pearson, H. Freyer, and W. Stocker, 1997, Phys. Rev. C **55**, 3166.
Onsi, M. and J. M. Pearson, 2002, Phys. Rev. C **65**, 047302.
Oppenheimer, J. R., and R. Serber, 1938, Phys. Rev. **54**, 540.
Orr, N. A., W. Mittig, L. K. Fifield, M. Lewitowicz, E. Plagnol, Y. Schutz, W. L. Zhan, L. Bianchi, A. Gillibert, A. V. Belozyorov, S. M. Lukyanov, Y. E. Penionzhkevich, *et al.*, 1991a, Phys. Lett. B **258**, 29.
Orr, N. A., W. Mittig, L. K. Fifield, M. Lewitowicz, E. Plagnol, Y. Schutz, W. L. Zhan, L. Bianchi, A. Gillibert, A. V. Belozyorov, S. M. Lukyanov, Y. E. Penionzhkevich, *et al.*, 1991b, Phys. Lett. B **271**, 468(E).
Otsuka, T., 2001, Hyperfine Interact. **132**, 409.
Otsuka, T., R. Fujimoto, Y. Utsuno, B. A. Brown, M. Honma, and T. Mizusaki, 2001, Phys. Rev. Lett. **87**, 082502.
Otsuka, T., Y. Utsuno, T. Mizusaki, and M. Honma, 2001, Nucl. Phys. A **685**, 100.
Ozawa, A., T. Kobayashi, T. Suzuki, K. Yoshida, and I. Tanihata, 2000, Phys. Rev. Lett. **84**, 5493.
Particle Data Group, 2002, Phys. Rev. D **66**, 010001.
Patyk, Z., A. Baran, J. F. Berger, J. Dechargé, J. Dobaczewski, P. Ring, and A. Sobiczewski, 1999, Phys. Rev. C **59**, 704.
Paul, A., S. Röttger, A. Zimbal, and U. Keyser, 2001, Hyperfine Interact. **132**, 189.
Paul, W., 1990, Rev. Mod. Phys. **62**, 531.
Pearson, J. M., 1980, Phys. Lett. B **91**, 325.
Pearson, J. M., 1982, Nucl. Phys. A **376**, 501.
Pearson, J. M., 2001, Phys. Lett. B **513**, 319.
Pearson, J. M., Y. Aboussir, A. K. Dutta, R. C. Nayak, M. Farine, and F. Tondeur, 1991, Nucl. Phys. A **528**, 1.
Pearson, J. M., and S. Goriely, 2001, Phys. Rev. C **64**, 027301.
Pearson, J. M., and S. Goriely, 2003, Phys. Rev. C, in press.

Pearson, J. M., R. C. Nayak, and S. Goriely, 1996, Phys. Lett. B **387**, 455.
Pearson, J. M., and G. Saunier, 1968, Phys. Rev. **173**, 991.
Penionzhkevich, Y. E., 2001, Hyperfine Interact. **132**, 265.
Pfützner, M., E. Badura, C. Bingham, B. Blank, M. Chartier, H. Geissel, J. Giovinazzo, L. V. Grigorenko, R. Grzywacz, M. Hellström, Z. Janas, J. Kurcewicz, *et al.*, 2002, Eur. Phys. J. A **14**, 279.
Pieper, S. C., V. R. Pandharipande, R. B. Wiringa, and J. Carlson, 2001, Phys. Rev. C **64**, 014001.
Poth, H., 1990, Phys. Rep. **196**, 135.
Preston, M. A., and R. K. Bhaduri, 1975, *Structure of the Nucleus* (Addison-Wesley, Reading, MA).
Radon, T., H. Geissel, G. Münzenberg, B. Franzke, T. Kerscher, F. Nolden, Y. N. Novikov, Z. Patyk, C. Scheidenberger, F. Attallah, K. Beckert, T. Beha, *et al.*, 2000, Nucl. Phys. A **677**, 75.
Radon, T., T. Kerscher, B. Schlitt, K. Beckert, T. Beha, F. Bosch, H. Eickhoff, B. Franzke, Y. Fujita, H. Geissel, M. Hausmann, H. Irnich, *et al.*, 1997, Phys. Rev. Lett. **78**, 4701.
Raimbault-Hartmann, H., G. Audi, D. Beck, G. Bollen, M. de Saint Simon, H.-J. Kluge, M. König, R. B. Moore, S. Schwarz, G. Savard, J. Szerypo, and the ISOLDE Collaboration, 2002, Nucl. Phys. A **706**, 3.
Raimbault-Hartmann, H., D. Beck, G. Bollen, M. König, H.-J. Kluge, E. Schark, J. Stein, S. Schwarz, and J. Szerypo, 1997, Nucl. Instrum. Methods Phys. Res. B **126**, 378.
Rainville, S., M. P. Bradley, J. V. Porto, J. K. Thompson, and D. E. Pritchard, 2001, Hyperfine Interact. **132**, 177.
Ravn, H. L., 2002, Ed., *Proceedings of the 5th International Conference on Radioactive Nuclear Beams RNB-5* (North-Holland and Elsevier Science, Amsterdam). Also published as volume 701 in Nucl. Phys. A.
Ravn, H. L., P. Bricault, G. Ciavola, P. Drumm, B. Fogelberg, E. Hagebø, M. Huyse, R. Kirchner, W. Mittig, A. Mueller, H. Nifenecker, and E. Roeckl, 1994, Nucl. Instrum. Methods Phys. Res. B **88**, 441.
Rayet, M., M. Arnould, F. Tondeur, and G. Paulus, 1982, Astron. Astrophys. **116**, 183.
Reinhard, P.-G., and H. Flocard, 1995, Nucl. Phys. A **584**, 467.
Retamosa, J., E. Caurier, F. Nowacki, and A. Poves, 1997, Phys. Rev. C **55**, 1266.
Riisager, K., D. V. Fedorov, and A. S. Jensen, 2000, Europhys. Lett. **49**, 547.
Rikovska Stone, J., P. D. Stevenson, J. C. Miller, and M. R. Strayer, 2002, Phys. Rev. C **65**, 064312.
Ring, P., and P. Schuck, 1980, *The Nuclear Many-Body Problem* (Springer, New York).
Roeckl, E., 2001, Hyperfine Interact. **132**, 153.
Roeckl, E., A. Blazhev, K. Burkard, J. Döring, H. Grawe, W. Hüller, R. Kirchner, C. Mazzocchi, I. Mukha, and C. Plettner, 2003, Nucl. Instrum. Methods Phys. Res. B **204**, 53.
Rowe, D. J., 1970, *Nuclear Collective Motion* (Methuen, London).
Rutz, K., M. Bender, T. Bürvenich, T. Schilling, P.-G. Reinhard, J. A. Maruhn, and W. Greiner, 1997, Phys. Rev. C **56**, 238.
Samaddar, S. K., M. M. Majumdar, B. C. Samanta, and J. N. De, 1986, Nucl. Phys. A **451**, 160.
Samyn, M., S. Goriely, P.-H. Heenen, J. M. Pearson, and F. Tondeur, 2002, Nucl. Phys. A **700**, 142.
Sarazin, F., H. Savajols, W. Mittig, F. Nowacki, N. A. Orr, Z. Ren, P. Roussel-Chomaz, G. Auger, D. Baiborodin, A. V. Belozyorov, C. Borcea, E. Caurier, *et al.*, 2000, Phys. Rev. Lett. **84**, 5062.
Satpathy, L., V. S. Uma Maheswari, and R. C. Nayak, 1999, Phys. Rep. **319**, 85.
Satpathy, L., and R. C. Nayak, 1983, Phys. Rev. Lett. **51**, 1243.
Satula, W., D. J. Dean, J. Gary, S. Mizutori, and W. Nazarewicz, 1997, Phys. Lett. B **407**, 103.
Satula, W., and R. Wyss, 1997, Phys. Lett. B **393**, 1.
Satula, W., and R. Wyss, 2000, Nucl. Phys. A **676**, 120.
Satula, W., and R. A. Wyss, 2002, nucl-th/0211044.
Saunier, G., and J. M. Pearson, 1967, Phys. Rev. **160**, 740.
Savajols, H., 2001, Hyperfine Interact. **132**, 245.
Savajols, H., 2002, private communication.
Savard, G., 2003, Nucl. Instrum. Methods Phys. Res. B **204**, 771.
Savard, G., J. Schwartz, J. Caggiano, J. P. Greene, A. Heinz, M. Maier, D. Seweryniak, and B. J. Zabransky, 2002, Nucl. Phys. A **701**, 292.
Savard, G., and G. Werth, 2000, Annu. Rev. Nucl. Part. Sci. **50**, 119.
Schatz, H., A. Aprahamian, J. Görres, M. Wiescher, T. Rauscher, J. F. Rembges, F.-K. Thielemann, B. Pfeiffer, P. Möller, K.-L. Kratz, H. Herndl, B. A. Brown, *et al.*, 1998, Phys. Rep. **294**, 167.
Scheidenberger, C., 2002, Eur. Phys. J. A **15**, 7.
Scheidenberger, C., F. Attallah, A. Casares, U. Czok, A. Dodonov, S. A. Eliseev, H. Geissel, M. Hausmann, A. Kholomeev, V. Kozlovski, Y. A. Litvinov, M. Maier, *et al.*, 2001, Hyperfine Interact. **132**, 531.
Schlitt, B., K. Beckert, T. Beha, H. Eickhoff, B. Franzke, H. Geissel, H. Irnich, H. C. Jung, T. Kerscher, O. Klepper, K. E. G. Löbner, G. Münzenberg, *et al.*, 1996, Hyperfine Interact. **99**, 117.
Schmidt, K.-H., J. Benlliure, T. Enqvist, A. R. Junghans, F. Rejmund, and M. V Ricciardi, 2002, Nucl. Phys. A **701**, 115.
Schröder, S., R. Klein, N. Boos, M. Gerhard, R. Grieser, G. Huber, A. Karafillidis, M. Krieg, N. Schmidt, T. Kühl, R. Neumann, V. Balykin, *et al.*, 1990, Phys. Rev. Lett. **64**, 2901.
Schwarz, S., F. Ames, G. Audi, D. Beck, G. Bollen, C. de Coster, J. Dilling, O. Engels, R. Fossion, J.-E. Garcia Ramos, S. Henry, F. Herfurth, *et al.*, 2001, Nucl. Phys. A **693**, 533.
Schwarz, S., F. Ames, G. Audi, D. Beck, G. Bollen, J. Dilling, F. Herfurth, H.-J. Kluge, A. Kellerbauer, A. Kohl, D. Lunney, R. B. Moore, *et al.*, 2001, Hyperfine Interact. **132**, 337.
Schwarz, S., M. Baird, G. Bollen, D. Lawton, P. Lofy, D. J. Morrissey, J. Ottarson, R. Ringle, P. Schury, T. Sun, and V. Varentsov, 2003, in *Exotic Nuclei and Atomic Masses (ENAM2001)*, edited by J. Äystö, P. Dendooven, A. Jokinen, and M. Leino (Springer-Verlag, Heidelberg), p. 431.
Schwarz, S., G. Bollen, D. Lawton, A. Neudert, R. Ringle, P. Schury, and T. Sun, 2003, Nucl. Instrum. Methods Phys. Res. B **204**, 474.
Seeger, P. A., and W. M. Howard, 1975, Nucl. Phys. A **238**, 491.
Seifert, H. L., J. M. Wouters, D. J. Vieira, H. Wollnik, X. G. Zhou, X. L. Tu, Z. Y. Zhou, and G. W. Butler, 1994, Z. Phys. A **349**, 25.
Seth, K. K., 1996, in *Proceedings of the 1st Conference on Exotic Nuclei and Atomic Masses ENAM95*, edited by M. de Saint Simon and O. Sorlin (Editions Frontières, Gif-sur-Yvette), p. 109.
Sharma, M. M., G. Lalazissis, J. König, and P. Ring, 1995, Phys. Rev. Lett. **74**, 3744.

Sherrill, B. M., 2003, Nucl. Instrum. Methods Phys. Res. B **204**, 765.
Shibata, M., A. Odahara, S. Mitarai, Y. Gono, M. Kidera, K. Miyazaki, and T. Kuroyanagi, 1996, J. Phys. Soc. Jpn. **65**, 3172.
Sikler, G., D. Ackermann, F. Attallah, D. Beck, J. Dilling, S. A. Elisseev, H. Geissel, D. Habs, S. Heinz, F. Herfurth, F. Heßberger, S. Hofmann, *et al.*, 2003, Nucl. Instrum. Methods Phys. Res. B **204**, 482.
Sikler, G., G. Audi, D. Beck, G. Bollen, O. Engels, F. Herfurth, A. Kellerbauer, H.-J. Kluge, D. Lunney, M. Oinonen, C. Scheidenberger, S. Schwarz, *et al.*, 2003, in *Exotic Nuclei and Atomic Masses (ENAM2001)*, edited by J. Äystö, P. Dendooven, A. Jokinen, and M. Leino (Springer-Verlag, Heidelberg), p. 48.
Sorlin, O., S. Leenhardt, C. Donzaud, J. Duprat, F. Azaiez, F. Nowacki, H. Grawe, Z. Dombrádi, F. Amorini, A. Astier, D. Baiborodin, M. Belleguic, *et al.*, 2002, Phys. Rev. Lett. **88**, 092501.
Stancu, F., D. M. Brink, and H. Flocard, 1977, Phys. Lett. B **68**, 108.
Starodubsky, V. E., and N. M. Hintz, 1994, Phys. Rev. C **49**, 2118.
Steck, M., K. Beckert, H. Eickoff, B. Franzke, F. Nolden, H. Reich, B. Schlitt, and T. Winkler, 1996, Phys. Rev. Lett. **77**, 3803.
Stevenson, P., M. R. Strayer, and J. Rikovska Stone, 2001, Phys. Rev. C **63**, 054309.
Stevenson, P. D., J. Rikovska Stone, and M. R. Strayer, 2002, Phys. Lett. B **545**, 291.
Strutinsky, V. M., 1967, Nucl. Phys. A **95**, 420.
Strutinsky, V. M., 1968, Nucl. Phys. A **122**, 1.
Sumiyoshi, K., S. Yamada, H. Suzuki, and W. Hillebrandt, 1998, Astron. Astrophys. **334**, 159.
Swiatecki, W. J., 1951, Proc. Phys. Soc., London, Sect. A **64A**, 226.
Szerypo, J., D. Habs, S. Heinz, J. Neumayr, P. Thirolf, A. Wilfart, and F. Voit, 2003, Nucl. Instrum. Methods Phys. Res. B **204**, 512.
Szerypo, J., A. Jokinen, V. S. Kolhinen, A. Nieminen, S. Rinta-Antila, and J. Äystö, 2002, Nucl. Phys. A **701**, 588.
Tabakin, F. and K. T. R. Davies, 1966, Phys. Rev. **150**, 793.
Tagaya, Y., S. Hashimoto, K. Morita, Y. H. Pu, T. Ariga, K. Ohta, T. Minemura, I. Hisanaga, T. Motobayashi, and T. Nomura, 1999, Eur. Phys. J. A **5**, 123.
Tanihata, I., 1996, J. Phys. G **22**, 157.
Tanihata, I., 1998, in *Exotic Nuclei and Atomic Masses ENAM98*, edited by B. M. Sherrill, D. J. Morrissey, and C. N. Davids, AIP Conf. Proc. No. 455 (AIP, Woodbury, NY), p. 943.
Tanihata, I., H. Hamagaki, O. Hashimoto, Y. Shida, N. Yoshikawa, K. Sugimoto, O. Yamakawa, T. Kobayashi, and N. Takahashi, 1985, Phys. Rev. Lett. **55**, 2676.
Thibault, C., R. Klapisch, C. Rigaud, A. M. Poskanzer, R. Prieels, L. Lessard, and W. Reisdorf, 1975, Phys. Rev. C **12**, 644.
Tondeur, F., 1978a, Nucl. Phys. A **303**, 185.
Tondeur, F., 1978b, Nucl. Phys. A **311**, 51.
Tondeur, F., M. Brack, M. Farine, and J. M. Pearson, 1984, Nucl. Phys. A **420**, 297.
Tondeur, F., A. K. Dutta, J. M. Pearson, and R. Behrman, 1987, Nucl. Phys. A **470**, 93.
Tondeur, F., S. Goriely, J. M. Pearson, and M. Onsi, 2000, Phys. Rev. C **62**, 024308.
Treiner, J., W. D. Myers, W. J. Swiatecki, and M. S. Weiss, 1986, Nucl. Phys. A **452**, 93.
Trötscher, J., K. Balog, H. Eickhoff, B. Franczak, B. Franzke, Y. Fujita, H. Geissel, C. Klein, J. Knollmann, A. Kraft, K. E. G. Löbner, A. Magel, *et al.*, 1992, Nucl. Instrum. Methods Phys. Res. B **70**, 455.
Typel, S., and B. A. Brown, 2001, Phys. Rev. C **64**, 027302.
Van der Meer, S., 1985, Rev. Mod. Phys. **57**, 689.
Van Dyck, R. S., Jr., S. L. Zafonte, and P. B. Schwinberg, 2001, Hyperfine Interact. **132**, 163.
Van Giai, N., and H. Sagawa, 1981, Phys. Lett. B **106**, 379.
Van Isacker, P., and O. Juillet, 1999, J. Phys. G **25**, 675.
Van Isacker, P., O. Juillet, and F. Nowacki, 1999, Phys. Rev. Lett. **82**, 2060.
Van Isacker, P., D. D. Warner, and D. S. Brenner, 1995, Phys. Rev. Lett. **74**, 4607.
Vautherin, D., 1973, Phys. Rev. C **7**, 296.
Vautherin, D., and D. M. Brink, 1972, Phys. Rev. C **5**, 626.
Vedel, F., and G. Werth, 1995, in *Practical Aspects of Ion Trap Mass Spectrometry*, edited by R. E. March and J. F. J. Todd (CRC Press, Boca Raton), Vol. II, p. 237.
Vertse, T., A. T. Kruppa, R. J. Liotta, W. Nazarewicz, N. Sandulescu, and T. R. Werner, 1998, Phys. Rev. C **57**, 3089.
Vertse, T., A. T. Kruppa, and W. Nazarewicz, 2000, Phys. Rev. C **61**, 064317.
Vervier, J., 2003, Nucl. Instrum. Methods Phys. Res. B **204**, 759.
Vieira, N., G. Audi, Z. Djouadi, H. Doubre, C. Gaulard, S. Henry, D. Lunney, M. de Saint Simon, C. Thibault, G. Bollen, and the ISOLDE Collaboration, 2003, in *Exotic Nuclei and Atomic Masses (ENAM2001)*, edited by J. Äystö, P. Dendooven, A. Jokinen, and M. Leino (Springer-Verlag, Heidelberg), p. 21.
von Weizsäcker, C. F., 1935, Z. Phys. **96**, 431.
Wagemans, C., J. Wagemans, and G. Goeminne, 2001, Hyperfine Interact. **132**, 321.
Wallerstein, G., I. Iben, P. Parker, A. M. Boesgaard, G. M. Hale, A. E. Champagne, C. A. Barnes, F. Käppeler, V. V. Smith, R. D. Hoffmann, F. X. Timmes, C. Sneden, *et al.*, 1997, Rev. Mod. Phys. **69**, 995.
Wang, J. C., J. Clark, K. S. Sharma, J. Vaz, J. P. Greene, A. Heinz, G. Savard, D. Seweryniak, Z. Zhou, F. Buchinger, J. E. Crawford, S. Gulick, *et al.*, 2002, Bull. Am. Phys. Soc. **47**, 82.
Wapstra, A. H. and G. Audi, 2002, Eur. Phys. J. A **15**, 1.
Wapstra, A. H., G. Audi, and R. Hoekstra, 1985, Nucl. Phys. A **432**, 185.
Weber, C., and the ISOLTRAP Collaboration, 2003, in preparation.
Werth, G., T. Beier, S. Djekic, H.-J. Kluge, W. Quint, T. Valenzuela, J. Verdu, and M. Vogel, 2003, Nucl. Instrum. Methods Phys. Res. B. **205**, 1.
Wheeler, J. A., 1955, in *Niels Bohr and the Development of Physics*, edited by W. Pauli (McGraw-Hill, New York), p. 163.
Wigner, E., 1937, Phys. Rev. **51**, 106.
Wiringa, R. B., 2001, private communication.
Wiringa, R. B., V. Fiks, and A. Fabrocini, 1988, Phys. Rev. C **38**, 1010.
Wiringa, R. B., S. C. Pieper, J. Carlson, and V. R. Pandharipande, 2000, Phys. Rev. C **62**, 014001.

Wollnik, H., and A. Casares, 2001, Hyperfine Interact. **132**, 439.
Yakovlev, D. G., A. D. Kaminker, O. Y. Gnedin, and P. Haensel, 2001, Phys. Rep. **354**, 1.
Youngblood, D. H., H. L. Clark, and Y.-W. Lui, 1999, Phys. Rev. Lett. **82**, 691.
Youngblood, D. H., Y.-W. Lui, and H. L. Clark, 2002, Phys. Rev. C **65**, 034302.
Yu, Y., and A. Bulgac, 2003, Phys. Rev. Lett. **90**, 222501.
Zeldes, N., T. S. Dumitrescu, and H. S. Köhler, 1983, Nucl. Phys. A **399**, 11.
Zerguerras, T., 2001, *Etude de l'émission proton et de deux protons dans les noyaux légers déficients en neutrons de la région* $A=20$, Ph.D. thesis (Université Paris 6).
Zhou, X. G., X. L. Tu, J. M. Wouters, D. J. Vieira, K. E. G. Löbner, H. L. Seifert, Z. Y. Shou, and G. W. Butler, 1991, Phys. Lett. B **260**, 285.
Zuker, A. P., 1994, Nucl. Phys. A **576**, 65.
Zuker, A. P., 2003, Phys. Rev. Lett. **90**, 042502.
Zuo, W., I. Bombaci, and U. Lombardo, 1999, Phys. Rev. C **60**, 024605.
Zuo, W., A. Lejeune, U. Lombardo, and J. F. Mathiot, 2002a, Nucl. Phys. A **706**, 418.
Zuo, W., A. Lejeune, U. Lombardo, and J. F. Mathiot, 2002b, Eur. Phys. J. A **14**, 469.